

**Investigating Mechanisms Responsible for the Pro-Regenerative Effects of Conditioning
Electrical Stimulation**

by

Leah Tamara Acton

A thesis submitted in partial fulfillment of the requirements for the degree of

Master of Science

Neuroscience
University of Alberta

© Leah Tamara Acton, 2022

Abstract

Though capable of regeneration, repair surgeries following peripheral nerve injury are often incomplete or entirely unsuccessful. The slow rate of regeneration (1-3mm/day) of a proximal injury requires up to two years to reach the distal target, whereas significant muscle atrophy occurs after 6-12 months; therefore, even if the regenerating axons reach these muscles they may no longer be amenable to reinnervation (Ginsell and Keating, 2014). Despite the advancements in surgical techniques, over half of patients with peripheral nerve injury experience lifelong deficits that can severely impact quality of life (Ruijs et al., 2005). The conditioning crush lesion (CCL), a technique in which a crush injury is performed one week prior to a nerve transection and repair surgery, increases the rate of nerve growth 2-4-fold (Richardson and Issa, 1984). CCL has not been clinically translated as it requires an intentional nerve injury which evokes an invasive inflammatory response. The Webber laboratory has demonstrated that conditioning electrical stimulation (CES) upregulates the same regeneration-associated genes (RAGs) as CCL to accelerate nerve regeneration and promote sensorimotor functional recovery (Senger et al., 2018; Senger et al., 2019). Prior to clinical application of CES we sought to confirm that unlike CCL, CES is non-injurious and non-inflammatory. Infiltrating and resident macrophages did not play a role in the pro-regenerative effects of CES, with decreased IBA-1 and dectin-1 immunofluorescence compared to CCL. Furthermore, macrophage ablation reduced the conditioning effect associated with CCL but not CES. We also investigated the heat-shock protein, alphaB-crystallin, previously found to support remyelination. Proteomics and mass spectrometry identified a five-fold decrease in alphaB-Crystallin protein expression in CES compared to CCL sensory neurons, which was not reproduced in Western Blot Analysis. AlphaB-crystallin null mice displayed increased inherent pCREB expression, all other

regeneration-associated genes were not different from wildtype mice, and the conditioning effect was unaffected.

Preface

This thesis is an original work by Leah Acton. The current research project was completed at the University of Alberta under the supervision of Dr. Webber, Dr. Plemel, and Dr. Zochodne. The research project, of which this thesis is a part, received research ethics approval from the University of Alberta Research Ethics Board, AUP00003034, September 2020. This research project received funding support from a Canada Graduate Scholarship-Masters-CIHR.

Dedication

I would like to dedicate this masters thesis to my family and friends who have supported me along the way. A special mention to my parents, Jody and Cynthia Acton, who have always encouraged me and taught me the value of perseverance in achieving my goals. I would also like to dedicate this to my brother, Matthew Acton, who inspired me by completing his own Master's thesis on top of many different degrees, and has taught me so much despite being in completely different fields. Lastly, I would like to dedicate this to Brett, who has been a continual source of undying support during graduate school. Without your unwavering belief in me, I could not possibly be where I am today.

I am so grateful to have all these wonderful people in my life.

Acknowledgements

I would like to express my deepest gratitude to my supervisor, Dr. Christine Webber. Thank you for sharing all your knowledge, passion for science, and patience as I completed this thesis. It is only with your support, motivation, and guidance that I am completing this Masters' thesis. I learned so much along the way from you, both skills relating to research and otherwise, that I will continue to draw upon in the future. This project could not have been completed without Dr's Douglas Zochodne and Jason Plemel, members of my supervisory committee. Your vast expertise guided me in completing crucial parts of this project, and I will always be grateful for your kindness, support, and willingness to make time for any of my questions and meetings. Thank you to our laboratory technician Susanne Lingrell for your technical expertise and all your suggestions when troubleshooting different experiments. Thank you to Dr Jenna Senger for completing the intricate microsurgeries with me, I will forever be impressed by your skill in surgeries and could not have completed this work without you. Thank you to our undergraduate student Paige Hardy, who assisted on various parts of this project and who gave me the opportunity to share my own skills with her. Thank you to members of the Plemel laboratory Charbel Baaklini and Madelene Ho for making time to show me how to handle injections and complete macrophage analysis. Thank you to Dr Andrew Simmonds for letting me spend countless hours on his microscopy and all his assistance in taking beautiful pictures. Thank you to the Cellular Imaging centre at the University of Alberta for the use of their confocal microscope.

Table of Contents

	Page
Abstract	ii
Preface	iv
Dedication	v
Acknowledgements	vi
Table of Contents	vii
List of Figures	xii
List of Abbreviations	xiv
CHAPTER 1: Introduction	1
1.1 Peripheral Nerve Injury	2
1.2 Nerve Injury Signalling	4
<i>1.2.1 Early Signalling</i>	4
<i>1.2.2 Delayed Signalling</i>	5
1.3 Wallerian Degeneration	7
<i>1.3.1 Multicellular Involvement in Wallerian Degeneration</i>	9
1.4 Nerve Regeneration	12
<i>1.4.1 PI3K-Akt and Ras-MEK-MAPK Pathways</i>	13
<i>1.4.2 Schwann Cell and Macrophage Responses during Nerve Regeneration</i>	14
<i>1.4.3 Growth Cone Extension and Guidance</i>	17
<i>1.4.4 Staggered Regeneration</i>	18
1.5 Limitations of Peripheral Nerve Regeneration	19

1.6 Strategies to Accelerate Nerve Regeneration	20
<i>1.6.1 Post-operative Electrical Stimulation</i>	21
<i>1.6.2 Conditioning Crush Lesion</i>	22
<i>1.6.3 Upregulating Pro-Regenerative Pathways</i>	26
<i>1.6.4 Conditioning Electrical Stimulation</i>	27
1.7 Thesis Statement and Aims	29
CHAPTER 2: Investigation of conditioning electrical stimulation as a strategy to promote peripheral nerve regeneration in a wildtype mouse model	30
2.1 Introduction	31
2.2 Methods	33
2.3 Results	37
<i>2.3.1 CES and CCL upregulate DRG RAGs following nerve repair surgery.</i>	37
<i>2.3.2 CES and CCL promote nerve regeneration in mice, similar to Sprague-Dawley rats.</i>	37
<i>2.3.3 CES, unlike CCL, does not upregulate ATF3, display overt inflammation, or cause Wallerian Degeneration compared to unconditioned controls.</i>	38
2.4 Discussion	40
2.5 Figures	42
CHAPTER 3: The immune profile and role of macrophages following CES and CCL	50
3.1 Introduction	51
<i>3.1.1 Inflammatory responses in the peripheral nerve</i>	51

3.1.2 <i>Tissue-Resident Macrophages (TRMs) and monocyte derived macrophages are found in the PNS</i>	52
3.1.3 <i>Macrophage Ontogeny</i>	52
3.1.4 <i>Genetically modified mouse models to study macrophage populations</i>	54
3.2 Methods	57
3.3 Results	61
3.3.1 <i>In both wildtype and CCR2^{-/-} mice, CCL, but not CES, increased ATF3 expression in DRG neuronal nuclei</i>	61
3.3.2 <i>IBA-1 is upregulated post CCL-conditioning in mice with deficient macrophage infiltration at the nerve, but not the DRG</i>	62
3.3.3 <i>CCR2^{-/-} mice continue to upregulate pCREB post-CCL and CES conditioning</i>	63
3.3.4 <i>CX3CR1^{CreER}; Rosa26 mice upregulate pCREB following CES and CCL, and the injury marker ATF3 is only increased following CCL</i>	63
3.3.5 <i>CCL promotes monocyte-derived macrophage infiltration at the DRG and conditioning site compared to CES and unconditioned animals.</i>	64
3.3.6 <i>CCL promotes activation of monocyte-derived macrophages.</i>	66
3.3.7 <i>Unlike CCL, the pro-regenerative effects of CES persist following macrophage depletion in iDTR;CX3CR1 mice.</i>	68
3.4 Discussion	71
3.5 Figures	78
CHAPTER 4: Investigation of the role of AlphaB-Crystallin in the pro-regenerative effects of CES and CCL	96

4.1 Introduction	97
4.2 Methods	99
4.3 Results	103
<i>4.3.1 Biomix identifies a difference between DRG alphaB-crystallin expression following CES and CCL.</i>	103
<i>4.3.2 The heat-shock protein αBC is upregulated 3 days following CES, but not CCL conditioning.</i>	103
<i>4.3.3 CES and CCL promote DRG RAG upregulation in WT and αBC^{-/-} mice</i>	104
<i>4.3.4 Similar to WT mice, only CCL, but not CES αBC^{-/-} mice increase ATF3 expression within DRG neurons.</i>	104
<i>4.3.5 αBC^{-/-} mice display inherently increased pCREB expression compared to WT mice.</i>	105
<i>4.3.6 The loss of αBC protein did not influence the pro-regenerative conditioning effects of CES or CCL.</i>	105
<i>4.3.7 Loss of αBC in the regenerating environment does not affect nerve growth.</i>	106
4.4 Discussion	108
4.5 Figures	112
Discussion	123
Bibliography	132
Appendices:	156

1. Conditioning Electrical Stimulation Is Superior to Postoperative Electrical Stimulation in Enhanced Regeneration and Functional Recovery Following Nerve Graft Repair. *Neurorehabil Neural Repair*. 2020 Apr;34(4):299-308. doi: 10.1177/1545968320905801.

2. Recovering the regenerative potential in chronically injured nerves by using conditioning electrical stimulation
J Neurosurg. 2021 Oct 15;1-13. doi: 10.3171/2021.4.JNS21398

List of Figures

Figure 2.5.1: Primary and Secondary Antibodies used for Immunohistochemistry

Figure 2.5.2: CES and CCL upregulate similar RAGs in wildtype mice

Figure 2.5.3: CES and CCL accelerate nerve regeneration in wildtype mice following surgical transection and repair compared to unconditioned animals.

Figure 2.5.4 CES does not upregulate the injury marker, ATF3

Figure 2.5.5 CES does not display overt inflammation, Wallerian degeneration, or macrophage upregulation

Figure 3.5.1: Primary and Secondary Antibody Protocols for Immunohistochemistry

Figure 3.5.2: ATF3 is upregulated following CCL, but not CES, compared to unconditioned animals in both WT and CCR2^{-/-} mice.

Figure 3.5.3 IBA-1 expression is upregulated in the DRG following CCL conditioning

Figure 3.5.4 IBA-1 expression is upregulated in the sciatic nerve following CCL conditioning

Figure 3.5.5: CCR2^{-/-} mice upregulate pCREB post-CES and CCL conditioning.

Figure 3.5.6 CES and CCL of CX3CR1^{CreER}; Rosa26 mice increase pCREB at the DRG, whereas CCL alone upregulates the injury marker ATF3.

Figure 3.5.7 CES and CCL do not affect DRG tissue-resident macrophage numbers; however, CCL allows infiltration of monocyte-derived macrophages.

Figure 3.5.8 CES and CCL do not affect nerve tissue-resident macrophage numbers; however, CCL allows infiltration of monocyte-derived macrophages

Figure 3.5.9 Macrophage numbers were significantly reduced in iDTR;CX3CR1 ablated mice that were conditioned with either CCL or CES prior to surgical repair.

Figure 3.5.10 The pro-regenerative effects of CCL and CES persist in littermate controls of iDTR;CX3CR1 mice.

Figure 3.5.11 Unlike CCL, the pro-regenerative effect of CES remains following macrophage ablation in iDTR;CX3CR1 mice.

Figure 4.5.1: Primary and Secondary Antibody Protocols for Western Blot Analysis

Figure 4.5.2: Primary and Secondary Antibodies Used for Immunohistochemistry

Figure 4.5.3 The heat-shock protein, α BC, is unchanged 1 day following CCL and CES compared to unconditioned Sprague-Dawley rats but upregulated 3 days post-CES.

Figure 4.5.4: CES and CCL upregulated RAGs in WT and α BC^{-/-} mice, whereas there is an increase in pCREB expression in the unconditioned α BC^{-/-} DRG.

Figure 4.5.5: α BC protein does not influence the pro-regenerative effects of CES and CCL.

Figure 4.5.6 A lack of α BC in the nerve growth environment does not affect sciatic nerve growth through a graft.

List of Abbreviations

αBC	alphaB-crystallin
ANOVA	analysis of variance
ATF3	activating transcription factor 3
ATP	adenosine triphosphate
BBB	blood-brain barrier
DCC	deleted in colorectal cancer
BDNF	brain-derived neurotrophic factor
BMDM	bone marrow derived monocytes
BNB	blood nerve barrier
cAMP	cyclic adenosine monophosphate
CCL	conditioning crush lesion
CCL2	class c chemokine ligand I
CCR2	class c chemokine receptor 2
CDC42	cell division cycle 42
CES	conditioning electrical stimulation
CMAP	compound muscle action potential
CNS	central nervous system
CR3	complement receptor 3
CREB	cAMP response element-binding protein
CSF	cerebrospinal fluid
DLK	dual leucine zipper-bearing kinase
DRG	dorsal root ganglion

EPAC	exchange protein directly activated by cAMP
GAP-43	growth-associated protein 43
GFAP	glial fibrillary acidic protein
GSK-3 β	glycogen synthase kinase 3beta
GTP	guanosine triphosphate
HSLAS	Health Sciences Laboratory Animal Services
IBA-1	ionized calcium binding adaptor molecule 1
IL-1α	interleukin-1alpha
IL-1β	interleukin 1-beta
JAK	janus kinase
JIP3	JNK interacting protein 3
JNK	JUN amino-terminal kinase
LIF	leukemia-inducible factor
LPS	lipopolysaccharide
MAGs	myelin-associated glycoproteins
MAPK	mitogen-activated protein kinase
MAP3K	mitogen-activated protein kinase III
MEK	MAP/ERK kinase
MHC II	major histocompatibility complex II
mTOR	the mammalian target of rapamycin
MUNE	motor unit number estimation
NAD⁺	nicotinamide adenine dinucleotide
NF200	neurofilament 200

NGF	nerve growth factor
NGS	normal goat serum
NLS	nuclear localization signals
NMN	nicotinamide mononucleotide
NMNAT2	nicotinamide mononucleotide adenylyltransferase 2
NT-3	neurotrophin 3
NT-4/5	neurotrophin 4/5
PAP III	pancreatitis associated protein III
PBS	phosphate-buffered saline
PCR	polymerase chain reaction
pERK	phosphorylated extracellular signalling related kinases
PES	post-operative electrical stimulation
PI3K	phosphatidylinositol 3,4,5 triphosphate
PIP3	phosphoinositide 3-kinase
PKA	protein kinase A
PMR	preferential motor regeneration
PNS	peripheral nervous system
PTEN	phosphatase and tensin homolog deleted on chromosome 10
RAG	regeneration-associated genes
SARM1	sterile alpha and armadillo motif-containing protein 1
STAT3	signal transducer and activator of transcription 3
TIR	toll/interleukin-1 receptor
TLRs	toll-like receptors

TNFα	tumor necrosis factor- α
Trk	tyrosine kinase receptor
TrkA	tropomyosin-receptor kinase A
TRM	tissue-resident macrophages
Unc5H	uncoordinated 5H
VEGF-A	vascular endothelial growth factor -A

CHAPTER 1: Introduction

1.1 Peripheral Nerve Injury

Of the two divisions of the nervous system, only the peripheral nervous system (PNS) is capable of regeneration following injury due to the intrinsic neuronal and microenvironmental properties to promote growth (Rigoni and Negro, 2020). However, in contrast to expectations, successful peripheral nerve regeneration is often associated with poor or incomplete recovery due to a variety of factors, including but not limited to, slow axonal growth rate, poor numbers and misdirection of extending axons, length of growth required, and cortical reorganization (Faroni et al., 2015). One of the major barriers to achieving functional recovery following nerve injury is that the rate of regeneration is only 1-2 mm/day in humans which means that proximal nerve injuries can require up to two years to reach distal targets even under ideal circumstances (Grinsell and Keating, 2014). As significant muscle atrophy occurs at 6-12 months following denervation, these muscles may no longer support reinnervation (Grinsell and Keating, 2014). Therefore, these nerve injury patients may not achieve satisfactory recovery due to lifelong disability and reduced quality of life.

To understand how the type of nerve injury can impact prognosis, nerve and axonal structure must be considered. At the smallest level, each individual axon (myelinated or not) is surrounded by a connective tissue layer, together called the endoneurium, composed of Type I and Type III collagen where mast cells, tissue-resident macrophages (TRMs), fibroblasts, and blood vessels reside (Zochodne, 2008; Richner et al., 2019). The endoneurium forms part of the blood-nerve barrier (BNB) as tight junctions between cells restrict the passage of most molecules to access axonal components, though it is less restrictive than the central nervous systems' blood-brain barrier (BBB). The second major component of the BNB is formed from the tight junctions between perineurial cells, composing the next layer of connective tissue that bundles

individual axons along with their endoneurial layer into fascicles (Zochodne, 2008; Richner et al., 2019). Finally, the largest connective tissue layer found in peripheral nerves is the epineurium, where collagen tissue, blood and lymphatic vessels, TRMs, fibroblasts, and mast cells can be found (Zochodne, 2008; Topp and Boyd, 2006). Overall, injury affecting the deepest nerve layers and varying on degree to which subsequent levels of the nerve are injured can cause increasing severity of dysfunction in patients.

Peripheral nerve injury is most often classified according to Seddon and/or Sunderland's criteria (Seddon, 1942; Sunderland, 1951) The Seddon categories of injury include: neurapraxia, axonotmesis, and neurotmesis. Neurapraxia is the least severe injury of focal demyelination with no axonal injury. Axonotmesis is a lesion of axonal function with intact connective tissue, for example, a crush injury in which the epineurium remains intact while axons are severed. Finally, neurotmesis includes the complete separation of both connective tissues and axons, thereby creating a proximal and distal end such as the case of transection injuries. Sunderland's classifications are similar but grouped from first degree-fifth degree injury. First degree injury involves local demyelination without structural deficits, akin to neurapraxia. Next, Seddon's axonotmesis is separated into three categories: second-degree includes axonal damage without endoneurial injury; third-degree includes axonal and endoneurial damage without perineurial injury; and fourth-degree includes axonal, endoneurial, and perineurial damage without complete transection of the epineurial sheath. Finally, fifth-degree injury is analogous to neurotmesis.

Due to the differing types of peripheral nerve injury, the prognosis of axonal re-growth and subsequent functional recovery varies clinically. For example, regrowth following transection injury is most difficult as axons may struggle to grow through the epineurial gap and become organized. Peripheral nerve surgeries seek to combat such difficulties by reconnecting

nerve bridges with coaptation by sutures and fibrinogen glue, whereas larger gaps are traversed by allo- (engineered) or autografts (typically a sensory nerve from the same patient that provides non-critical sensation). Though surgical techniques have made significant advancements in nerve recovery, approximately half of the patients who receive nerve repair surgeries have unsatisfactory outcomes as they experience lifelong sensory and motor deficits (Ruijs et al., 2005; Grinsell and Keating, 2014). As a result of these poor outcomes, it is evident that means to accelerate nerve regeneration to improve patient recovery following peripheral nerve injury are necessary.

1.2 Nerve Injury Signalling

Understanding the multicellular degeneration and regeneration processes following peripheral nerve injury is important to create clinical strategies. Following peripheral nerve injury, cellular changes occur at both the axonal injury site and where the neuronal cell bodies reside, which is the dorsal root ganglion (DRG) for sensory neurons or the ventral horn of the spinal cord for motor axons (Topp and Boyd, 2006; Zochodne, 2012). First and foremost, for the necessary cellular changes that support regrowth to occur, the event that an injury has occurred must be signalled to both the axon and their cell bodies. Therefore, the various signalling pathways that commence at the injury site and propagate to the cell bodies can be grouped into two classes: early and delayed. Early signalling involves ion propagation, happening within seconds to minutes after injury, whereas delayed signalling typically happens within hours to days following injury and involves protein translation and retrograde transport along dynein (Ambron and Walters, 1996).

1.2.1 Early Signalling

The early signal from the injured axon to the cell body primarily involves calcium waves. The rupture of the axonal membrane at the damaged distal nerve segment activates voltage-dependent sodium channels (Iwata et al., 2004). The subsequent intracellular rise in sodium in the distal axon causes the inversion of sodium/calcium exchange pumps (Mandolesi et al., 2004; Rishal and Fainzilber, 2014). Concurrently, the opened voltage-gated calcium channels at the injury site promotes calcium release from intra-axonal endoplasmic reticulum stores through ryanodine receptors and inositol triphosphate receptors. This increase in intracellular calcium levels at the injury site causes a propagation of transient calcium waves along the axon to alert the cell bodies of injury occurrence and activate the necessary downstream pathways (Zochodne, 2012; Ohtake et al., 2018).

One of the most important early signalling pathways downstream of calcium involves cyclic adenosine monophosphate (cAMP). The elevated intracellular calcium at the cell body activates calcium/calmodulin-dependent protein kinase which in turn activates the enzyme adenylyl cyclase to catalyze the formation of cAMP from adenosine triphosphate (ATP) (Sassone-Corsi, 2012; Senger et al., 2018). Following its activation, cAMP can dimerize protein kinase A (PKA) and activate exchange protein directly activated by cAMP (EPAC). Both PKA and EPAC are then translocated to the nucleus to activate the transcription factor cAMP response element-binding protein (CREB) via phosphorylation to influence gene transcription in favour of regeneration (Wei et al., 2016; Senger et al., 2018). PKA can also initiate dual leucine zipper-bearing kinase (DLK) activation, a component of delayed injury signalling discussed below (Mahar and Cavalli, 2018).

1.2.2 Delayed Signalling

The delayed injury signal from the axon to the cell body involves a large variety of macromolecular signalling complexes that travel along the established retrograde transport mechanisms, dynein (Rishal and Fainzilber, 2014). Importins were considered as a candidate injury signal in early studies completed in *Aplysia californica* (Ambron et al., 1995) due to their role in nucleocytoplasmic transport as karyophilic proteins with nuclear localization signals (NLS). Importin- α and importin- β were both identified in axons; importin- α is constitutively expressed in axons and is associated with dynein, whereas importin- β is locally translated following axonal injury (Hanz et al., 2003; Perry and Fainzilber, 2009; Rishal and Fainzilber, 2014). Upon axonal injury, importin- α and importin- β form heterodimers with high-affinity NLS-binding sites, allowing their retrograde transport to the cell body through dynein association (Rishal and Fainzilber, 2014). With the creation of this high-affinity NLS, other proteins present at the injury site can bind to it, thus accessing the retrograde signalling motors by dynein (Hanz et al., 2003). Specifically, the intermediate filament vimentin is locally translated after injury (Perlson et al., 2005; Mahar and Cavalli, 2018). The calcium-dependent cysteine protease, calpain, cleaves vimentin allowing the pieces to bind phosphorylated extracellular signal-related kinase (pERK), which lacks an NLS. Furthermore, vimentin blocks dephosphorylation of pERK, allowing it to function as an important retrograde signal (Perlson et al., 2006). Then, a macromolecular complex forms with the binding of importin- β 1 to vimentin in the vimentin-pERK complex, allowing it to be marked for nuclear transport via dynein (Rishal and Fainzilber, 2014). Once at the cell body, pERK activates transcription factors through phosphorylation to support regeneration and inhibits cAMP phosphodiesterases, thereby further increasing cAMP activity at the cell body after axon injury (Perlson et al., 2005; Zochodne, 2008).

Another member of the MAPK family, DLK is a mitogen-activated protein kinase III (MAPK3) implicated in processes such as axon growth, neuronal migration, and regeneration (Tedeschi and Bradke, 2013). Following injury, both elevations of cAMP and microtubule instability activate DLK which then associates with the mitogen-activated protein kinase (MAPK), JNK3, initiating its activation (Mahar and Cavalli, 2018). As part of the retrograde signalling complex JNK3 binds to the JNK scaffolding protein, JNK-interacting protein 3 (JIP3), and DLK-KN3-JIP3 is retrogradely transported to the cell body via dynein retrograde transport. DLK can also activate the transcription factor and injury signal, signal transducer and activator of transcription 3 (STAT3), which is locally translated at the injury site following calcium elevation, phosphorylated during injury, and transported retrogradely via importins (Mahar and Cavalli, 2018). At the soma, DLK-JNK-JIP3 signalling induces the activation of the transcription factor, Jun, to change the pattern of gene expression to support injury processes instead of homeostatic gene transcription. Both JNK and STAT3 can also be activated by microtubule disruption for retrograde transport at these later injury stages to evoke changes in gene transcription. Ultimately, the result of both early and delayed injury signalling is the upregulation of gene transcription that supports the processes of degeneration and regeneration in the PNS.

1.3 Wallerian Degeneration

As retrograde signalling to the cell body occurs, the myelin and axonal debris from injured axons must be cleared to remove inhibition and support regrowth, in a process first described by Augustus Waller in 1850, now collectively described as “Wallerian Degeneration” to refer to the sequenced axonal changes that occur following nerve transection which are remarkably similar in other types of nerve injury (Conforti et al., 2014). The rapid depolarization at the site of injury

is not only involved in retrograde signalling, but also hypothesized to initiate degeneration of the distal nerve segment which is maintained by ongoing calcium influx (George et al., 1995; Zochodne, 2008). This ongoing calcium influx triggers downstream pathways necessary for degeneration including the activation of proteases such as calpain (Yang et al., 2013; Christie and Zochodne, 2013). Much of what is known about degeneration was discovered through the spontaneous mutation of the “slow Wallerian degeneration” (*Wlds*) mouse, which resulted in axons resistant to degeneration, producing a delayed injury response, and providing the first piece of evidence that Wallerian Degeneration is an active process, not merely passive cell death as previously thought (Brown et al., 1994; Wang et al., 2018).

There are two key molecular events during Wallerian Degeneration that lead to the degradation of cellular debris: one of which is the removal of the survival factor nicotinamide mononucleotide adenylyltransferase 2 (NMNAT2) and the other involves the activation of sterile alpha and armadillo motif-containing protein 1 (SARM1), a degeneration trigger protein (Ding and Hammarlund, 2019). NMNAT2 is an axonal enzyme made at the cell body responsible for the catalysis of nicotinamide mononucleotide (NMN) to form nicotinamide adenine dinucleotide (NAD⁺) using ATP. In axons, NMNAT2 undergoes frequent anterograde transport due to its short half-life, thereby providing necessary survival signalling for proper axonal function (Walker et al., 2017). Anterograde transport is blocked following nerve injury and causes the reduction of NMNAT2 at the injury site and lack of its pro-survival cues. MAPK signalling induced following injury contributes to NMNAT2 breakdown, thereby allowing degeneration to occur (Walker et al., 2017; Ding and Hammarlund, 2019). The *Wlds* mouse undergoes slow degeneration due to the formation of a chimeric protein containing the N-terminal fragment of the ubiquitination factor, Ube4b, and the typically nuclear-bound NMNAT1 (Conforti et al.,

2000; Mack et al., 2001; Cohen et al., 2012; Ding and Hammarlund, 2019). With the abnormal formation of this chimeric protein, NMNAT1 is found axonally, where it remains following injury, thus compensating for the loss of NMNAT2 during injury and protecting the axons from degeneration (Ding and Hammarlund, 2019). Furthermore, any event that increases NMNAT2 levels such as the loss of Highwire, an E3 ubiquitin ligase responsible for NMNAT2 turnover, or even loss of a component of this E3 ubiquitin ligase results in delayed axon degeneration (Xiong et al., 2012; Yamagishi and Tessier-Lavigne, 2016). Conversely, SARM1 is found inactivated during healthy states. Following injury, the inhibition is released which allows dimerization of its C-terminus, Toll/interleukin-1 receptor (TIR) domain. When dimerized, TIR can induce rapid NAD⁺ loss through enzymatic cleavage and ATP depletion, causing cytoskeletal and axonal degradation (Ding and Hammarlund, 2019; Essuman et al., 2017). Since NMNAT2 is responsible for NAD⁺ synthesis, SARM1 pro-degenerative signaling requires removal of the pro-survival signal, NMNAT2 to promote Wallerian degeneration. The induction of SARM1 is largely unknown; however, it is hypothesized that removal of NMNAT2 induces SARM1 activation (Ding and Hammarlund, 2019). Overall, the actions of these two molecular proteins are important for Wallerian Degeneration to proceed to eventually make space for regeneration.

1.3.1 Multicellular Involvement in Wallerian Degeneration

Wallerian degeneration is not only a neuronal event, but also relies on the activation of nearby glial and immune cells, including Schwann cells and macrophages, respectively (Chen et al., 2015; Jang et al., 2016). Schwann cells can envelope healthy axons to form myelin sheaths (myelinating Schwann cells) or support unmyelinated axons in Remak bundles (unmyelinating Schwann cells). After sensing that injury has occurred, due in part through the induction of toll-like receptors (TLRs), it is necessary for the previously myelinating Schwann cells to withdraw

their production of structural and myelin-associated glycoproteins (MAGs) as they differentiate to a proliferative state through the upregulation of *JUN*, peaking at 4 days post-injury (De-Francesco-Lisowitz et al., 2015). Schwann cells then commence phagocytosis of myelin and extracellular debris following the activation of phospholipase-A2, which is activated in the cytosol upon injury (Gaudet et al., 2011; Murakami et al., 1997). This enzyme hydrolyzes phosphatidylcholine to lysophosphatidylcholine and arachidonic acid, thereby initiating myelin degradation (Gregson and Hall, 1973; Gaudet et al., 2011). Lysophosphatidylcholine is a strong demyelinating factor with extensive research demonstrating its contribution to nerve degeneration, and ability to activate and recruit immune cells including macrophages, neutrophils, and T cells (Hall, 1972; Gregson and Hall, 1973; Ousman and David, 2000; Ousman and David, 2001; De et al., 2003; Gaudet et al., 2011)

Schwann cells further contribute to immune cell recruitment to the axonal injury site by producing pro-inflammatory cytokines and chemokines (Chan et al., 2014). The loss of the BNB allows access to the immune cells of the blood. The first immune cell to infiltrate to the injured nerve are neutrophils where they start phagocytosis of axonal and myelin debris before their rapid apoptosis after 24 hours (Gaudet et al., 2011; Perkins and Tracey, 2000). At day 2-3 post-injury, the release of inflammatory cytokines by both the Schwann cells and axotomized neuron leads to subsequent infiltration of monocyte-derived macrophages, the most dominant cell for phagocytosis of myelin debris (Rotshenker, 2011; Shen et al., 2000). Major cytokines that produce the macrophage infiltration following peripheral nerve injury includes leukemia-inducible factor (LIF), class c chemokine ligand I (CCL2, also known as monocyte chemoattractant protein-1), interleukin 1-beta (IL-1 β) and tumor necrosis factor- α (TNF α), some of which are partly dependent on calpain activity as neither TNF- α nor IL-1 β are induced

following injury with calpain block (De-Francesco-Lisowitz et al., 2015). Monocyte-derived macrophages express class c chemokine receptor 2 (CCR2), the major receptor mediating macrophage infiltration due to neuronal and Schwann cell regulated release of its ligand CCL2 (Kuziel et al., 1997; Rossi and Zlotnik, 2000; White et al., 2005) CCR2^{-/-} mice exhibit deficient macrophage infiltration following sciatic nerve injury, but interestingly, Wallerian Degeneration remains unaffected (De-Francesco-Lisowitz et al., 2015). Further studies demonstrated that neutrophils compensate for the lack of CCR2 in these mice as their depletion via anti-Ly6G injection to CCR2^{-/-} mice produced deficits in Wallerian Degeneration (Lindborg et al., 2017). With the breakdown of the BNB, opsonins from the blood are allowed to enter the injury site including both antibodies and complement proteins (Brück and Friede, 1990; Vargas and Barres, 2007; Vargas et al., 2010). Macrophage interactions with B cells are evidenced during Wallerian degeneration as endogenous autoantibodies are upregulated following nerve injury. Further, the complement system is activated during nerve injury and phagocytosis of myelin debris is opsonin-dependent (Vargas and Barres, 2007; Vargas et al., 2010). Following opsonization of myelin by the complement protein C3, binding to macrophages through their receptor CR3 allows for subsequent phagocytosis (Rotshenker 2003; van der Laan et al., 1996). Depletion of complement proteins during nerve injury produces defective macrophage phagocytosis leading to sustained myelin presence and delayed nerve regeneration (Vargas et al., 2010). Interestingly, a second site of macrophage infiltration was identified at the cell body, leading to increased recognition of macrophages beyond Wallerian degeneration, which will be discussed below (Niemi et al., 2013). Ultimately, the removal of myelin and axonal debris clears a path for subsequent regenerating axons to ideally reach their distal targets.

1.4 Nerve Regeneration

As degeneration occurs at the distal stump, nerve regeneration commences proximally. Following the integration of retrograde signalling, the cell body produces several changes associated with injury that impacts the subsequent regenerative processes (Schmidt and Modert, 1984). For instance, morphological changes including early cell body swelling, delayed atrophy, loss of Nissl bodies in the ribosomes, and displacement of the nucleus from the centre of the neuron to a lateral placement occur (Zochodne, 2012). Akin to the Schwann cell de-differentiation from myelinating to a proliferative phenotype following axonal injury, the neuron changes its phenotype from a mature, innervating neuron to a regenerating neuron. Nuclear displacement makes room for newly synthesized proteins (Levine et al., 2004; Zochodne, 2008). Importantly, neurons change their pattern of protein expression to downregulate constitutively expressed molecules and myelin-related proteins while upregulating those involved in regeneration, collectively referred to as regeneration-associated genes (RAGs) (Verge et al., 1996). The pattern of change in gene expression that occurs following peripheral nerve injury is often comparable to that of development, when neurons are first born and migrate to their respective targets prior to myelination, which highlights the regenerative response that is found in injured neurons (Gordon, 2020; Hilton et al., 2022). Though there are many RAGs, some examples include brain-derived neurotrophic factor (BDNF), growth-associated protein 43 (GAP-43), and phosphorylated-CREB (pCREB) which promote the upregulation of structural proteins that will be trafficked to the growing axon including tubulin and actin (Chan et al., 2014). Aside from the pathways previously mentioned that upregulate transcription of RAGs including cAMP, EPAC, pERK, and STAT3 (discussed in Chapter 1.2 and 1.3), prominent

pathways implicated in nerve regeneration are the phosphoinositide 3-kinase (PI3K)-Akt pathway and the Ras-MEK-MAPK pathway.

1.4.1 PI3K-Akt and Ras-MEK-MAPK Pathways

After injury, a transient upregulation of nerve growth factor (NGF) at the injury site evokes PI3K activation following tropomyosin receptor A (TrkA) binding and the subsequent activation of adaptor proteins Gab-1 or Ras which have separate effects on PI3K signalling (Kaplan and Miller, 2000; Chan et al., 2014). PI3K is activated by phosphorylation of PIP2 to phosphatidylinositol 3,4,5 triphosphate (PIP3) which then phosphorylates the downstream pathway associated with Gab-1 (Hemmings and Restuccia, 2012). Through Gab-1-mediated PI3K activation, Akt is activated by phosphorylation, whereas Ras activation causes downstream ERK-1/2 phosphorylation (Chan et al., 2014). Akt is anti-apoptotic by inhibition of pro-apoptotic transcription factors Forkhead and Bad, causing subsequent downregulation of the Fas ligand Akt and reduced apoptosis (Brunet et al., 1999; Vanhaesebroeck and Alessi, 2000; Dudek et al., 1997; Read and Gorman, 2009; Chan et al., 2014). To promote growth through upregulation of protein and ribosome synthesis, Akt phosphorylates the mammalian target of rapamycin (mTOR), activating this pathway (Jaworski et al., 2005; Read and Gorman, 2009; Christie and Zochodne, 2013). Furthermore, Akt inhibits glycogen synthase kinase 3 β (GSK-3 β), an inhibitory brake on nerve regeneration found at the growth cone involved in targeting proteins for proteolysis (Cross et al., 1995; Zochodne, 2009). Another brake on nerve regeneration is phosphatase and tensin homolog deleted on Chromosome 10 (PTEN), that typically dephosphorylates PIP3, thereby decreasing neural regeneration and inhibiting growth by reducing activity of the PI3K pathway (Leslie et al., 2008; Christie and Zochodne, 2013). The increase in NGF following nerve injury inhibits PTEN through phosphorylation by casein kinase

II, allowing nerve growth to occur (Arevalo and Rodríguez-Tébar, 2006; Christie and Zochodne, 2013). Similarly, the activation of ERK-1/2 occurs following Ras activation of the serine-threonine kinase Raf which can subsequently activate MAP/ERK kinase (MEK) (Klesse et al., 1999; Pernet et al., 2005). MEK phosphorylation of ERK-1/2 then promotes neural regeneration, and upregulates CREB (Mazzoni et al., 1999; Atwal et al., 2000; Chan et al., 2014). MEK phosphorylation also activates anti-apoptotic pathways. Instead of inhibiting pro-apoptotic factors like Akt, ERK-1/2 typically activates anti-apoptotic proteins such as Bcl-2 (Hetman et al., 1999; Kaplan and Miller, 2000; Hausott and Klimaschewski, 2019). Overall, the activation of PI3K and Ras pathways promote growth and reduce cell death through downstream effectors including Akt and ERK, while reducing the activity of inhibitory brakes on regeneration.

1.4.2 Schwann Cell and Macrophage Responses during Nerve Regeneration

Similar to Wallerian degeneration, nerve regeneration is not solely a neuronal response, and involves pro-regenerative actions by Schwann cells, satellite glial cells, and even macrophages (Zochodne, 2012). In their proliferative, de-differentiated state, Schwann cells produce high levels of neurotrophic factors and ultimately guide axonal growth along the endoneurium tube by forming the Bands of Bungner after degeneration has occurred (Parrinello et al., 2010; Jopling et al., 2011; Rosenberg et al., 2014; Xiao et al., 2015; Cattin and Lloyd, 2016). In transection injuries, the gap that is formed between proximal and distal stumps is filled with laminin and fibronectin, basement membrane proteins produced by Schwann cells, macrophages, and fibroblasts (Tonge et al., 1998; Chen et al., 2007; Webber and Zochodne, 2010). This environment then entices regenerating neurons to extend forwards, albeit there is much hesitation by regenerating neurons. Fibroblasts can activate Schwann cell migration, and then the subsequent neuronal regeneration follows, by their release of ephrin B. This binds to the

receptor, EphB2, on Schwann cells, which ultimately produces an attractive behavior that allows Schwann cells to migrate across the gap (Parrinello et al., 2010; Jessen et al., 2015). A key signalling molecule involved in the interactions of regenerating neurons and Schwann cells is neuregulin-1, a growth factor typically found in developing axons that is associated with proper migration of Schwann cells and eventual myelination phenotypes (Harrisingh et al., 2004; Woodhoo and Sommer, 2008; Webber and Zochodne, 2010). After injury, neuregulin is once more produced by axons following the expression of growth factors by Schwann cells, thereby further contributing to their proliferation, survival, and eventual myelination (Stassart et al., 2013; Fricker et al., 2011; Zochodne, 2012). The Raf-ERK pathway is also important for maintaining the regenerative phenotype of Schwann cells as exogenous activation can trigger Schwann cell de-differentiation and breakdown of the myelin-barrier without injury which is subsequently resolved following removal of ERK activation (Harrisingh et al., 2004; Napoli et al., 2012). Furthermore, the activation of transcription factor *c-Jun* is particularly important in the regenerative response of Schwann cells as knock-out Schwann cells fail to upregulate neurotrophic factors required for neuronal growth and produce abnormal regeneration, resulting in reduced functional recovery and cell death (Mirsky et al., 2008; Arthur-Farraj et al., 2012). Overall, Schwann cells de-differentiate and proliferate to aid in nerve regeneration by producing neurotrophic factors and guiding regenerating axons to distal targets (Chen et al., 2007; Parrinello et al., 2014; Xiao et al., 2015; Cattin and Lloyd, 2016).

Satellite glial cells are another supportive cell ensheathing the perikarya of sensory neurons with functions that are being increasingly recognized in peripheral nerve regeneration research. Findings that support their potential role in nerve regeneration includes their production of neurotrophins including BDNF, NGF, and NT-3 and cytokines following injury (Wetmore and

Olson, 1995; Pannese and Procacci, 2002; Zhou et al., 1999; Ohtori et al., 2004; Hanani, 2005). Furthermore, satellite glial cells have been shown to proliferate extensively after neuronal damage including axotomy, and even phagocytose debris similar to Schwann cells and macrophages (Shinder et al., 1999; Aldskogius and Arvidsson, 1978). Overall, following nerve regeneration these perineuronal satellite glial cells proliferate, release neurotrophic factors, and perform some degree of phagocytosis.

Traditionally thought to be involved primarily in Wallerian or Wallerian-like Degeneration, macrophages have recently been shown to participate in regenerative processes (Lu and Richardson, 1993; Niemi et al., 2013). Reducing the infiltration of macrophages to the DRG in *CCR2*^{-/-} mice did not impair Wallerian Degeneration; however, axonal regeneration was significantly reduced (Niemi et al., 2013). Additionally, macrophages are hypothesized to contribute to peripheral nerve regeneration by their release of inflammatory cytokines, which recently has been suggested to act as trophic factors once regeneration commences, alongside more traditional neurotrophic factors produced by proliferative Schwann cells and macrophages (Hikawa and Takenaka, 1996; Fleur et al., 1996; Heumann et al., 1987; Gaudet et al., 2011; Liu et al., 2019; Jha et al., 2021). At the nerve bridge, macrophages also drive angiogenesis by producing vascular endothelial growth factor A (VEGF-A), which may contribute to the migration of Schwann cells during regeneration as they move across the bridge along new blood vessels (Cursiefen et al., 2004; Pollard, 2009; Fantin et al., 2010; Cattin et al., 2015). Furthermore, macrophage-derived VEGF-A is crucially important for end target muscle function due to its major role in promoting neuromuscular junction reinnervation (Lu et al., 2020). Interestingly, a recent study demonstrated that macrophages may be mobilized ahead of Schwann cells and directly contribute to neuronal guidance separately from its angiogenesis

function by secretion of the new axon guidance protein, plexin-b2 (Li et al., 2022). Altogether, it is evident that neuronal regeneration is a multicellular process involving Schwann cells, satellite glial cells, and macrophages alongside the injured neurons.

1.4.3 Growth Cone Extension and Guidance

Regeneration occurs through the formation of a dynamic structure called a growth cone emerging at the distal tip of the proximal nerve stump. Extensively studied *in vitro*, the growth cone is composed mostly of actin and microtubules and displays exploratory behavior during regeneration: collapsing and extending in response to environmental cues. Guiding growth cone extension is both substrate-bound cues and chemotropic cues, including neurotrophins, and Netrin-1 that can lead to subsequent activity by Rho guanosine triphosphate (GTP) hydrolase enzymes (GTPases) within the axon to mediate extension or collapse (Hall and Lalli, 2010). The GTPase RhoA promotes myosin II contractile activity leading to growth cone retraction and collapse and is typically decreased in areas where the growth cone is attracted (Wu et al., 2005; Cheng et al., 2008; Lowery and Vactor, 2009). Other members of the GTPase family instead mediate growth cone extension such as cell division cycle 42 (CDC42) and Rac (Wang et al., 2007; Zochodne, 2008; Hall and Lalli, 2010). The filopodia are finger-like projections at the tip of the growth cone that extend from their distal tips via actin monomers. Filopodium increase the surface area for cell surface receptors including growth or guidance receptors (such as TrkA) that can respond to and grow towards concentration gradients of secreted guidance molecules. Similar to developmental states, NGF can facilitate growth cone attraction in *in vitro* turning assays following injury (Webber et al., 2008). Most often studied during CNS development, Netrin-1 has also been shown to be involved in peripheral nerve regeneration (Zochodne, 2012). At the nerve, one of Netrin-1's receptor's, deleted in colorectal cancer (DCC), is upregulated

following injury, whereas another, uncoordinated 5H (Unc5H) is decreased. DCC is increased at the injury site and localizes with de-differentiated Schwann cells, indicating a role in axonal regrowth whereas Unc5H is inhibitory to nerve regeneration and knock-down of its function produces increases in regeneration (Webber et al., 2011). Overall, the complex interplay between guidance cues can contribute to axonal outgrowth past transection sites and eventual reinnervation of target tissues following injury.

1.4.4 Staggered Regeneration

Cajal's work with silver staining suggested regenerating axons taking roundabout routes at differing lengths following injury, in lieu of axons projecting straight to their targets (Cajal, 1928). These findings were later expanded on and confirmed, as regenerating neuronal growth was found to be asynchronous and officially referred to as 'staggered regeneration' (Al-Majed et al., 2000; Zochodne 2008). After nerve repair surgeries, only 25% of axons grow past the coaptation site (Witzel et al., 2005). This highlights the important conclusion that regenerating axons must differ in their exposure to certain environmental cues, as neurotrophic factors, cytokines, and guidance cues evolve during the regenerative process. It also explains certain limitations of peripheral nerve injury recovery since the supposed speed of axonal growth is around 1-2mm/day, but many axons do not behave according to these standards and take much longer to extend past the injury site. As the first neurons extend past this site of injury, it has been hypothesized that their early passage could be another neurotrophic signal that further directs the delayed axonal outgrowth to regenerate (Zochodne, 2008). Furthermore, the growth of regenerative axons is not only guided past the injury site, but also to an extent, towards their correct targets. Findings have indicated that motor axons tend to growth towards motor pathways, instead of sensory, indicating the process of preferential motor regeneration (PMR)

(Brushart, 1988). As this asynchronous growth occurs, some axons extent incorrect projections; however, over time, this decreases while correct projections increase (Gordon, 2020). Overall, reducing staggered regeneration and improving correct target reinnervation are two important avenues to improve functional recovery following nerve injury.

1.5 Limitations of Peripheral Nerve Regeneration

Though capable of regeneration, injury to the peripheral nerves rarely results in complete recovery. Deficits at any stage of regeneration could negatively impact recovery while the intrinsic properties of re-growing nerve, such as staggered regeneration, may also limit complete reinnervation. Aside from the relative severity of the injury, several factors can impact recovery including speed of regeneration, age, type of injury, and location of the injury. The slow rate of regeneration decreases the change of likelihood of functional recovery, as after a significant time period of denervation, degeneration of the motor end plate occurs and cannot be reversed (Grinsell and Keating, 2014). This is exacerbated in proximal nerve injuries, where regenerating axons have a large distance to grow before reaching targets compared to distal injuries, at the fingertips for example. Further, this highlights the importance of increasing the growth rate of axons, as denervated Schwann cells could lose their regenerative effects and no longer support subsequent axonal regeneration (Gordon, 2020). A lack of neuronal contact at all will result in Schwann cell loss and subsequent downregulation of growth factors; highlighting the importance of axonal guidance by neurotrophic Schwann cells to support neuronal survival, and ultimately impact recovery (Cattin and Lloyd, 2016). The combination of slow nerve regeneration and progressive muscular atrophy strongly indicates a need to increase the intrinsic rate of regeneration to ultimately support functional recovery in patients. Transection injuries are most

prominently severe as regenerating axons need to find the correct pathway forward, and without their endoneurium to guide them to their correct target, the axons can be misguided to the wrong tissue or even form neuromas. At the target tissue, misdirection of regenerating axons is limited by pruning of growth cones that extend towards an incorrect target; however, misdirection remains a problem difficult to address. With misdirection comes potential cortical reorganization, which could help with regaining recovery but can require extensive training to regain appropriate function (Abrams and Widenfalk, 2005).

Peripheral nerve injury can be associated with retrograde neuronal loss, meaning that the number of regenerating axons is inherently reduced, thereby decreasing the number of axons available to eventually regenerate to the end target, though these findings are debated in the literature (Oliveira, 2001; Scholz et al., 2005; Zochodne, 2008). Likewise, advanced age is associated with fewer numbers of regenerating axons, as well as decreased capacity to complete processes such as Wallerian degeneration and production of growth factors (Verdú et al., 2000; Abrams and Widenfalk, 2005). Overall, there are many factors that negatively impact recovery following peripheral nerve injury and necessitate means to improve regeneration for patients.

1.6 Strategies to Accelerate Nerve Regeneration

Current strategies to improve outcomes following nerve injury often target one or multiple events that occur during the multicellular degeneration/regeneration processes. Though microsurgery has advanced nerve regeneration, even patients who undergo repair surgeries have deficits with only approximately 50% of patients achieving satisfactory recovery (Ruijs et al., 2005). As a result, strategies to improve nerve injury recovery alongside microsurgeries have been considered, including post-operative electrical stimulation (PES), conditioning crush

lesions (CCL), upregulating pro-regenerative pathways, and conditioning electrical stimulation (CES).

1.6.1 Post-operative Electrical Stimulation (PES)

Electrical stimulation following nerve repair is clinically safe and promotes nerve regeneration (Chan et al., 2016; Wong et al., 2015). Electrical stimulation of the nerve at 20 Hz for one hour following surgical transection and repair promoted nerve regeneration (Al-Majed et al., 2000). Increased time of electrical stimulation (up to 2 weeks) and increased frequency (up to 200 Hz) either failed to improve or had poorer outcomes, respectively, on nerve regeneration (Al-Majed et al., 2000). Blocking retrograde action potential transmission reduced the effect of electrical stimulation on regeneration indicating electrical stimulation relies on a cell body response (Al-Majed et al., 2000). Importantly, PES increases the number of axons extending across the coaptation site, but it does not inherently accelerate the rate of nerve regeneration (Brushart et al., 2002). PES increases the amount of correct axonal projections of both motor and sensory axons, thereby limiting the amount of inappropriate growth that hinders recovery (Al-Majed et al., 2000; Brushart et al., 2005). Furthermore, the clinically useful effects of PES are associated with upregulated RAGs, prominently including BDNF and GAP-43, as well as upregulation of the PI3K pathway (Al-Majed et al., 2000; Geremia et al., 2007; Singh et al., 2015). BDNF is induced following nerve injury and has been shown to have neuroprotective effects, as well as enhanced sprouting *in vitro*, whereas blocking BDNF after injury leads to deficits in regeneration and remyelination (Zhang et al., 2000; Streppel et al., 2002; Al-Majed et al., 2000; Geremia et al., 2010). These actions of BDNF are mediated through the cAMP pathway as PES upregulates cAMP levels, increasing the activation of this pathway and downstream effects (Geremia et al., 2007). Furthermore, PES has been shown to improve

Schwann cell function and remyelination, not solely regeneration, *in vitro* and *in vivo* (Huang et al., 2010; Singh et al., 2012; McLean et al., 2014).

Following the abundance of promising data completed in mouse and Sprague-Dawley rat animal models, PES has undergone clinical trials demonstrating its effectiveness for peripheral nerve injury patients. The first trial demonstrated significantly increased motor unit number estimation (MUNE) in patients undergoing carpal tunnel decompression surgery, indicating a higher amount of muscle innervation by motor neurons (Gordon et al., 2010). Further, PES was demonstrated to be effective in patients with transection injury, traction injury, and chronic compression neuropathy as it was associated with improved MUNE scores, compound muscle action potential (CMAP) amplitudes, and sensory function (Wong et al., 2015; Barber et al., 2018; Power et al., 2020; Zuo et al., 2020). Overall, PES is effective in reducing staggered regeneration and improving recovery after multiple types of nerve injury, but does not inherently accelerate the rate of re-growth.

1.6.2 Conditioning Crush Lesion

Forty years of research have extensively studied the conditioning crush lesion (CCL) that has been found to enhance the growth rate of neurons 2-4-fold (Richardson and Issa, 1984; McQuarrie and Jacob, 1991; Senger et al., 2018). CCL involves the application of a proximal nerve crush one week prior to nerve transection and surgical repair, and in this way, the injured neurons are already primed for regeneration by the time that the second injury occurs (Allodi et al., 2012). Unfortunately, CCL is not clinically applicable due to the invasive nature of applying an intentional nerve crush on patients; therefore, CCL remains useful in research to study enhanced regeneration and as a positive control, but alternative strategies to enhance nerve regeneration without such an invasive nature remain necessary and sought after. On the other

hand, in instances of deliberate surgical repair that require a transection as part of the procedure, CCL (and CES below) might improve surgical outcome.

The mechanisms associated with CCL include upregulation of regeneration-promoting pathways, RAGs, and inflammation. Like PES, the cAMP pathway is upregulated following conditioning, ultimately leading to increases in RAGs, such as GAP-43 and activating transcription factor 3 (ATF3) (Senger et al., 2018). Attempts to produce the conditioning effect without causing prior injury infused the cAMP analogue, dibutyryl cAMP, were promising as they increased neurite length *in vitro* and overcame MAG inhibition (Cai et al., 1999; Blesch et al., 2012). Furthermore, upregulation of the cAMP pathway via constitutive CREB activation produces similar pro-regenerative effects (Gao et al., 2004). However, solely increasing the cAMP pathway ultimately did not accelerate the rate of nerve growth, demonstrating that this approach, at least alone, would not be beneficial in patients (Cai et al., 1999; Blesch et al., 2012). In summary, CCL upregulates the cAMP pathway which, alongside the activation of other growth-supporting factors, produces the conditioning effect and results in more robust growth after subsequent injury.

Other pathways altered by CCL include the PI3K/AKT and the Janus Kinase and Signal Transducer and activator of transcription 3 (JAK/STAT3) pathway. Conditioning produces an increase in cytokines such as CNTF and LIF from adjacent Schwann cells or infiltrating macrophages which bind to the gp130 receptor on injured neurons causing JAK phosphorylation (Wu et al., 2007; Cafferty et al., 2001). JAK then activates STAT3 to dissociate from the receptor and translocate to the nucleus where it upregulates RAG transcription (Liu and Snider, 2001; Qui et al., 2005; Senger et al., 2018). Blocking this pathway via JAK2 inhibition by pharmacological inhibition decreases neurite outgrowth, STAT3 phosphorylation, spinal axon

regeneration, and GAP-43 upregulation (Qui et al., 2005). Importantly, the cAMP and JAK/STAT3 pathways are linked as ligands of the JAK/STAT3 pathway such as CNTF and LIF are also products of the cAMP pathway (Cao et al., 2006; Wu et al., 2007; Senger et al., 2018). As a result, both the JAK/STAT3 and cAMP pathways are highly upregulated to produce enhanced growth following CCL, but these pathways do not display enhanced regeneration when inherently upregulated together due to the cross-over between them (Wu et al., 2007; Hannila and Filbin, 2008; Senger et al., 2018).

RAGs associated with the conditioning effect, such as GAP-43, BDNF, and ATF3, are induced downstream of cAMP elevation and display JAK/STAT3 interactions. GAP-43 is highly expressed in the developing nervous system and following injury, in both the cell bodies and found at the distal growth cones of regenerating axons (Meiri et al., 1986; Skene and Willard, 1981; Jacobson et al., 1986). Deficiencies in GAP-43 are associated with deficits in pathway finding and neurite extension, whereas GAP-43 overexpression is associated with increased axonal sprouting and growth (Fu and Gordon, 1997). However, GAP-43 is not solely responsible for nerve outgrowth as its removal does not inhibit CCL-induced axon regeneration; therefore, it is defined as a non-essential regeneration marker correlating with nerve outgrowth. GAP-43 is hypothesized to interact with F-actin at the growth cone following phosphorylation by protein kinase C (Meiri et al., 1986; Zochodne, 2008). Similarly, BDNF is a neurotrophic factor synthesized by nonneuronal cells following injury with well-established roles in survival and growth (Fu and Gordon, 1997; Geremia et al., 2010; Duraikannu et al., 2019). In addition to its role in PES, BDNF is strongly upregulated in DRG neurons following conditioning. Blocking the increase of endogenous BDNF following conditioning is associated with poor axon outgrowth, remyelination, and reduced GAP-43 expression (Song et al., 2008; Geremia et al.,

2010). Conversely, exogenous BDNF treatment produces increased regeneration of sensory axons and improvement of motor functions (Song et al., 2008). However, exogenous BDNF treatment potential is limited by the fact that it is also associated with hyperalgesia and allodynia, highlighting its role in chronic pain (Duraikannu et al., 2019). ATF3 is a transcription factor that is upregulated following nerve injuries and conditioning lesions, which lead to its grouping as a RAG (Seijffers et al., 2006; Seijffers et al., 2007; Patodia and Raivich, 2012; Senger et al., 2018). However, it is better used as a marker for injury in conditioning paradigms rather than a RAG, even though ATF3 overexpression has been found to increase neurite outgrowth (Seijffers et al., 2006). One reason is that solely upregulating ATF3 is not enough to overcome MAG inhibition, as well as the fact that these effects are more likely mediated by interactions with other pro-regenerative factors including CREB and STAT3, and ATF3 is not induced following electrical stimulation or other pro-regenerative paradigms (Seijffers et al., 2007; Senger et al., 2018; Tsujino et al., 2000; Geremia et al., 2007). Altogether, the conditioning effect associated with CCL strongly upregulates RAGs downstream of pathway activation to produce enhanced growth.

The CCL conditioning effect also relies on a robust inflammatory response to produce pro-regenerative effects. The upregulation of inflammation via *Corynebacterium parvum* DRG injection prior to a second lesion produces pro-regenerative effects similar to conditioning including increased regeneration, and upregulation of Schwann cell and satellite glial cell proliferation (Lu and Richardson, 1991). Similarly, the overexpression of the chemotactic ligand CCL2 results in increased axon regeneration. (Kwon et al., 2015; Niemi et al., 2013; Niemi et al., 2016). Conversely, depletion of macrophages through clodronate liposomes, drug delivery vehicles containing dichloromethylene diphosphonate, results in a lack of regenerative capacity

following conditioning sciatic nerve injury (van Rooijen and van Nieuwmegen, 1984; Salegio et al., 2011). A reduction in macrophage infiltration in CCR2^{-/-} mice or CCL2^{-/-} mice similarly abolishes the conditioning lesion effect (Niemi et al., 2013; Kwon et al., 2015). Overall, CCL relies on inflammation produced by macrophage infiltration to produce pro-regenerative effects.

1.6.3 Upregulating Pro-Regenerative Pathways

In addition to the previously mentioned pathways that promote RAG upregulation and have been targeted as potential therapeutic molecules, there are many other avenues in peripheral regeneration that have been identified similarly, notably the PI3K pathway and neurotrophins. Within the PI3K pathway there are many candidates that could be manipulated to improve peripheral nerve growth. For example, inhibition of PTEN would increase activity of the PI3K pathway with subsequent growth promoting effects (Ohtake et al., 2015). This increase in growth was demonstrated following both in DRG *in vitro* and *in vivo* studies where PTEN pharmacological inhibition by dipotassium bisperoxo(pyridine-2-carboxyl) oxovanadate or using siRNA was associated with increased neurite extension, and axonal outgrowth (Christie et al., 2010). In addition to BDNF, other members of the neurotrophin family with growth promoting effects include NGF, neurotrophin 3 (NT-3) and neurotrophin 4/5 (NT-4/5). NGF has traditional roles in survival and differentiation during development and injury (Levi-Montalcini, 1987; Rich et al., 1987; Horie et al., 1991; Duraikannu et al., 2019). However, the effect of NGF varies by receptor activation. When solely p75, the low affinity pan-neurotrophin receptor, is activated, NGF causes neuronal apoptosis which would be detrimental to growth (Duraikannu et al., 2019). Typically following nerve injury, there is an upregulation of both NGF and the TrkA receptor, causing neurotrophic effects and protecting from apoptosis (Rich et al., 1987; Verge et al., 1989). Exogenous NGF treatment is associated with increased neurite outgrowth, myelination, and

conduction velocity (Horie et al., 1991; Chen and Wang, 1995). Similarly, NT-3 increases neurite outgrowth and promotes survival following peripheral nerve injury by actions mediated through its TrkC receptor (Rosenthal et al., 1990; Verge et al., 1996). Likewise, NT-4/5 increases axonal regeneration, myelination, and functional recovery (Friedman et al., 1995; Yin et al., 2001; Duraikannu et al., 2019). Overall, agents that promote the PI3K pathway or neurotrophin release have growth-promoting effects on peripheral nerve regeneration and present potential therapeutic targets.

1.6.4 Conditioning Electrical Stimulation

CES is another conditioning paradigm that upregulates RAGs, accelerates nerve regeneration and promotes functional recovery to the same extent as CCL (Senger et al., 2018, 2019, 2020). Prior to our laboratory's *in vivo* work, the Fouad laboratory demonstrated that in culture, CES for one hour to an intact sciatic nerve prior to *in vitro* assays 1 or 7 days later enhances neurite outgrowth 4 times that of control which is similar to the maximum pro-regenerative effects from CCL (Udina et al., 2008). Following this study, *in vivo* work demonstrated CES to the tibial or common peroneal nerve for 60 minutes at 20Hz one week prior to nerve transection enhances RAG expression, accelerates sensory and motor nerve regeneration and reinnervation, and promotes functional recovery similar to the gold-standard CCL (Senger et al., 2018, 2019). The electrical stimulation paradigms for CES are identical to the clinically safe PES paradigm (Senger et al., 2019). PES is applied following nerve repair surgery whereas in animal studies CES is applied one week prior to the nerve repair surgery (Senger et al., 2019; Senger et al., 2020). Important for clinical translation, gross observation of the conditioning site after CES indicates an absence of an inflammatory response and lack of macrophage infiltration (Senger et al., 2020). Part of the mechanistic effect of CES is the upregulation of RAGs

including BDNF, pCREB, GAP-43, and glial fibrillary acidic protein (GFAP) (Senger et al., 2018; 2019; 2020). These RAGs are also upregulated through the conditioning effect associated with CCL, indicating that these two methods to increase nerve regeneration may act through similar mechanisms; however, the absence of an overt inflammatory response of nerve swelling in CES suggests convergent pathways where the ultimate result is that both CCL and CES upregulate RAGs. To elucidate the mechanism associated with CES, the absence of an inflammatory response and possible key players in producing the enhanced regeneration must be thoroughly investigated. Ultimately, CES is a clinically feasible method to accelerate regeneration, unlike CCL, if confirmed at a cellular level to be non-injurious and non-inflammatory.

1.7 Thesis Statement and Aims

Hypothesis: CES and CCL both promote nerve regeneration through convergent RAG actions; however, CES, unlike CCL, initiates this process independently of the inflammatory response.

Aim 1: Determine if CES upregulates RAGs and increases nerve regeneration in a mouse model.

Aim 2: Determine the immune profile and role of macrophages following CES and CCL.

Aim 3: Investigate the role of AlphaB-Crystallin, as a keynote inflammatory mediator, in the pro-regenerative effects of CES and CCL using a transgenic mouse model (α BC^{-/-}).

CHAPTER 2: Investigation of conditioning electrical stimulation as a strategy to promote peripheral nerve regeneration in a wildtype mouse model

2.1 Introduction

To date, the research on conditioning electrical stimulation (CES) solely as a conditioning paradigm has been applied *in vivo* to Sprague-Dawley rats. Electrical stimulation applied as a conditioning paradigm to Sprague-Dawley rat tissue *in vivo* 3 days prior to culturing showed neurite extension was increased to the same extent as the conditioning crush lesion (CCL) (Udina et al., 2008). In mice, electrical stimulation applied to dorsal root ganglia (DRG) neurons *in vitro* promotes neurite extension and *in vivo*, post-crush electrical stimulation improved regeneration, electrophysiological scores, and behavioral indices (Singh et al., 2009; 2015). The effect of electrical stimulation *in vitro* will likely utilize the same key molecular players for CES (which is performed *in vivo*). Pharmacological inhibitors, agonists, and antagonists applied to DRG neurons *in vitro* at the time of electrical stimulation may help unveil the mechanism of CES *in vivo*. Alternatively, DRG neurons from transgenic mice could be used to determine the effects of CES *in vivo*. Prior to the utilization of transgenic mouse studies, however, CES must first be demonstrated to promote nerve regeneration in wildtype mice in a similar manner to rat (Senger et al., 2018; 2019; 2020). Though electrical stimulation and post-operative electrical stimulation (PES) have been studied in mice, the effect of CES, has not been studied (Singh et al., 2009; 2015). It is likely that, since the PES had identical effects to promote nerve regeneration and functional recovery in both rat and mice, CES will also exert a conditioning effect in both rodent models. It is not uncommon to assume that rat and mouse research should be considered identical; however, there are several differences between these species highlighting the importance of fully evaluating CES in mice before moving to transgenics. A microarray study in hippocampal neurons demonstrated that 4713 genes were differentially expressed from the total 10 833, dramatically contrasted from only 54 genes being

differentially expressed in two different mouse strains (Francis et al., 2014). Furthermore, rat and mouse have been shown to display different neurotransmitter distributions, particularly in the case of serotonin, as well as various other neurotransmitters and hormones (Ellenbroek and Youn, 2016). Due to the evident species differences of rat and mouse, it is essential to evaluate the effectiveness of CES to promote nerve regeneration in wildtype mice. Transspecies effectiveness of CES may support the likelihood of clinical CES translation to promote human nerve regeneration. Traditionally, the use of solely rat animal data to support human clinical trials has not been reliable and transspecies studies may limit any species-specific variables that could confound data (Kaplan et al., 2015). Furthermore, there is an abundance of rat data in the peripheral nerve field; therefore, using mice could also provide a fuller understanding of nerve regeneration as a whole (Kaplan et al., 2015; Vela et al., 2020).

The use of transgenic mice allows for molecular manipulations to investigate the mechanism of CES. Research on CCL has demonstrated its effectiveness in upregulating regeneration associated genes (RAGs) and increasing the rate of nerve regeneration both in Sprague-Dawley rats and in wildtype or genetically modified mouse strains; therefore, CCL will be used as a positive control for conditioning, whereas naïve mice that do not undergo conditioning will serve as negative controls (Neumann and Woolf, 1999; Gardiner et al., 2007; Navarro and Kennedy, 1990; Tanaka et al., 1992). In summary, evaluating the effectiveness of CES in wildtype mice to accelerate nerve regeneration will allow us to begin investigating the mechanism of CES through molecular manipulation, first through transgenic mouse models.

2.2 Methods

Animals: Adult 129S6/SvEvTac (wildtype) mice were obtained from Taconic Biosciences (New York, USA) (and housed with the Health Sciences Laboratory Animal Services (HSLAS) (AUP 00003034) at the University of Alberta (Simpson et al., 1997). The mice were housed in flat-bottomed betachip-lined cages with ad libitum standard mice chow and water. Lighting was cycled with 12h on/off rotations.

Surgical Procedures: The University of Alberta Animal Research Ethics Board approved all experimental procedures (AUP 00003034). Cohorts consisted of CCL (positive control for DRG RAG upregulation and accelerated nerve regeneration), CES (experimental group), and unconditioned/naive animals (negative control to demonstrate there is no DRG RAG upregulation or accelerated nerve regeneration). Eighteen animals were used for nerve regeneration (n=6/cohort) and 24 animals were used for RAG analysis (n=4/cohort). All surgical procedures were adapted from the Webber laboratory's previous experimental procedures on Sprague Dawley rats (Senger et al., 2019). Surgeries were performed in a dedicated animal surgery facility at the University of Alberta.

Conditioning: Animals were given analgesics by subcutaneous buprenorphine injection (0.05 mg/Kg/animal) and anesthetized by oral isoflurane (2%, titrated at 1-2L/min). A 2 cm incision was made at the mid-thigh and the sciatic nerve was isolated via blunt dissection proximal to the trifurcation point. CES animals received 20Hz electrical stimulation at 0.1 ms duration for 60 minutes to the sciatic nerve using an SD-9 stimulator (Grass Instruments, Quincy, MA). CCL animals received a sciatic crush injury with a non-toothed fine hemostat for 10 s. Unconditioned

(naïve) animals did not receive conditioning or surgical intervention. Sham electrical stimulation was not used as previous studies indicated no difference between unconditioned and sham animals (Senger et al., 2018; Senger et al., 2019). The skin was closed using 5-0 vicryl sutures (Ethicon, USA, Somerville, NJ). Seven days following, all 18 animals per cohort underwent nerve transection and repair by Dr Jenna-Lynn Senger. These animals received 0.05 mg/Kg buprenorphine analgesic and isoflurane anesthesia (2%, titrated at 1-2 L/min). The sciatic nerve was exposed, transected distally to the conditioning site (for CES and CCL groups), and subsequently repaired using 10-0 ethilon sutures supplemented with Evicel fibrinogen gel (Ethicon, USA). The skin was closed with 5-0 vicryl sutures. 4 animals per cohort were harvested at day 1 and day 3 to measure RAG expression and macrophage accumulation at both the nerve and DRG.

Tissue Collection: Eighteen animals were harvested for nerve regeneration studies and twenty-four animals were harvested for RAG analysis: twelve at 1 day post-conditioning and twelve at 3 days post-conditioning. Animals were euthanized via deep isoflurane inhalation followed by cardiac puncture. At 1 and 3 days following conditioning, the ipsilateral L4 and L5 DRGs were harvested and placed in 4% paraformaldehyde (PFA) (American MasterTech Scientific, Lodi, CA) overnight at 4°C. Seven days following transection and repair (day 14 post conditioning), the injury site and distally at the sciatic nerve was harvested, stabilized against a toothpick, and placed in 4% PFA overnight at 4°C. The following day, harvested tissue was rinsed in 30% sucrose in phosphate-buffered saline (PBS) (Thermo Fisher Scientific, Waltham, MA) before postfixation in 30% sucrose for 48 hours at 4°C. Tissue was then frozen in Optimal Cutting Temperature medium (OCT; Tissue-Tek) (Sakura Finetek, Torrance CA) by indirect exposure to

liquid nitrogen and stored in -80°C until cryosectioning (Leica) at $9\ \mu\text{m}$. The nerve and DRG sections were thaw-mounted on Superfrost Plus microscope slides (Thermo Fisher Scientific) and stored at -80°C .

Immunohistochemistry: Specific antibody procedures and concentrations are listed below (Figure 2.5.1). Slides were warmed to room temperature before undergoing three washes for five minutes in 0.01 M phosphate-buffered saline (PBS) (Thermo Fisher Scientific) followed by permeabilization with 0.1% Triton-100 x (Thermo Fisher Scientific) for five minutes. Slides were blocked in 10% normal goat serum (MP Biomedicals, Santa Ana, CA) with 3% bovine serum albumin (Sigma-Aldrich, St Louis, MO) in 0.01M PBS for 90 minutes. Primary antibodies included BDNF, GAP-43, ATF3, pCREB, and NF200 and were applied overnight at 4°C in a solution of 3% BSA and 0.01M PBS. The following day, slides were washed two times in 0.05% Tween in PBS followed by two washes for five minutes in PBS. Secondary antibodies were applied for 60 minutes at room temperature in a solution of 3% BSA and 0.01M PBS. The nuclei were stained with DAPI (NucBlue) (Thermo Fisher Scientific) which was applied to DRG sections in PBS for five minutes before a final PBS rinse was applied to slides. Slides were sealed with aquapoly mount (Polysciences) and stored at -20°C .

Imaging: All digital images taken were processed in a parallel manner with identical fluorescent exposures using either a 20X (DRG analysis) or 10X (nerve regeneration analysis) objective with a Zeiss Axio Imager fluorescence microscope. Two representative DRG sections were analyzed for each animal using Image J software. BDNF and GAP-43 were analyzed through cytosolic pixel intensity (a.u.), whereas ATF3 and pCREB were analyzed through binary evaluation

(positive or negative nuclei). For length of nerve regeneration, each image required the processing of two nerve sections for each animal followed by serial capture of each image and post-production ‘stamping’ of the image to display the extent of nerve regeneration past the injury site. A minimum of 10 axons were required for length of regeneration, and axons were counted every 500 μm 's.

Statistical Analysis: Experimental results are written as the mean \pm standard error mean (*s.e.m*). Significance of RAG analysis and length of regeneration was determined using a one-way analysis of variance (ANOVA) to determine any differences in the mean between groups followed by a post-hoc Dunnett's test to compare experimental groups against unconditioned animals. A level of $p < 0.05$ was the cut-off for statistical significance. To determine statistical significance between axon counts, a two-way ANOVA was completed to determine differences between the mean of each group in a paired data set followed by Dunnett's post-hoc for comparison against unconditioned animals. Statistics were completed using Prism 9.3.1 (GraphPad Software, San Diego, CA).

2.3 Results

2.3.1 CES and CCL upregulate DRG RAGs following nerve repair surgery.

The sciatic nerve of 129S6/SvEvTac (WT) mice were conditioned by CES, CCL, or remained unconditioned (n=4/cohort). Three days post-conditioning, the animals were euthanized and their L4 and L5 DRGs were harvested and processed for tissue sectioning (9 μ m) and brain-derived neurotrophic factor (BDNF), growth-associated protein 43 (GAP-43) and phosphorylated-cyclic adenosine monophosphate (cAMP) response element binding protein (pCREB) RAG immunohistochemistry. Using identical methods in rat studies, these RAGs were upregulated following both CES and CCL compared to unconditioned (naïve) DRGs (Senger et al., 2018, 2019, 2020). Immunohistochemistry demonstrated increased cytosolic expression of BDNF following CCL (91.8 a.u. \pm 6.2 a.u.; $p < 0.01$) compared to unconditioned animals (65.2 a.u. \pm 6.5 a.u.). CES BDNF was not significantly upregulated compared to naïve (73.0 a.u. \pm 2.7 a.u.; $p > 0.05$) and (Figure 2.5.2). The cytosolic immunofluorescence of GAP-43 was significantly upregulated in CES (79.8 a.u. \pm 3.0 a.u.; $p < 0.05$) and CCL (88.5 a.u. \pm 3.7 a.u.; $p < 0.01$) compared to the baseline expression of GAP-43 in the unconditioned animals (68.2 a.u. \pm 0.8 a.u.). Furthermore, CES and CCL showed a significant increase in nuclear pCREB immunofluorescence (24.1% \pm 0.9%, $p < 0.05$; 28.6% \pm 3.0%, $p < 0.01$ respectively) compared to unconditioned control animals (10.1% \pm 4.5%) (Figure 2.5.2).

2.3.2 CES and CCL promote nerve regeneration in mice, similar to Sprague-Dawley rats.

The extent of regeneration was determined by analyzing nerves seven days following a sciatic nerve repair surgery in which the animals were previously conditioned by CES, CCL or unconditioned controls (n=6/cohort). As regenerating and degenerating axons have differing

morphology, neurofilament 200 (NF200) labelling allowed for quantification of the number of regenerating axons past the cut/coaptation site (Figure 2.5.3). Both CES and CCL had significantly increased mean numbers of axons extending past the site of coaptation with maximums reaching 66.6 ± 2.5 axons and 65.6 ± 5.9 axons, respectively, compared to unconditioned animals with 34.2 ± 3.7 axons. This pattern of significantly more regenerating axons at every 0.5 mm intervals distal to the coaptation site continued throughout the regenerating length (at least $p < 0.05$). Further, both CES and CCL groups attained significantly greater distances of regeneration. The maximum length of regeneration following CES was $5.4 \text{ mm} \pm 0.2 \text{ mm}$ ($p < 0.05$) and CCL was $5.6 \text{ mm} \pm 0.6 \text{ mm}$ ($p < 0.05$), whereas unconditioned animals only reached $3.1 \text{ mm} \pm 0.7 \text{ mm}$. Together, these data demonstrate that CES increases the extent of regeneration and upregulates RAGs including pCREB and GAP-43 in WT mice, like Sprague-Dawley rats.

2.3.3 CES, unlike CCL, does not upregulate ATF3, display overt inflammation, or cause Wallerian Degeneration compared to unconditioned controls.

Activating transcription factor 3 (ATF3) is an early injury marker that upregulates in DRG nuclei following nerve injury and our rat studies showed that ATF3 was increased in DRG nuclei 24 hours following CCL but not CES, suggesting that CES does not cause axonal injury (Senger et al., 2020). A new cohort ($n=4/\text{cohort}$) of wildtype animals underwent CES, CCL, or remained unconditioned, and their L4, L5 DRGs were harvested the following day. The neuronal nuclei of animals conditioned with CCL displayed upregulated expression of the injury marker ATF3 ($41.7\% \pm 6.2\%$, $p < 0.001$), while the DRG nuclei of CES ($3.5\% \pm 1.9\%$; $p > 0.05$) and

unconditioned ($0.09\% \pm 0.09\%$) animals did not, indicating CES does not cause axonal injury response in mice (Figure 2.5.4).

Gross observation of the conditioning site (asterisk) at 7 days post-CES, CCL, was compared to naïve nerve and it was observed that the sciatic nerve was swollen following CCL, but not CES (Figure 2.5.5). Immunohistochemistry against NF200 was performed to assess axonal morphology and indicated that axons underwent Wallerian degeneration past the CCL conditioning site. The axons were intact distal to the site of CES, similar to naïve nerves, suggesting the CES axons did not undergo Wallerian Degeneration (Figure 2.5.5). We assessed immune cell proliferation or infiltration at the conditioning site using IBA-1 immunohistochemistry which labels both tissue resident and infiltrating macrophages. There was an obvious increase in macrophage presence following CCL, compared to CES and naïve mice (Figure 2.5.5).

2.4 Discussion

Our data demonstrates that, similar to our Sprague-Dawley rat studies (Senger et al., 2018, 2019, 2020), CES upregulates RAGs and accelerates nerve regeneration in WT mice. The RAGs GAP-43, and pCREB were upregulated at three days following conditioning, indicating the presence of a regenerative environment at the DRG. Compared to naïve rat data, BDNF levels in the mouse had higher innate expression. We predict this increase in baseline BDNF expression in our WT mice could be attributed to either the stress that animals might have had during transport to the surgery suite or the relatively low number of animals (n=4) used in this study. We believe that an increase in the number of animals, it is likely both CES and CCL would show significantly higher BDNF expression compared to naive mice.

Similar to Sprague-Dawley rats, CES and CCL allowed for an increased number of axons to regenerate past the cut/coaptation site, as well as an increased lengths of regeneration compared to unconditioned animals (Senger et al., 2018). Overall, the upregulation of RAGs and increased extent of regeneration indicates that CES promotes a pro-regenerative response in wildtype mice. These data are supported by in vitro studies that demonstrated an increase in neurite extension and RAG expression following electrical stimulation (Singh et al., 2009, 2015). Similar to our rat studies, the injury marker, ATF3 was significantly upregulated in the nuclei of the CCL DRGs, compared to both CES and unconditioned animals. These data add support to our hypothesis that unlike CCL, CES is non-injurious.

This data supports the published data in Sprague-Dawley rats, showing that CES and CCL upregulate similar RAG expression, highlighting a convergence of their pathways (Senger et al., 2018, 2019, 2020). Further, the absence of Wallerian degeneration and macrophage

presence in CES nerve and the lack of ATF3 activation in their neuronal nuclei further supports that this modality is non-injurious as it does not evoke nerve degeneration or evoke an immune cell response. This chapter did not discern between tissue resident or blood born macrophages at the nerve or the DRG. There is a possibility that while CES did not demonstrate an obvious increase in the number of macrophages at the conditioning site, the tissue-resident macrophages (TRMs) could have been activated. Exploration into the relative contributions of TRMs to the conditioning effect associated with CCL is also unknown.

Overall, this data supports that CES is translatable from Sprague-Dawley rats to mice and therefore transgenic mice can be used to try to determine the mechanism through which CES evokes its conditioning effects.

2. 5 Figures

Primary Antibody	Antigen Retrieval 40 minutes in 60 °C citrate buffer (10mM sodium citrate, 0.05% Tween-20, pH 6.0)	Primary Antibody Dilution	Secondary Antibody	Secondary Antibody Dilution
ATF3 (rabbit) Abcam 207434	Yes	1:500	AlexaFluor 488 goat anti-rabbit Invitrogen, Carlsbad, CA A-11008	1:1000
pCREB (rabbit) Cell Signalling 9198	Yes	1:500	AlexaFluor 488 goat anti-rabbit	1:1000
NF200 (rabbit) Sigma-Alrich N4142	No	1:500	AlexaFluor 488 goat anti-rabbit	1:500
GAP-43 (rabbit) Novus Biochemicals Centennial, CO NB300-143	No	1:500	Alexa Fluor 488 goat anti-rabbit	1:1000
BDNF (rabbit) Abcam Cambridge, UK Ab108319	Yes	1:200	AlexaFluor 488 goat anti-rabbit	1:1000

Figure 2.5.1 Primary and Secondary Antibodies used for Immunohistochemistry

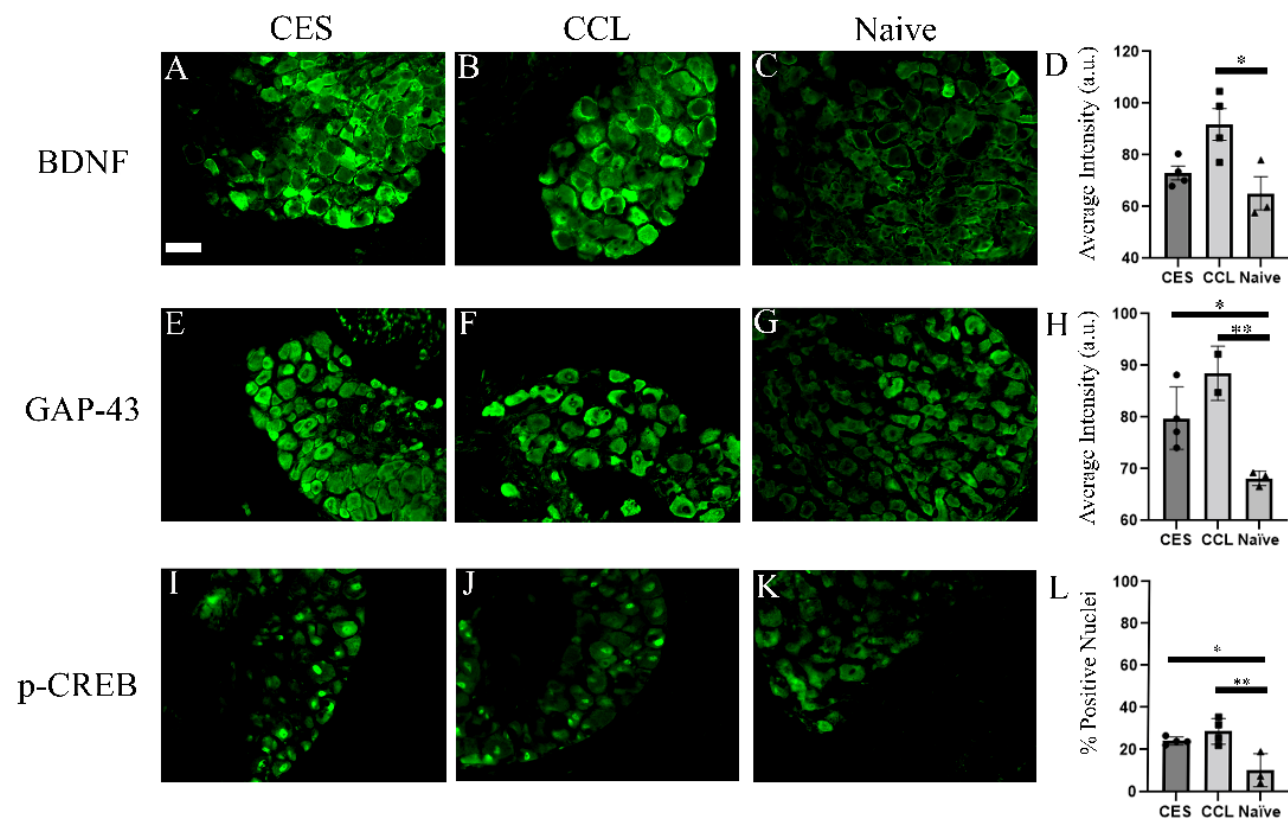


Figure 2.5.2: CES and CCL upregulate similar RAGs in wildtype mice.

A) The average intensity of BDNF immunofluorescence in arbitrary units 3 days following B) CES (n=4), C) CCL (n=4), or D) no-conditioning (n=4). E) The average intensity of GAP-43 immunofluorescence in arbitrary units 3 days following F) CES (n=4), G) CCL (n=4), or H) no-conditioning (n=4). I) The immunohistochemical expression of p-CREB 3-days following J) CES (n=4) K) CCL (n=4) or L) no-conditioning (n=4). The scale bar in B indicates a distance of 100 μm . CCL had significant increases in the expression of RAGs including BDNF, GAP-43, and pCREB ($*p < 0.05$; $**p < 0.01$). CES had significant increases in RAG expression of GAP-43 and pCREB ($*p < 0.05$), and an increase in BDNF, though not statistically significant.

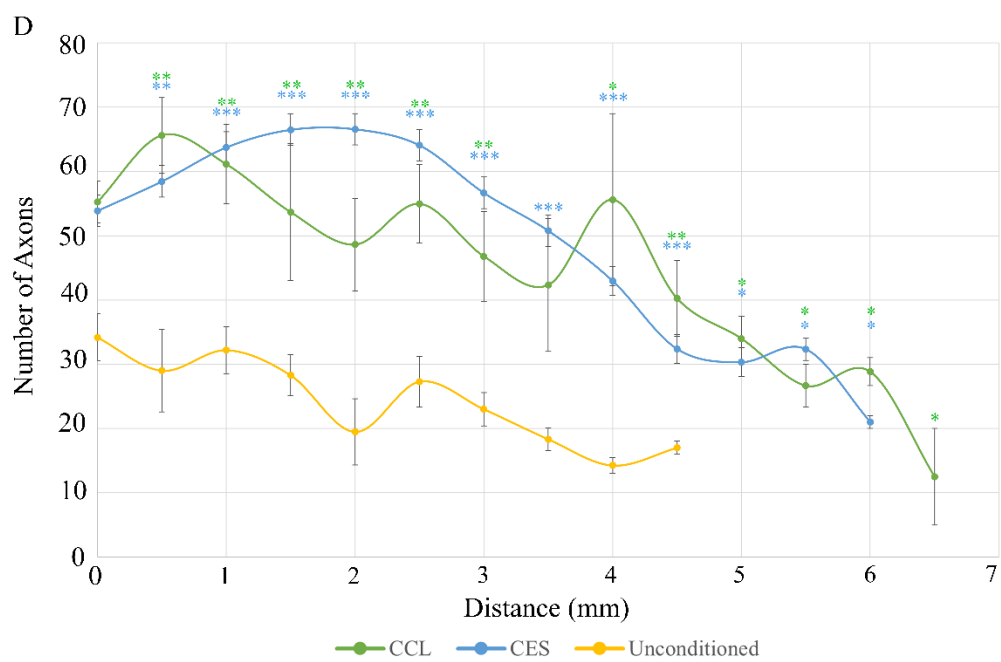
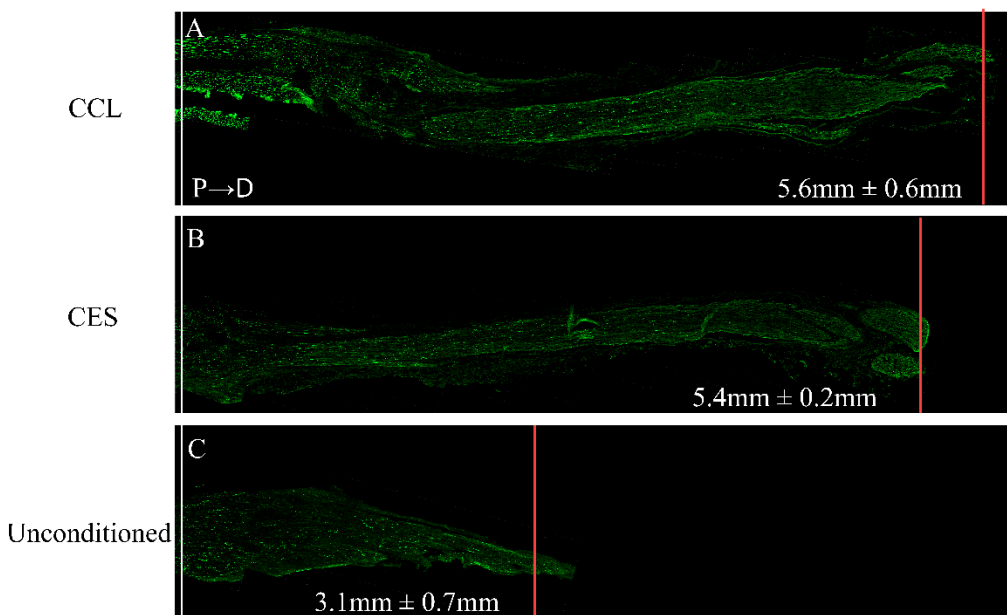


Figure 2.5.3: CES and CCL accelerate nerve regeneration in wildtype mice following surgical transection and repair compared to unconditioned animals.

NF200 immunofluorescence of the sciatic nerve at 7 days following surgical transection and repair of animals who had received either A) CCL (n=6) B) CES (n=6) or C) no-conditioning (n=6). The scale bar in C measures 500 μm A-C) White line indicates the site of surgery repair and is the location from which regeneration is measured. Red line indicates the distance at which < 10 axons were counted. D: Extent of nerve regeneration from the surgery repair site is quantified by the number of axons (y-axis) and distance in micrometers (x-axis) every 500 μm distal to the site of coaptation. Statistical significance at each 500 μm length where the number of axon counts of CES or CCL animals were different than the rate of regeneration of the unconditioned axons is indicated on the graph (* $p < 0.05$, ** $p < 0.01$, *** $p < 0.001$).

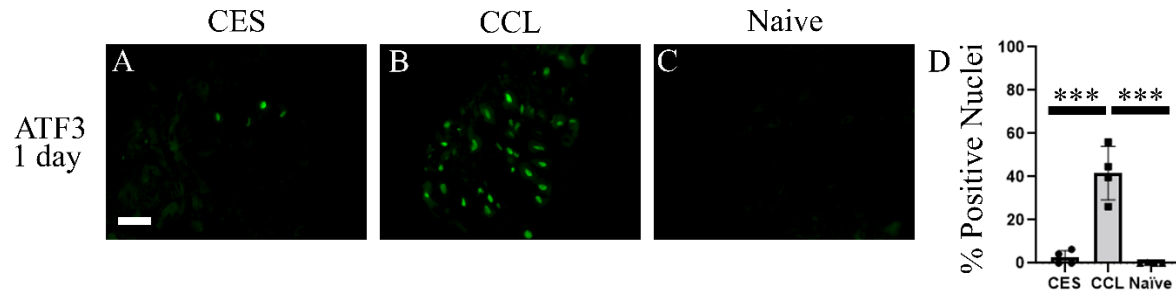


Figure 2.5.4: CES does not upregulate the injury marker, ATF3.

A) The immunohistochemical expression of ATF3 at the L4 and L5 DRGs 1 day following A) CES (n=4) B) CCL (n=4) or C) no-conditioning (n=4). The scale bar in A indicates a distance of 100 μm . D) The percentage of ATF3 positive neuronal nuclei. CCL had a significant increase in the injury marker, ATF3 (** $p < 0.001$).

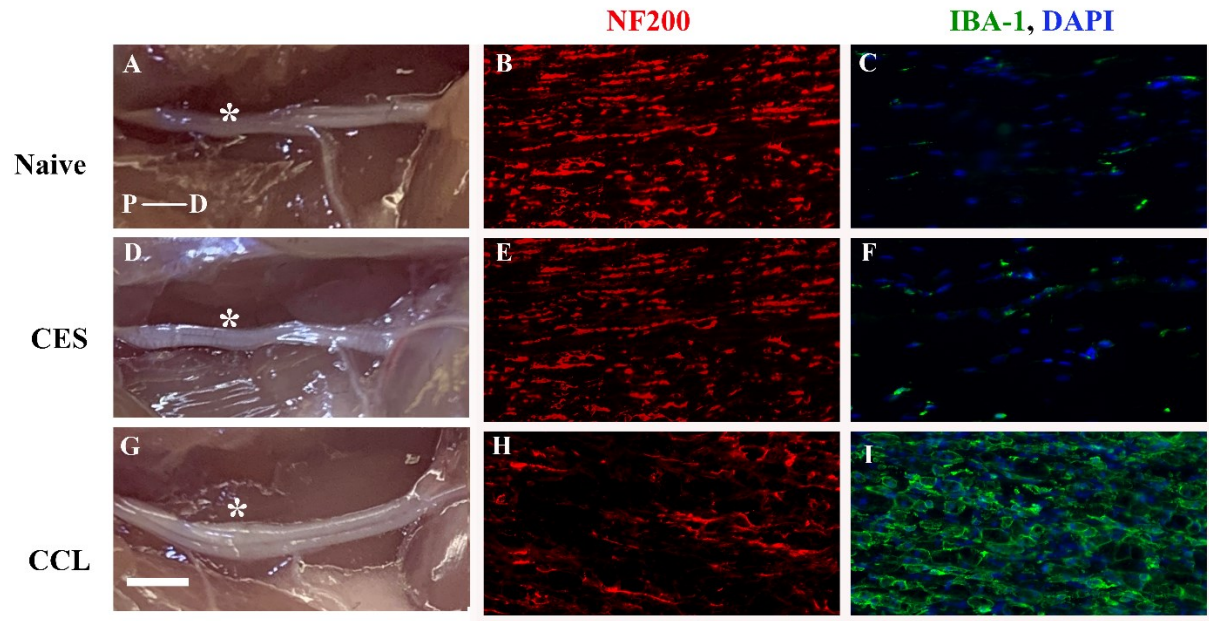


Figure 2.5.5 CES does not display overt inflammation, Wallerian degeneration, or macrophage upregulation.

A,D,G) Gross appearance of unconditioned (A), CES (D) or CCL (G) nerves confirms swelling in the CCL but not CES or naïve nerves 5 days post-conditioning. Conditioning site in D, G is shown by asterisks. B, E, H) NF200 immunofluorescence shows healthy axons in naïve (B) and CES (E) but Wallerian degeneration following CCL (H). C, F, I) IBA-1 labels tissue resident and monocyte-derived macrophages. Naïve nerve (C) and CES (F) has little macrophage presence unlike CCL (I) which demonstrates a large number of macrophages. Nuclear staining with DAPI confirms the increase in cells at the nerve conditioned with CCL (I) compared to CES (F) or naïve nerve (C). Scale bar in G is 100 μm .

CHAPTER 3: The immune profile and role of macrophages following CES and CCL

3.1 Introduction

3.1.1 Inflammatory responses in the peripheral nerve

Macrophages are largely responsible for the inflammatory response that is initiated following peripheral nerve injury. The pro-regenerative effect of a conditioning lesion benefits from the inflammation produced by monocyte-derived macrophages as they clear the injury site of axonal, myelin, and other cellular debris which produces an environment conducive to axonal regrowth (Lu and Richardson, 1991; Dahlin, 1992; Senger et al., 2018). The infiltration of monocytes to the site of injury occurs following the production of inflammatory cytokines, such as class C chemokine ligand 2 (CCL2), by injured Schwann cells and neurons (Tanaka et al., 2004; Kwon et al., 2015; Zhang and De Koninck, 2006). The binding of CCL2 to the class C chemokine receptor 2 (CCR2) receptor expressed on the plasma membrane of these circulatory monocytes binds CCR2 after their infiltration and initiates the participation of monocyte-derived macrophages in Wallerian Degeneration (Perrin et al., 2005). Once activated in the injured nerve, macrophages participate in the phagocytosis of debris necessary to clear the injury site, allowing axons to regenerate through to their distal targets (Dahlin, 1992; Senger et al., 2018).

Overexpression of CCL2 enhances neurite regeneration in vitro similar to the conditioning crush lesion (CCL), and CCR2^{-/-} mice display deficient regeneration even following CCL conditioning (Niemi et al., 2013; 2016; Kwon et al., 2015). CCR2^{-/-} mice do not continue to exert their conditioning effect following nerve crush injury, while Wallerian degeneration is intact due to compensation from neutrophils (Niemi et al., 2013, 2016). Neutrophil ablation in CCR2^{-/-} mice allows Wallerian degeneration to occur, indicating redundancy in these mice, while the conditioning effect of CCL relies on macrophages. It is not known if CCR2 macrophages are involved in CES-induced conditioning.

3.1.2 Tissue-resident macrophages (TRMs) and monocyte-derived macrophages are found in the PNS

Macrophages can be divided into two separate classes: monocyte-derived macrophages that are derived from bone-marrow monocytes, or TRMs which fate-mapping studies have indicated derive from the yolk sac or fetal liver (Zhao et al., 2018; Hashimoto et al., 2013). TRMs are found in all tissues, including the dorsal root ganglia (DRG) and peripheral nerves. In the peripheral nerve, the role of circulatory monocyte-derived macrophages following injury is well-described, whereas due to the more recent discovery of TRMs and methods to study them, their role following peripheral nerve injury, including conditioning, is unclear. It is accepted that TRMs are responsible for the upregulation of interleukin-13 expression as early as 4 hours post-injury since monocyte-derived macrophages are not yet found in the injured nerve (Ydens et al., 2012; Ydens et al., 2020). Furthermore, TRMs proliferate following nerve injury, contributing to the inflammatory response and phagocytosis of myelin debris (Davies et al., 2013; Mueller et al., 2001). Due to their expression of major histocompatibility complex II (MHC II) molecules and complement receptor 3 (CR3), TRMs are thought to be involved in antigen presenting and surveillance functions during homeostatic conditions (Mueller et al., 2003; Bruck and Friede 1991). Overall, it is accepted that these cells are involved in both homeostatic nerve maintenance and proliferation and phagocytosis during injury, while their potential role in the conditioning effect to promote nerve regeneration is unknown.

3.1.3 Macrophage Ontogeny

The ontogeny of macrophage subtypes is important when discerning between their unique roles. Traditionally, TRMs were thought to originate from bone marrow derived

monocytes (BMDMs) that were replenished as necessary (Fogg et al., 2006; Yona et al., 2013). However, it is now accepted that these TRMs have embryonic origins of either the yolk sac or the fetal liver before they migrate to peripheral tissues including peripheral nerves and the DRG (Yona et al., 2013; Ydens et al., 2020). TRMs maintain themselves locally and are capable of proliferation and self-renewal, in contrast to the previously assumed monocyte-derived replenishment (Ydens et al., 2020; Ginhoux et al., 2010; Ajami et al., 2007). Though TRMs and monocyte-derived macrophages share similarities including phagocytotic function, cytokine release, and tissue repair, they have differing roles as TRMs are already present in the event of injury and help initiate the injury and inflammatory response (Mueller et al., 2001; Mueller et al., 2003; Krishnan et al., 2018; Bautista and Krishnan, 2022). Both monocyte-derived macrophages and TRMs are increasingly demonstrating further subtypes. monocyte-derived macrophages are typically subdivided into $Ly6C^{high}CCR2^{+}$ and the $Ly6C^{low}CX3CR1^{+}$, with $CCR2^{+}$ monocytes having a more evident role in inflammation and $CX3CR1^{+}$ in patrolling endothelium layers (Ydens et al., 2020; Bautista and Krishnan, 2022). Evidence suggests that the function and gene expression of TRMs is highly tailored to the specific tissue and physiological needs of that region (Lavin et al., 2014). For example, TRMs of either the endoneurium or epineurium within the sciatic nerve were found to differentially express genes, and even further, endoneurial macrophages were more associated with immediate-early genes following injury compared to epineurial macrophages, with endoneurial macrophages much more active overall (Ydens et al., 2020). Furthermore, the skeletal system is increasingly being recognized as an additional reservoir for myeloid cells as monocytes and neutrophils have been shown to infiltrate to the central nervous system (CNS) in injury conditions from adjacent bone marrow (Cugurra et al., 2021). In the CNS, the infiltrating monocytes and neutrophils use direct ossified vascular

channels that connect the skull bone marrow to the overlying meninges to gain access to the brain (Herisson et al., 2018; Yao et al., 2018; Cai et al., 2019; Cugurra et al., 2021). Following experimental autoimmune encephalomyelitis (EAE), spinal cord injury, and optic nerve crush injury, Cugurra et al., traced a substantial portion CNS-infiltrating monocytes separately from blood origins, indicating that these cells are not only involved during homeostatic conditions, but also following injury (Cugurra et al., 2021). It could be possible, therefore, that monocytes from the vertebrae could infiltrate into the nearby DRG or nerve post-injury. In summary, macrophages display vast heterogeneity which could impact their activation and function following peripheral nerve injury and conditioning. To our knowledge, the role of TRMs in the nerve regenerating effects of CCL and CES is not known. We hypothesize that CES is non-injurious and non-inflammatory; therefore, both TRMs and monocyte-derived macrophages will not have a significant role in the CES conditioning effect. Alternatively, we hypothesize that CCL promotes both TRM and monocyte-derived macrophage activation to accelerate nerve regeneration.

3.1.4 Genetically modified mouse models to study macrophage populations

Distinguishing TRMs from monocyte-derived macrophages has been difficult due to the fact that they express similar receptors and cytokines. For example, ionized calcium binding adaptor molecule 1 (IBA-1), a pan-macrophage marker, labels both TRMs and monocyte-derived macrophages (Imai et al., 1996; Köhler, 2007). The use of genetically modified mice is necessary to distinguish between the two populations. Tamoxifen inducible timed expression of CX3CR1+ fluorescence using the CreER system can differentiate TRMs from monocyte-derived macrophages depending on the timing of tamoxifen injection (Zhao et al., 2019; Bautista and Krishnan, 2022). Overall, the use of these genetically modified mice is crucial to immune cell

research and will allow the investigation of TRMs separately from monocyte-derived monocytes in the conditioning effect.

Herein we use two transgenic mice, the CX3CR1^{CreER}; Rosa26 mice were used as a tracer for TRMs while the iDTR;CX3CR1 mice were used to ablate CX3CR1 expressing cells, including both TRMs and monocyte-derived macrophages (Buch et al., 2005; Zhao et al., 2019; Plemel et al., 2020). Of note, CX3CR1 is also expressed in microglia and therefore in addition to the effects on macrophages, these mice have fluorescently labeled microglia and ablated microglia, respectively. We did not investigate microglia in our studies as it was outside the scope of these experiments.

Neonatal tamoxifen injection induces CX3CR1^{CreER}; Rosa26 mice to express TdTomato, a red fluorescent marker, in CX3CR1 cells. Infiltrating monocytes expressing TdTomato eventually die, and without a consistent source of tamoxifen, the bone-marrow stem cells replenish these infiltrating monocytes without TdTomato fluorescence. Alternatively, TRMs perform self-renewal and continue to express TdTomato. Thus, a 1-3 day neonatal tamoxifen treatment followed by a 4 week washout results in animals with TRM CX3CR1 TdTomato fluorescence and no labelling of infiltrating monocytes (Plemel et al., 2020).

Alternatively, iDTR;CX3CR1 express the inducible diphtheria toxin receptor (iDTR), not endogenous to mice, downstream of the Rosa26 locus. With tamoxifen injection into adult mice, iDTR is expressed in CX3CR1 cells. One week after tamoxifen, injection of diphtheria toxin 1 day prior to and during the week of conditioning (CCL and conditioning electrical stimulation (CES)) ablates CX3CR1 macrophages. Littermate controls did not express iDTR and were insensitive to diphtheria toxin mediated cellular ablation.

In summary, we aimed to determine the presence and activation of TRMs by utilizing a mouse model in which these macrophages fluoresce (CX3CR1^{CreER}; Rosa26). We then went on to determine if the conditioning effect associated with CES persists in the absence of tissue-resident and monocyte-derived macrophages (iDTR;CX3CR1). These genetic mouse models allowed us to both label TRMs and ablate macrophages to explore their potential role in CES and CCL.

3.2 Methods

Animals: CCR2^{-/-} mice were obtained from the Jackson Laboratory (Bar Harbor, MA, USA) and housed as above (Boring et al., 1997). Animals used for RAG and immune cell analysis at the DRG were culled 1 and 3 days post-conditioning (n=4/cohort).

CX3CR1^{CreER}; Rosa26 mice were obtained from the Plemel Laboratory at the University of Alberta and bred at the Health Sciences Laboratory Animal Services (HSLAS). Tamoxifen dissolved in corn oil (Sigma, T-5648) was injected intraperitoneally once/day for 3 days to each animal at 100mg/kg at 12-15 days post-birth to enable tissue-resident macrophage fluorescence. At 8 weeks of age these mice were used to analyze regeneration associated gene (RAG) expression and macrophage quantification and activation analysis at 1 and 3 days post-CES and CCL conditioning (n=4/cohort).

CX3CR1^{CreER}; Rosa26 mice were crossed with iDTR;Rosa26 mice to produce CX3CR1^{CreER+/-};Rosa^{tdtom+/-};Rosa^{iDTR+/-} mice, abbreviated hereafter as iDTR;CX3CR1 mice (n=4/cohort) from the Plemel laboratory at the University of Alberta. All mice were genotyped by the Plemel laboratory and transferred to the Webber laboratory at 9 weeks old for experimental procedures. Half of the mice had the genotype DTR⁺, tdRFP⁻ and the remaining mice had the genotype DTR⁻, tdRFP⁺. Similar to the CX3CR1^{CreER};Ai9 mice, 100 mg/kg tamoxifen dissolved in corn oil (Sigma, T-5648) was injected intraperitoneally once/day for 3 days into each animal. Five days following tamoxifen injections, 1 µg of diphtheria toxin (Cedarlane; #150) injections were given intraperitoneally 1/day for seven days (10µL of DT in 2000µL of Sterile 1X PBS; 1 µg).

Surgical Procedures: Conditioning and cut/coaptation surgical procedures were completed as described in Chapter 2. CCR2^{-/-} mice underwent CES or CCL conditioning and surgical transection/repair surgeries to the tibial nerve, whereas all other mice underwent sciatic nerve surgeries. The timeline for surgical procedures of the iDTR;CX3CR1 mice was executed as follows: conditioning (Day 1) was completed on the second day of diphtheria injections; surgical transection and repair was completed one week after conditioning (Day 7) and tissue was harvested one week later (Day 14).

Tissue Collection: L4, L5 DRG tissue collection was completed as stated in chapter 2 at days 1 and 3 post-conditioning with the addition of a 2cm nerve segment from the conditioning site being harvested at 3 days post-conditioning for CCR2^{-/-} and CX3CR1^{CreER}; Rosa26 mice. Likewise, tibial and sciatic nerves were harvested at day 14 as stated in chapter two for nerve regeneration studies of CCR2^{-/-} and iDTR;CX3CR1 mice including the harvest of L4, L5 DRG tissue from each animal.

Immunohistochemistry: Immunohistochemistry was completed as stated above for activating transcription factor 3 (ATF3), phosphorylated cyclic adenosine monophosphate (cAMP) response element binding protein (pCREB), and neurofilament 200 (NF200) primary antibodies. For macrophage analysis, DRG and conditioning site slides with 3 day post-conditioning tissue were warmed to room temperature before washing with 1X phosphate-buffered saline (PBS) for 10 minutes. Slides were then blocked in 10% Normal Donkey Serum, 0.1% fish stain gelatin, 0.1% TritonX100, and 0.05% Tween-20 in 0.01M PBS for 45 minutes. The primary antibodies included IBA-1, and Dectin-1 and were applied in 0.01M PBS, 0.1% fish stain gelatin, and 0.5%

Triton X-100 overnight at 4°C. The following day, slides were washed 7 times for 6 minutes each in PBS before application of the secondary antibodies in 0.01M PBS, 0.1% fish stain gelatin, and 0.5% Triton X-100 at room temperature for 1 hour. Slides were then rinsed 7 times for 6 minutes before DAPI application for five minutes. Slides were mounted with aqua-poly mount. Specific procedures are listed in Figure 3.5.1.

Polymerase Chain Reaction (PCR) Genotyping: Splenic tissue from each animal (approximately 10 mg) was processed using DNeasy Blood and Tissue Handbook Protocol with a Qiagen Kit. Briefly, spleen tissue was digested in proteinase K overnight at 56 °C in a water bath. The next day, using spin column technology the genomic DNA was isolated and measured using a NanoDrop Microvolume Spectrophotometer. The following day, PCR genotyping was performing using touchdown cycling according to protocol for CCR2^{-/-} mice from the Jackson Laboratory. On ice, DNA master mix was made from 10x PCR buffer, 50mM Mg, 25mM dNTPs, 10µM Common F, 10 µM Wt R, 10 µM Ko R, 0.1 µL Platinum Taq and 1.95 µL water. DNA (150ng) was added to the master mix in each sample, alongside a negative control (master mix and water), before undergoing PCR and gel electrophoresis (1.5% agarose). Each sample was added to the gel with 6X TriTrack DNA Loading Dye and ran for 20 minutes at 120V.

Imaging: Imaging for RAG analysis and nerve regeneration analysis was completed as in chapter two. For macrophage analysis, slides were visualized with a Laser Scanning Confocal Microscope (Leica TCS SP5) at the Cell Imaging Core of the University of Alberta. Macrophage area was determined with thresholding FIJI analysis of IBA-1 fluorescence divided by total DRG area. Macrophage cell numbers were counted with binary evaluation of IBA-1 and TdTom

fluorescence with a DAPI nucleus and total nonneuronal DAPI cells were counted. Two DRG and nerve sections for each animal were processed and analyzed in an identical manner.

Statistical Analysis: Experimental results are written as the mean \pm standard error mean (*s.e.m.*). Significance of RAG analysis, length of regeneration, and macrophage areas and cell counts were determined using a one-way analysis of variance (ANOVA) to determine any differences in the mean between groups followed by a post-hoc Dunnett's test to compare experimental groups against unconditioned animals. A level of $p < 0.05$ was the cut-off for statistical significance. To determine statistical significance between axon counts, a two-way ANOVA was completed to determine differences between the mean of each group in a paired data set followed by Dunnett's post-hoc for comparison against unconditioned animals. To compare between genetically modified mice conditions and littermate controls, unpaired t-tests were performed on each group. Statistics were completed using Prism 9.3.1 (GraphPad Software, San Diego, CA).

3.3 Results

3.3.1 In both wildtype and CCR2^{-/-} mice, CCL, but not CES, increased ATF3 expression in DRG neuronal nuclei

PCR genotyping on wildtype (WT) and CCR2^{-/-} spleen tissue was performed to confirm that wildtype mice expressed the *Ccr2* gene at the expected 494 bp (lanes 1-3). As expected, the CCR2^{-/-} mice had the lower signal at 390 bp (lanes 4-6) (Figure 3.5.2).

We first wanted to confirm our previous findings that CCL, and not CES, upregulated ATF3 expression at the DRG (Lindå et al., 2011; Senger et al., 2020). The sciatic nerve of wildtype (WT) and CCR2^{-/-} mice were conditioned by CES, CCL (positive control ATF3 DRG expression), or remained unconditioned (negative control for ATF3 DRG expression) (n=4/cohort). On days 1 and 3 post-conditioning, the animals were euthanized and their L4, L5 DRGs as well as nerves at their conditioning sites, were harvested and processed for tissue sectioning (9 µm) and ATF3 immunohistochemical analysis (Figure 3.5.2). Similar to Sprague-Dawley rat models (Senger et al., 2018; 2019) and the WT mouse results of Chapter 2, there was a significant upregulation of ATF3 1 and 3 days following CCL in WT mouse DRG neuronal nuclei (Day 1: 63.5% ±8.4%, ***p*<0.01; Day 3: 80.5% ±4.3%, ****p*<0.001) compared to unconditioned animals. CES and unconditioned animals displayed low levels of ATF3 at 1 day (1.9% ±0.3%; 0.0±0.0%) and 3 days (7.2% ±1.0%; 3.2% ±1.0%), respectively (Figure 3.5.2).

This pattern of ATF3 upregulation persisted in CCR2^{-/-} animals, despite their deficient macrophage infiltration. One- and 3-days following CCL, CCR2^{-/-} mice DRG neurons had a mean ATF3 expression of 66.8% ±12.7% (***p*<0.01) and 89.6% ±0.7% (****p*<0.001) compared to unconditioned animals of 4.2% ±4.2% and 8.3% ±0.6% (Figure 3.5.2), respectively. CES continued to display low levels of ATF3 at one and three days in CCR2^{-/-} mice (7.9% ±4.2%;

8.0% \pm 3.4%) indicating a lack of injury. In summary, there were no significant differences between ATF3 expression in CCR2^{-/-} and WT mice as CCL-induced axonal injury upregulates ATF3 in the presence and absence of CCR2-expressing macrophages (Figure 3.5.2).

3.3.2 IBA-1 is upregulated post CCL-conditioning in mice with deficient macrophage infiltration at the nerve, but not the DRG

We next assessed whether macrophage levels were reduced following CCL in CCR2^{-/-} mice. WT and CCR2^{-/-} mice underwent CCL, CES, or no conditioning to the sciatic nerve and 3 days later the L4, L5 DRGs and nerve conditioning sites were harvested and processed for IBA-1 immunohistochemistry (Figure 3.5.3). At the DRG, CCL to WT mice increased the proportion of cells expressing IBA-1 (44.2% \pm 2.5%; ** p <0.01) compared to naïve mice (21.6% \pm 3.9%), demonstrating that there was an accumulation of macrophages within the DRG following CCL to the sciatic nerve (Figure 3.5.3). CES did not result in DRG macrophage accumulation (19.5% \pm 3.4%). In CCR2^{-/-} mice, there was a significant decrease in IBA-1⁺ macrophages at the DRG following CCL (20.1% \pm 5.9%; ** p <0.01) mice compared to WT CCL. CES (14.8% \pm 1.1%) and naïve (16.5% \pm 2.3%) CCR2^{-/-} mice were similarly expressed to their WT counterparts.

At the conditioning site of the sciatic nerve, WT mice that underwent CCL displayed upregulated IBA-1 macrophages (83.7% \pm 3.5% (***) p <0.001) compared to CES (20.2% \pm 2.1%) and naïve (12.4% \pm 0.7%) mice (Figure 3.5.4). Despite the decrease in CCR2-expressing macrophages post-CCL in CCR2^{-/-} mice, macrophages were still significantly upregulated compared to CES (21.0% \pm 2.6%; (***) p <0.001) and naïve (13.6% \pm 3.4%; (***) p <0.001) at the conditioning site. Notably, fewer macrophages accumulated at the conditioning site post-CCL

(51.6% \pm 2.8%; *** p <0.001) in the CCR2^{-/-} mice compared to the CCL WT mice (*** p <0.001) (Figure 3.5.4).

3.3.3 CCR2^{-/-} mice continue to upregulate pCREB post-CCL and CES conditioning.

We confirmed that similar to our findings in Chapter 2, both CCL (79.4% \pm 8.8% ; * p <0.05) and CES (83.6% \pm 2.7%; * p <0.05) promoted pCREB upregulation at the DRG compared to naïve (51.1% \pm 4.1%) in the WT mice. CCR2^{-/-} mice that underwent CCL and CES expressed similar levels of pCREB at their DRGs (CCL: 75.9% \pm 8.7%, * p <0.05; CES: 87.5% \pm 2.9%, ** p <0.01) compared to naïve CCR2^{-/-} mice (41.8% \pm 4.8%) (Figure 3.5.5)

3.3.4 CX3CR1^{CreER}; Rosa26 mice upregulate pCREB following CES and CCL, and the injury marker ATF3 is only increased following CCL

Next, we visualized TRMs through a genetically modified mouse model with tracer TdTomato fluorescence to analyze the separate macrophage populations following CES and CCL conditioning. Newly weaned CX3CR1^{CreER}; Rosa26 mice had early tamoxifen exposure to evoke TdTomato expression in all CX3CR1 cells. One month later, the monocyte-derived CX3CR1-expressing macrophages were replaced by bone-marrow progenitors without TdTomato fluorescence, whereas the TRMs and their progeny remained TdTomato positive (Buch et al., 2005; Zhao et al., 2019; Plemel et al., 2020). This TRM tracing experiment was devised to discern the involvement of TRMs post nerve injury and following CES or CCL conditioning.

As the fluorescent marking of CX3CR1 TRMs should not have an impact on the function of these cells, we expected CES and CCL to have growth promoting effects at the DRG and

regenerating nerve front in these mice. The sciatic nerve of CX3CR1^{CreER}; Rosa26 mice were conditioned by CES, CCL, or remained unconditioned (n=4/cohort). On days 1 and 3 post-conditioning, the animals were euthanized and their L4, L5 DRGs were harvested and processed for tissue sectioning (Figure 3.5.5). Immunohistochemistry was performed to determine if similar patterns of pCREB upregulation and the injury marker, ATF3, were present despite the insertion of TdTomato fluorescence into CX3CR1+ cells. Immunohistochemistry demonstrated a significant increase in immunofluorescence of the RAG, pCREB at the nuclei of both CES and CCL mice ($38.1\% \pm 7.1\%$, $p < 0.05$; $44.2\% \pm 2.4\%$, $p < 0.01$) compared to unconditioned mice at 3 days post-conditioning.

Similar to our wildtype findings, 1 day post-conditioning, CX3CR1^{CreER}; Rosa26 mice displayed an upregulation of the injury marker ATF3 following CCL ($27.6\% \pm 6.3\%$, $*p < 0.05$) whereas following CES ($5.0\% \pm 1.0\%$, $p > 0.05$) ATF3 levels were similar to unconditioned CX3CR1^{CreER}; Rosa26 animals ($5.1\% \pm 4.8\%$) (Figure 3.5.5). Overall, these data indicate that similar to our wildtype findings, both CCL and CES upregulate RAG expression at the DRG whereas CCL alone causes neuronal injury.

3.3.5 CCL promotes monocyte-derived macrophage infiltration at the DRG and conditioning site compared to CES and unconditioned animals.

To confirm the accumulation of macrophages in CX3CR1^{CreER}; Rosa26 mice after CCL we measured IBA-1 three days post-conditioning in the DRG and nerve. We found that IBA-1+ DRG area was higher in CCL ($2.4\% \text{ area} \pm 0.3\% \text{ area}$, $*p < 0.05$) as compared to CES ($1.4\% \text{ area} \pm 0.4\% \text{ area}$) and unconditioned mice ($1.1\% \text{ area} \pm 0.4\% \text{ area}$) (Figure 3.5.6). Furthermore, there was a significant increase in IBA-1 expression at the conditioning site, with CCL upregulating

IBA-1 levels ($3.1\% \text{ area} \pm 0.9\% \text{ area}$; $**p < 0.01$) compared to unconditioned mice ($0.5\% \pm 0.04\% \text{ area}$). CES ($0.4\% \text{ area} \pm 0.1\% \text{ area}$) mice were similar to the unconditioned controls (Figure 3.5.7).

The CX3CR1^{CreER}; Rosa26 mice have TdTomato-expressing (TdTom+) TRMs whereas the monocyte-derived macrophages are TdTomato negative (TdTom-). Therefore, these genetically modified mice can determine the effect of conditioning on these populations of macrophages. To determine whether the macrophage accumulation is due to monocyte-derived infiltration or tissue-resident macrophages expansion we examined the percentage of macrophages (IBA1+) expressing the TRM-specific fluorophore TdTom in the DRG and conditioning site after CCL, CES, or in naïve mice. There were no significant differences in numbers of TRMs at the DRG in CCL ($14.8\% \pm 4.9\%$) or CES ($19.6\% \pm 2.6\%$) compared to unconditioned ($17.7\% \pm 3.9\%$) animals (Figure 3.5.6). Similarly, there were no significant differences in numbers of TRMs at the conditioning sites of CCL ($15.6\% \pm 2.8\%$) and CES ($16.4\% \pm 5.2\%$) mice compared to unconditioned ($17.1\% \pm 2.1\%$) animals (Figure 3.5.6; Figure 3.5.7). In addition to measure the percentage of TRMs at the DRG we also determined macrophage density to ensure our quantity determination was unaffected by any alterations in adjacent cell populations. The densities of TRMs at the DRG post-CCL ($189.7 \text{ cells/mm}^2 \pm 47.4 \text{ cells/mm}^2$) and post-CES ($453.4 \text{ cells/mm}^2 \pm 62.2 \text{ cells/mm}^2$) were not significantly different from naïve ($300.6 \text{ cells/mm}^2 \pm 62.6 \text{ cells/mm}^2$). The densities of TRMs at the conditioning site were similarly unaffected by conditioning post-CCL ($1.4\text{E}^{-4} \text{ cells/mm}^2 \pm 2.5\text{E}^{-5} \text{ cells/mm}^2$) and post-CES ($1.4\text{E}^{-4} \text{ cells/mm}^2 \pm 5.1\text{E}^{-5} \text{ cells/mm}^2$) compared to naïve ($9.1\text{E}^{-5} \text{ cells/mm}^2 \pm 1.2\text{E}^{-5} \text{ cells/mm}^2$). Overall, these data suggest TRMs do not alter their overall population in the DRG or nerve following CCL or CES compared to unconditioned animals.

To determine if monocyte-derived macrophage infiltration was responsible for the increased IBA-1 levels at the DRG and nerve following CCL, the number of IBA-1+ cells that were TdTom- were quantified. Following CCL, there was a mean percentage of $26.6\% \pm 2.8\%$ IBA-1+/TdTom- cells at the L4, L5 DRGs ($***p < 0.001$), whereas both CES and unconditioned mice displayed low levels at $6.4\% \pm 1.1\%$, and $4.4\% \pm 1.1\%$, respectively (Figure 3.5.6). Likewise, this increase of infiltrating macrophages was also observed at the conditioning sites, with CCL displaying significantly increased IBA-1+/TdTom- cells ($24.6\% \pm 9.2\%$ $p < 0.05$), compared to CES ($2.4\% \pm 1.0\%$), and unconditioned mice ($1.3\% \pm 0.5\%$) (Figure 3.5.7). Density measurements similarly indicated an increase in monocyte-derived macrophages post-CCL ($550.6 \text{ cells/mm}^2 \pm 218.7 \text{ cells/mm}^2$; $349.1 \text{ cells/mm}^2 \pm 98.1 \text{ cells/mm}^2$; $p < 0.05$; $p < 0.01$) compared to CES ($160.1 \text{ cells/mm}^2 \pm 44.5 \text{ cells/mm}^2$; $22.2 \text{ cells/mm}^2 \pm 11.5 \text{ cells/mm}^2$) and naïve ($66.5 \text{ cells/mm}^2 \pm 18.6 \text{ cells/mm}^2$; $8.3 \text{ cells/mm}^2 \pm 3.8 \text{ cells/mm}^2$) at the DRG and conditioning sites, respectively. In summary, these data suggest that CCL causes monocyte-derived macrophage infiltration at the conditioning sites and at their DRG.

3.3.6 CCL promotes activation of monocyte-derived macrophages

To determine if the TRMs or monocyte-derived macrophages were activated following CCL and CES conditioning, immunohistochemistry against dectin-1 was performed on CX3CR1^{CreER}; Rosa26 mice. Dectin-1 is a C-type lectin receptor found on macrophages that is most characterized in response to fungal pathogens; it is upregulated following events that induce inflammation and exogenous injection elicits demyelination responses in the absence of injury (Schorey and Lawrence, 2008; Gensel et al., 2015). Therefore, we hypothesized that dectin-1+/IBA-1+ cells could be identified as activated macrophages. Given that macrophages

can respond without necessarily recruiting monocytes or proliferating, we wanted to determine if CCL and CES increased macrophage activation based on dectin-1 expression. Thus, we quantified the number of dectin-1 expressing IBA-1+/TdTTom+/- cells at the DRG and conditioning sites. Both at the DRG and nerve conditioning sites respectively, there were no differences in dectin-1 upregulation in TRMs of CCL ($2.6\% \pm 1.1\%$; $5.4\% \pm 2.0\%$) and CES ($3.3\% \pm 1.2\%$; $3.4\% \pm 0.2\%$) mice compared to unconditioned ($3.1\% \pm 1.2\%$; $6.2\% \pm 1.3\%$) mice (Figures 3.5.6; 3.5.7). Overall, these data suggest TRMs do not alter their activity levels in the DRG or nerve following CCL or CES compared to unconditioned animals.

We quantified the number of activated monocyte-derived macrophages following CCL, CES, or no conditioning at the DRG with dectin-1 immunofluorescence overlaying the infiltrating macrophages (Figure 3.5.6). There was a significant dectin-1 increase in the infiltrating macrophages in the DRG of mice that underwent CCL ($9.5\% \pm 2.9\%$; $p < 0.01$) compared to unconditioned mice ($0.9\% \pm 0.5\%$). CES ($0.7\% \pm 0.3\%$; $p > 0.05$) animals had similar dectin-1 levels in the monocyte-derived macrophages to the unconditioned mice (Figure 3.5.6). This finding persisted at the CCL conditioning site with a significant dectin-1 upregulation in IBA-1+/TdTTom- cells of CCL mice ($16.6\% \pm 4.4\%$; $p < 0.01$), compared to CES ($0.4\% \pm 0.3\%$) or unconditioned mice ($0.8\% \pm 0.4\%$) (Figure 3.5.7). In summary, these data suggest that unlike CES, CCL causes monocyte-derived macrophage activation at the conditioning sites and at their DRG. Alternatively, it is possible that monocyte-derived macrophages express dectin-1, and due to their enhanced presence, there was a rise in dectin-1 that does not necessarily signify activation.

3.3.7 Unlike CCL, the pro-regenerative effects of CES persist following macrophage depletion in iDTR;CX3CR1 mice.

We obtained 16 iDTR;CX3CR1 mice to assess whether the depletion of CX3CR1 macrophages would abolish the pro-regenerative effects of CES or CCL. The experimental animals received intraperitoneal tamoxifen injections one week prior to CES or CCL conditioning to drive the expression of the iDTR in all CX3CR1 cells (n=4/cohort) so that both monocyte-derived and TRMs could be targeted. The control mice were littermate controls with the CX3CR1^{CreER}; Rosa26 genotype and thus did not receive the insertion of the diphtheria toxin receptor onto the plasma membrane of CX3CR1 expressing cells during tamoxifen injections. One day prior to conditioning and daily for 6 days, all animals underwent diphtheria toxin i.p. injections to ablate the CX3CR1 macrophage populations in the experimental animals for the duration of the conditioning effect. On day 7, all animals underwent a sciatic nerve transection and repair surgery. On day 14, mice were euthanized and the sciatic nerve and L4,L5 DRGs were harvested and processed for immunohistochemistry to determine the extent of regeneration.

First, to confirm a significant ablation of CX3CR1 macrophages in the experimental animals one week following nerve repair surgery, anti-IBA-1 immunofluorescence at the DRGs was performed (Figure 3.5.9). Littermate control mice lacking the iDTR demonstrated the expected increase in IBA-1 immunofluorescence in CCL ($12.9\% \pm 3.7\%$), CES ($6.7\% \pm 1.2\%$), and unconditioned ($7.6\% \pm 0.4\%$) animals one week following nerve repair surgery (Figure 3.5.9). These studies measured macrophage expression levels at the DRG at the time of nerve harvest, 2 weeks after CCL and CES were performed. The nerve repair surgery understandably resulted in an increased of macrophages in the CES and naïve DRG as this procedure involves cutting the sciatic nerve. Notably however, the CCL cohort have elevated macrophages at their

DRG compared to CES and naïve cohorts due to the nerve crush (CCL) 2 weeks prior to the nerve repair surgery.

The experimental mice expressing the iDTR (CX3CR1;iDTR+ mice) had decreased IBA-1 expression following both CCL ($2.8\% \pm 0.8\%$; $p < 0.05$) and CES ($2.1\% \pm 0.8\%$; $p < 0.05$) one week following nerve repair surgery. This data suggests that CCL conditioning did not increase macrophage levels. Surprisingly, unconditioned animals ($8.0\% \pm 0.9\%$) did not display a decrease in IBA-1 immunofluorescence, indicating that the macrophage ablation was unsuccessful in this group and thus, these animals were discounted from further analysis. This experiment is scheduled to be repeated.

We went on to determine if CX3CR1 macrophages are required for the conditioning effects of CCL and CES. First, the sciatic nerves of all iDTR- animals (CX3CR1; DTR-) underwent immunohistochemistry against NF200 to confirm that the conditioning effect of CCL and CES persisted in these littermate control mice. As anticipated, both CES and CCL significantly increased the mean numbers of axons extending past the site of coaptation with maximums reaching 73.3 ± 6.8 axons and 56.5 ± 5.8 axons, respectively, compared to unconditioned animals with 35.8 ± 3.4 axons (Figure 3.5.10). The pattern of significant increases in axon numbers continued throughout the regenerating length (at least $p < 0.05$). Further, both conditioned groups accelerated nerve regeneration compared to unconditioned nerves. The distance of regeneration following CES was $6.9 \text{ mm} \pm 1.0 \text{ mm}$ ($**p < 0.01$) and CCL was $6.0 \text{ mm} \pm 0.5 \text{ mm}$ ($*p < 0.05$), whereas unconditioned animals only reached $3.1 \text{ mm} \pm 0.2 \text{ mm}$. These data demonstrate that diphtheria toxin injections, in lieu of the DTR, does not affect the regenerative effects of CCL and CES conditioning on the sciatic nerve.

Finally, the length of regeneration obtained in axons following sciatic nerve repair in CX3CR1; DTR+ mice following CES or CCL conditioning were compared to their littermate control mice (Figure 3.5.10). DTR+ mice that underwent CES ($5.8 \text{ mm} \pm 0.5 \text{ mm}$) displayed no significant differences in length of regeneration to littermate controls with CES ($6.9 \text{ mm} \pm 1.0 \text{ mm}$), whereas DTR+ mice that underwent CCL ($3.0 \text{ mm} \pm 0.5 \text{ mm}$) displayed a significant decrease in regeneration length compared to DTR- mice ($6.0 \text{ mm} \pm 0.5 \text{ mm}$; $p < 0.01$) indicating that the conditioning effect associated with CCL did not persist following CX3CR1 macrophage ablation ($p < 0.01$). Furthermore, there were significant decreases in numbers of axons regenerating in CCL DTR+ mice compared to CCL DTR- mice ($p < 0.05$ - $p < 0.001$).

In summary, these data suggest that unlike CCL, CES does not rely on CX3CR1 macrophages to exert the conditioning effect to promote nerve regeneration.

3.4 Discussion

ATF3 upregulation persisted in mice that underwent CCL, despite a lack of CCR2+ macrophage infiltration to the conditioning site and DRG, suggesting that other cell types including the damaged neurons and de-differentiated Schwann Cells, are involved in the multifaceted injury response of peripheral axons. Further, this ATF3 upregulation was not seen in mice following CES, corroborating that CES is non-injurious. As expected, there was a large increase in macrophage accumulation at both the DRG and conditioning site following CCL conditioning, but not CES. The increase of macrophages further supports our hypothesis that CES does not rely on the inflammatory response by macrophages to produce its pro-regenerative effects. Interestingly, the reduction of macrophage accumulation was more drastic at the nerve compared to the DRG following CCL. This draws attention to possible compensatory mechanisms, likely by neutrophils, by these CCR2^{-/-} mice to still produce inflammation, despite lacking CCL2-CCR2 signalling responsible for CCR2⁺ macrophage infiltration to the nerve (Niemi et al., 2013, 2016). Furthermore, the upregulation of DRG pCREB expression associated with both CES and CCL following conditioning was maintained in CCR2^{-/-} mice. We anticipated that pCREB upregulation would persist in mice that underwent CES, as thus far the pro-regenerative effects have been shown to be non-inflammatory and non-injurious; however, we anticipated if CCL relies on inflammation, then its pCREB upregulation would cease. As a result, both the upregulated IBA-1 and pCREB immunofluorescence that persist in CCR2^{-/-} mice indicate a compensatory mechanism that could potentially be responsible for these data. Blocking of the CCL-induced conditioning effect following neutrophil ablation by Ly6G injection in the CCR2^{-/-} mice prior to CCL would confirm if neutrophils were compensation for the loss of CCR2⁺ macrophages.

The conditioning lesion effect in CCR2^{-/-} animals was studied by Niemi et al., (2013) *in vitro* and found that in DRG explants the CCL conditioning lesion effect from axotomy was abolished, and in dissociated neurons it was substantially reduced. These *in vitro* studies do not support our findings as the pro-regenerative environment associated with CCL persisted in our *in vivo* CCR2^{-/-} mice. It is not surprising however, that the pro-regenerative effect of pCREB upregulation associated with CES persisted in CCR2^{-/-} mice, as we hypothesized that CES does not rely on macrophages or monocyte infiltration to produce a conditioning response due to its lack of cluster of differentiation 68 (CD68), ATF3 upregulation, and absence of Wallerian degeneration (Senger et al., 2020). Unfortunately, since our positive control did not establish altered pCREB immunofluorescence, the upregulated pCREB expression in CCR2^{-/-} mice is not enough to fully support our hypothesis as we cannot discount the possibility that compensatory mechanisms are also involved in CES.

There are several limitations to this experiment which could ultimately explain the discrepancy between our hypothesis and these findings. Firstly, a major limitation of this experiment lies in this mouse model itself as redundancy of other immune cells compensate for the loss of CCR2-expressing macrophages. CCR2^{-/-} mice do not display significant reductions in myelin clearance following nerve injury despite a decrease in macrophage infiltration evidenced by decreased Cd11b staining (Niemi et al., 2013). Further, these knockout mice display increased phagocytic Schwann cell activity, increased neutrophil infiltration and phagocytosis, and do ultimately produce a reduction in Wallerian degeneration following neutrophil depletion (Lindborg et al., 2017). There is also the possibility that other chemokine/cytokine signalling pathways are responsible for infiltration of monocyte-derived macrophage populations in knockout mice. Though signalling through the CCL2/CCR2 pathway is commonly thought to be the

dominant pathway of macrophage infiltration to the peripheral nerve and DRG, other cytokine signalling pathways have been shown to be involved such as LIF, IL-1 α , IL-1 β , and pancreatitis associated protein III (PAPIII) (Liu et al., 2019). The use of other signalling pathways to cause infiltration into the nerve could be responsible for non-CCR2⁺ macrophage infiltration or the infiltration of CCR2⁺ macrophages using other signalling methods to infiltrate. As we did continue to see a high amount of IBA-1 immunofluorescence in the CCL CCR2^{-/-} mice at the conditioning site, it is possible that this is due to any of these methods of compensation. Lastly, the possibility that tissue-resident macrophages are involved both in wildtype mice as well as CCR2^{-/-} mice during the conditioning response remains to be explored. It is known that TRMs residing in the DRG and nerves can proliferate and contribute to both pro-inflammatory and anti-inflammatory actions during peripheral nerve injury (Lindborg et al., 2017; Mueller et al., 2003). Altogether, it is possible that the redundancy and lifelong genetic mutations made unforeseen changes in this mouse model, ultimately showing that CCL retained a pro-regenerative environment with upregulated IBA-1 and pCREB immunofluorescence and the difference between CES and CCL cannot be determined using this mouse model.

CX3CR1^{CreER}; Rosa26 mice were developed to evoke TdTomato fluorescence in TRM to assess TRM proliferation or activation following CES and CCL compared to unconditioned animals. In order to confirm a similar phenotype to wildtype mice, immunohistochemistry was performed where the data indicated that fluorescent-labelling transgenic modifications causing TdTomato fluorescence in CX3CR1 cells does not alter the pro-regenerative effects associated with either CES or CCL. We confirmed an upregulation of the RAG, pCREB following CES and CCL in the TdTom TRM tracer mice. Further, the upregulation of the injury marker, ATF3, persisted in only CCL animals, confirming the injurious nature of the conditioning paradigm,

while CES animals did not display an upregulation of ATF3, like unconditioned animals. To compare the macrophage responses of CCL and CES, immunofluorescent analysis showed that infiltrating macrophages were increased both in quantity and activation levels at the DRG and conditioning site following CCL, but not CES. This supports the extensive previous literature describing that the conditioning effect associated with a crush lesion relies heavily on upregulated macrophage infiltration and inflammation to mount its robust regenerative response (Niemi et al., 2013; 2016). Further, this strongly supports our hypothesis that CES does not rely on pro-inflammatory infiltrating macrophages to evoke its pro-regenerative response.

Our data suggest that TRMs do not seem to be involved in the conditioning response of both CCL and CES. Though capable of proliferation and activation under homeostatic conditions, as well as upregulated following peripheral nerve injury to participate in events such as phagocytosis of myelin debris, TRMs showed no changes in quantity or activation in CCL and CES compared to unconditioned animals. It is possible that following CCL, the robust response by infiltrating monocyte-derived macrophages was sufficient to forego a response by TRMs, which remain inactivated unless absolutely necessary such as the case when infiltrating macrophages are abolished or under more injurious states, such as axotomy, not merely crush injury. Another possibility is that like neutrophils, TRMs may play a role earlier on in producing the conditioning effect and were deactivated at day 3. Indeed, research has shown that TRMs and other resident cells such as Schwann cells are activated early, at 1 day post-injury, in comparison to the slightly delayed infiltration of monocytes often commencing at day 2 and peaking around day 5 (Ydens et al., 2012). However, this research also shows that TRM proliferation peaks at day 2-3; therefore, further supporting the idea that if TRMs were proliferating in CCL or CES, it still would have been evident at day 3, when our tissue was harvested (Ydens et al., 2012).

Together, this data supports that both TRM and monocyte-derived macrophages are not involved in producing the conditioning effect associated with CES, indicating that its mechanism is not based in the upregulation of inflammation. Our data does suggest that monocyte-derived macrophages, likely not TRMs, are required for CCL conditioning.

We next utilized a tamoxifen induced diphtheria toxin receptor mouse model to ablate the CX3CR1 population of macrophages, allowing us to circumvent the redundancies such as described for the *CCR2*^{-/-} mice. After establishing a significant reduction in macrophages with IBA-1+ immunofluorescence, we were able to compare the conditioning effects of CCL and CES associated with a decrease in both TRMs and monocyte-derived macrophages. Due to the persistence of pro-regenerative responses associated with CCL and CES in DTR- mice, we concluded that diphtheria toxin and tamoxifen were not causing unwarranted toxic effects. Important to note are recent studies demonstrating that diphtheria toxin ablation through the iDTR system has been associated with CSF deficiencies and ventricular shrinkage (Bedolla et al., 2022). While the conclusions of this study remain important to be investigated thoroughly, we do not believe it to be an issue with the results of this experiment due to our controls and the fact that this is a PNS study that is assumed to not be impacted by ventricular deficits. To our knowledge, there is no interaction between ventricular function and PNS regeneration. Similar to data from the *CCR2*^{-/-} mice, DTR+ mice that underwent CCL displayed significantly reduced regeneration, indicating by a decrease in both axon numbers and lengths of regeneration past the coaptation site. However, in contrast to data from the *CCR2*^{-/-} mice, DTR+ mice that underwent CES continued to display a robust regenerative response, with no significant differences found in extent of regeneration. This supports our hypothesis that CES upregulates nerve regeneration without macrophage involvement. This data does not discount the fact that this mouse model

does not distinguish between TRMs and monocyte-derived macrophage infiltration, both of which could be involved in CCL or CES, despite data from the CX3CR1^{CreER}; Rosa26 mouse model previously discussed. It is important to note; however, that this experimental model using diphtheria toxin tends to target monocyte-derived macrophages more robustly compared to TRMs; therefore, combined with our data that TRMs do not seem to proliferate or activate following CES and CCL, it is likely that any changes occurred due to ablation of monocyte-derived macrophages.

Although not statistically significant, DTR+ mice that underwent CES demonstrated slight decrease in mean lengths of regeneration compared to DTR- mice that underwent CES. This alludes to the possibility that although CES does not seem to depend on macrophages for mounting a pro-regenerative response, combined with the CCR2^{-/-} mice data, perhaps macrophages are involved to some extent, whether it is pro-inflammatory or anti-inflammatory in nature. Due to vast macrophage heterogeneity, it is possible that the reduction in macrophages was partly targeting CES' mechanism, but not enough to produce complete abolishment. Similarly, it could also represent variability between groups associated with CES. Due to the lack of macrophage ablation in unconditioned DTR+ mice, this experiment is scheduled to be repeated to confirm the proper DTR+ control for this experiment. Furthermore, increasing the number of animals in this experiment might reduce any variability in individual animal responses.

These findings also generate intriguing concepts for further research. As the diphtheria toxin model used did not necessarily distinguish between monocyte-derived macrophages and TRMs, it would be relevant to complete the respective abolishment for both in the future. This could provide insight as to the slight decrease in length in CES animals with DTR+ genotypes. If

TRMs were involved in some capacity, for example by secretion of anti-inflammatory cytokines, this could both generate new concepts about how macrophages are involved in pro-regenerative responses, not solely for phagocytic debris clearance, as well as elucidate clinical avenues for human patients even beyond CES. Dectin-1 upregulation is strongly associated with pro-inflammatory states and responses; therefore, looking into anti-inflammatory activation states might be useful for a more comprehensive analysis of TRMs in CCL and CES, as well as support CES as non-inflammatory. It will also be necessary to determine if the rise in dectin-1 is associated with increased activation, since it is possible that dectin-1 was solely upregulated because there was an increase in monocyte-derived macrophages which tend to express dectin-1. Furthermore, if the conditioning effect associated with CES were to persist similarly with monocyte-derived macrophage abolishment, this would even further support our research that has thus far indicated an absence of an inflammatory response associated with CES.

Ultimately, these findings strongly support our hypothesis that CES does not rely on the inflammatory infiltration of monocyte-derived macrophages to produce its growth enhancing effect on peripheral nerve regeneration.

3.5 Figures

Primary Antibody	Antigen Retrieval 40 minutes in 60 °C citrate buffer (10mM sodium citrate, 0.05% Tween-20, pH 6.0)	Primary Antibody Dilution	Secondary Antibody	Secondary Antibody Dilution
ATF3 (rabbit) Abcam 207434	Yes	1:500	AlexaFluor 488 goat anti-rabbit	1:1000
pCREB (rabbit) Cell Signalling 9198	Yes	1:500	AlexaFluor 488 goat anti-rabbit	1:1000
NF200 (rabbit) Sigma-Alrich N4142	No	1:500	AlexaFluor 488 goat anti-rabbit	1:500
IBA-1 (rabbit) Wako Chemicals Richmond, VA 019-19741	No	1:1000	Alexa Fluor 488 goat anti-rabbit	1:400
Dectin-1 (rat) Invivogen San Diego, CA Mabg-mdect	No	1:50	AlexaFluor 647 donkey anti-rat Jackson ImmunoResearch 712-606-153	1:400

Figure 3.5.1: Primary and Secondary Antibody Protocols for Immunohistochemistry

Figure 3.5.2 ATF3 is upregulated following CCL, but not CES, compared to unconditioned animals in both WT and CCR2^{-/-} mice.

A) PCR Genotyping of wildtype and CCR2^{-/-} mice confirming the expected lower *ccr2* transcript at 390 bp in the CCR2^{-/-} mice. The sciatic nerve of wildtype mice underwent B) CCL (n=2) C) CES (n=2) or D) remained unconditioned (n=2) and their L4, L5 DRGs were harvested 1 day later. The sciatic nerve of CCR2^{-/-} mice underwent E) CCL (n=2), F) CES (n=2) or G) remained unconditioned (n=2). ATF3 immunohistochemistry was performed and the positive nuclei were counted. H) Wildtype and CCR2^{-/-} mice that underwent CCL had significantly higher ATF3 levels in the DRG nuclei ($p < 0.01$) compared to unconditioned controls. I-O) Three days following CCL (I,L), CES (J,M), or no conditioning (K,N) both wildtype (I-K) and CCR2^{-/-} (L-N) L4, L5 DRGs were processed for immunohistochemistry against ATF3. O) ATF3 immunofluorescence was significantly upregulated in CCL animals of both wildtype and CCR2^{-/-} mice ($p < 0.05$; $p < 0.01$) and there were no significant differences in baseline ATF3 expression in both CES or unconditioned mice for either wildtype or CCR2^{-/-} mice. The scale bar in B indicates a distance of 100 μm .

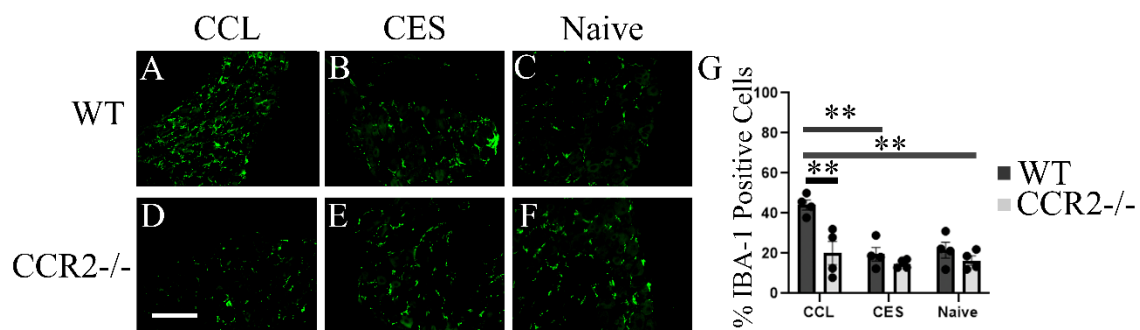


Figure 3.5.3 IBA-1 expression is upregulated in the DRG following CCL conditioning.

A-F) IBA-1 immunofluorescence at the L4, L5 DRGs three days following sciatic nerve conditioning in wildtype (A-C) and CCR2^{-/-} (D-F) mice that underwent A,D) CCL, B,E) CES or C,F) naive (n=4/cohort). G) The percentage of IBA-1 positive cells was upregulated in WT mice following CCL compared to CES and naïve mice. There was a significant decrease in IBA-1 immunofluorescence in CCR2^{-/-} mice following CCL compared to WT CCL mice (***p*<0.01). The scale bar in D indicates a distance of 100 μ m.

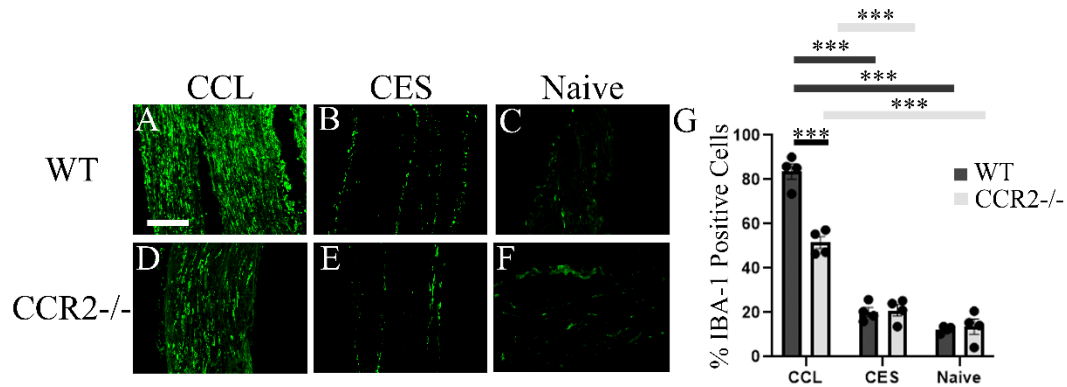


Figure 3.5.4 IBA-1 expression is upregulated in the sciatic nerve following CCL conditioning.

A-F) IBA-1 immunofluorescence at the nerve three days following sciatic nerve conditioning in wildtype (A-C) and CCR2^{-/-} (D-F) mice that underwent CCL (A-D), CES (B,E), or naïve (C-F) (n=4/cohort). G) The percentage of IBA-1 positive cells was upregulated following CCL in both wildtype and CCR2^{-/-} mice compared to CES and naïve mice. There was a significant decrease in IBA-1 immunofluorescence in CCR2^{-/-} mice that underwent CCL compared to WT CCL mice (***) ($p < 0.001$). The scale bar in A indicates a distance of 100 μ m.

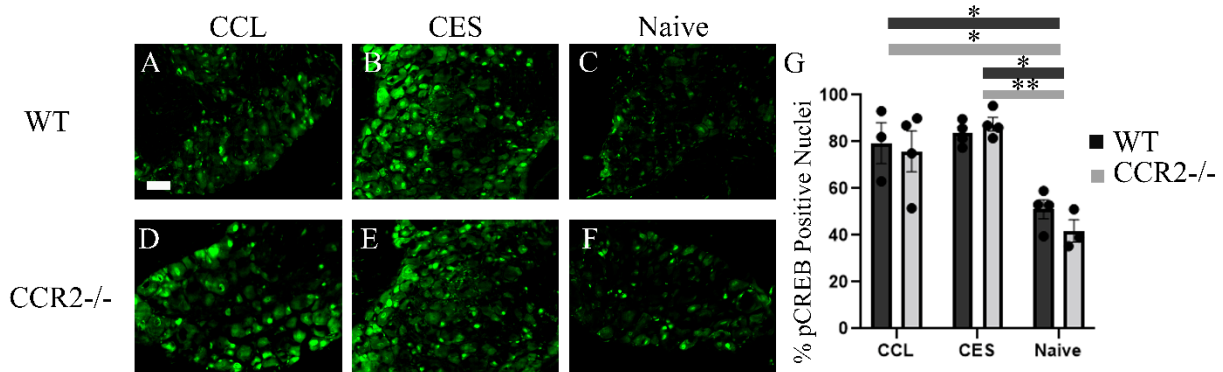


Figure 3.5.5: CCR2^{-/-} mice upregulate pCREB post-CES and CCL conditioning.

The sciatic nerve of A-C) wildtype and D-F) CCR2^{-/-} mice underwent A,D) CCL, B,E) CES or C,F) remained unconditioned (n=4/cohort) and their L4, L5 DRGs were harvested 3 days later.

pCREB immunohistochemistry was performed and the positive nuclei were counted. G)

Wildtype and CCR2^{-/-} mice that underwent CCL and CES conditioning had significantly higher pCREB levels in the DRG nuclei (* $p < 0.05$; ** $p < 0.01$) compared to unconditioned controls.

There was no significant difference in baseline pCREB expression of naive mice for either wildtype or CCR2^{-/-} mice. The scale bar in A indicates a distance of 100 μm.

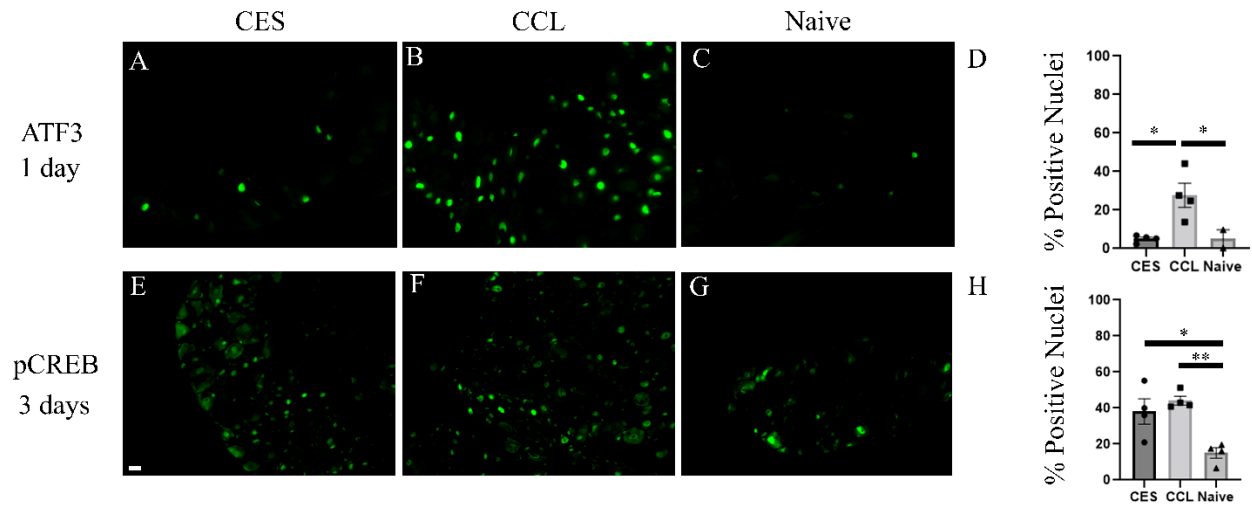


Figure 3.5.6: CES and CCL of $CX3CR1^{CreER}; Rosa26$ mice increase pCREB at the DRG, whereas CCL alone upregulates the injury marker ATF3.

A-C) ATF3 Immunohistochemistry of L4, L5 DRGs from $CX3CR1^{CreER}; Rosa26$ mice 1 day following CES (A) CCL (B) or unconditioned (C) ($n=4$ /cohort). D) ATF3 is upregulated in the DRG nuclei of CCL mice compared to CES or uninjured mice ($*p<0.05$). E-G) pCREB immunohistochemistry of L4, L5 DRGs 3 days following E) CES, F) CCL, or G) no conditioning ($n=4$ /cohort). H) Phospho-CREB was increased in $CX3CR1^{CreER}; Rosa26$ mice three days following CES and CCL compared to unconditioned mice ($*p<0.05$, $**p<0.01$). The scale bar in E indicates a distance of 100 μm .

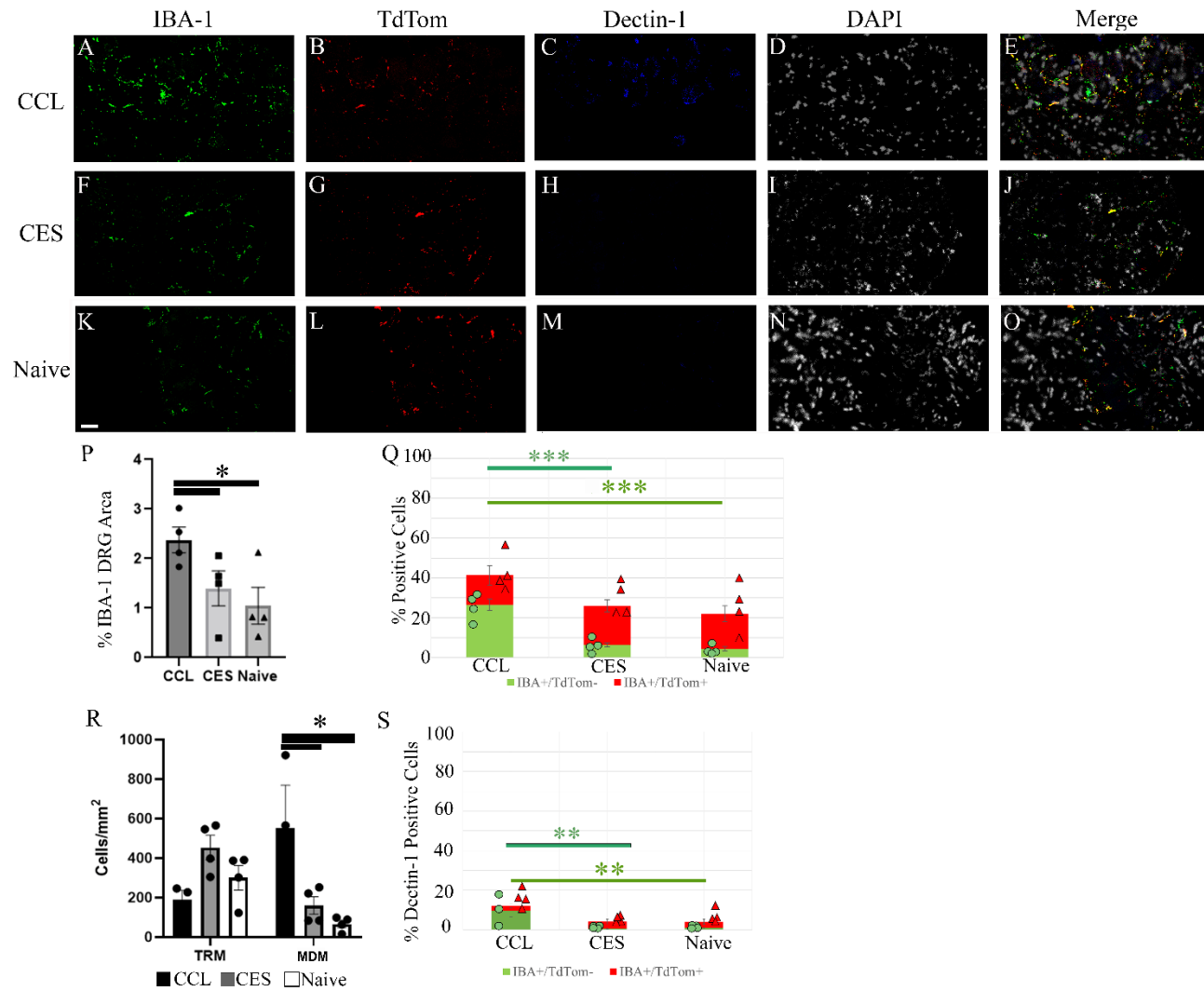


Figure 3.5.7 CES and CCL do not affect DRG tissue-resident macrophage numbers; however, CCL allows infiltration of monocyte-derived macrophages.

IBA-1, TdTom, Dectin-1, and Dapi immunofluorescence of L4, L5 DRGs from CX3CR1^{CreER}; Rosa26 mice 3 days following CCL (A-E) CES (F-J) and unconditioned (K-O) (n=4/cohort). P) Graph indicating area percentage of IBA-1+ immunofluorescence demonstrating a significant upregulation following CCL compared to CES or unconditioned mice ($p < 0.05$). Q) Graph indicating the percentage of infiltrating monocyte-derived macrophages (IBA-1+/TdTom-; green) and tissue-resident macrophages (IBA-1+/TdTom+; red) following CCL, CES, or no-conditioning. There was a significant upregulation of infiltrating macrophages at the DRG following CCL, not CES, compared to unconditioned animals ($p < 0.001$). Tissue-resident macrophages were similar in all groups. R) Graph indicating density of TRMs or monocyte-derived macrophages in DRG area ($p < 0.01$). S) Graph indicating the percentage of dectin-1+ macrophages that were either IBA-1+/TdTom- or IBA-1+/TdTom+. There was a significant upregulation of dectin-1 in IBA-1+/TdTom- macrophages following CCL, not CES, compared to unconditioned animals ($p < 0.01$). The scale bar in I represents 100 μm .

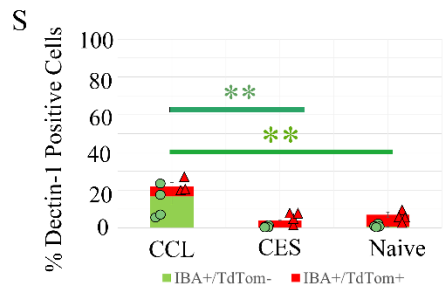
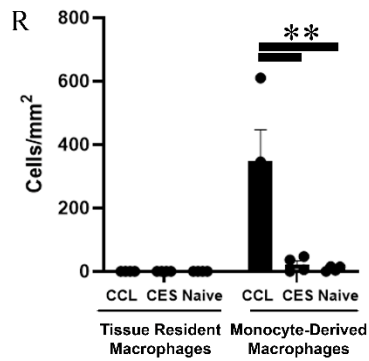
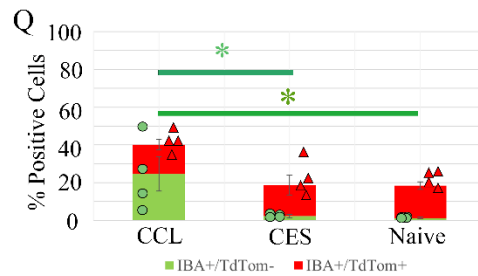
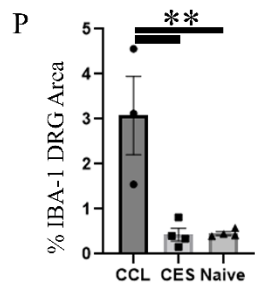
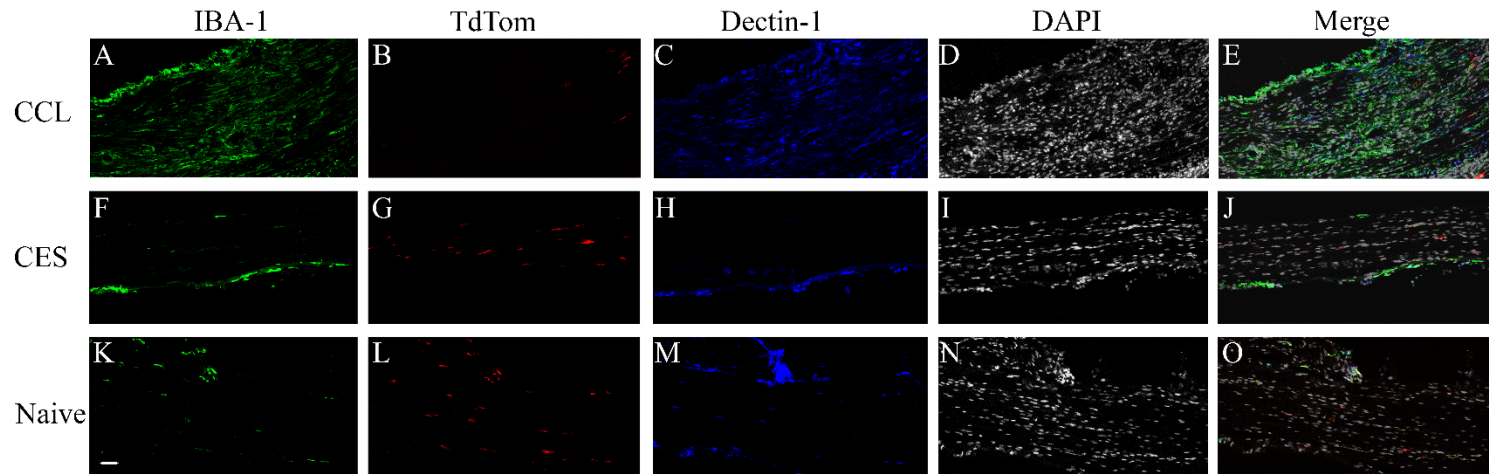
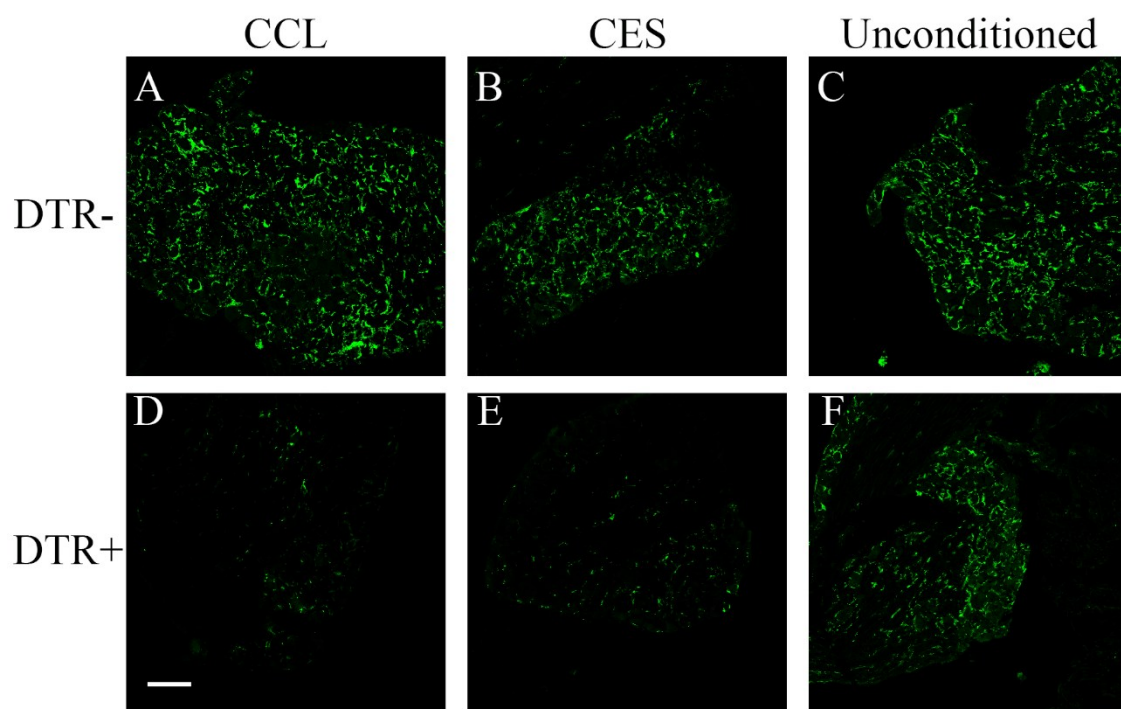


Figure 3.5.8 CES and CCL do not affect nerve tissue-resident macrophage numbers; however, CCL allows infiltration of monocyte-derived macrophages.

IBA-1, TdTom, Dectin-1, and Dapi immunofluorescence of nerve from CX3CR1^{CreER}; Rosa26 mice 3 days following CCL (A-E), CES (F-J). K-O) Unconditioned CX3CR1^{CreER}; Rosa26 nerve served as negative controls (n=4/cohort). P) Graph indicating area percentage of IBA-1+ immunofluorescence demonstrating a significant upregulation following CCL compared to CES or unconditioned mice ($p<0.05$). Q) Graph depicting the percentage of infiltrating monocyte-derived macrophages (IBA-1+/TdTom-; green) and tissue-resident macrophages (IBA-1+/TdTom+; red) following CCL, CES, or no-conditioning. There was a significant upregulation of infiltrating macrophages at the DRG following CCL, not CES, compared to unconditioned animals ($p<0.001$). Tissue-resident macrophages were similar in all groups. R) Graph indicating density of TRMs or monocyte-derived macrophages in sciatic nerve ($p<0.01$). S) Graph indicating the percentage of dectin-1+ macrophages that were either IBA-1+/TdTom- or IBA-1+/TdTom+. There was a significant upregulation of dectin-1 in IBA-1+/TdTom- macrophages following CCL, not CES, compared to unconditioned animals ($p<0.01$). The scale bar in I represents 100 μm .



G

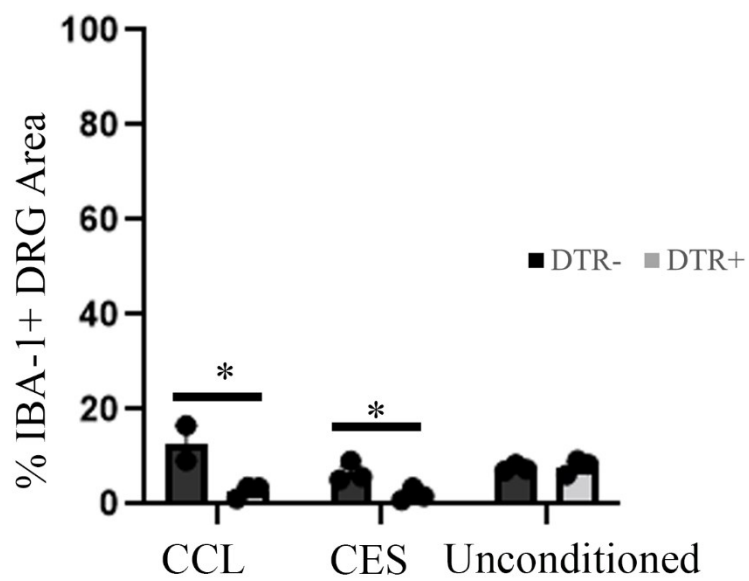


Figure 3.5.9 Macrophage numbers were significantly reduced in iDTR;CX3CR1 ablated mice that were conditioned with either CCL or CES prior to surgical repair.

A-F) IBA-1 immunofluorescence at the L4, L5 DRGs of iDTR;CX3CR1 mice that underwent CCL (A,D) CES (B,E) or remained unconditioned (C,F) (n=4/cohort). Diphtheria toxin was injected one day prior and daily for the duration of conditioning. Macrophages of mice that expressed the inducible diphtheria toxin receptor (DTR+) were ablated (D-F) whereas the macrophages of the mice that did not express the diphtheria toxin receptor (DTR-) remained viable (A-C). Seven days post-conditioning, all animals underwent sciatic nerve transection and repair and the DRG and nerve were collected one week later. G) The area percentage of IBA-1 immunofluorescence was quantified and confirmed a significant decrease in IBA-1 expression in DTR+ mice following CCL and CES ($p < 0.05$), but not in unconditioned mice. The scale bar in D represents a distance of 100 μm .

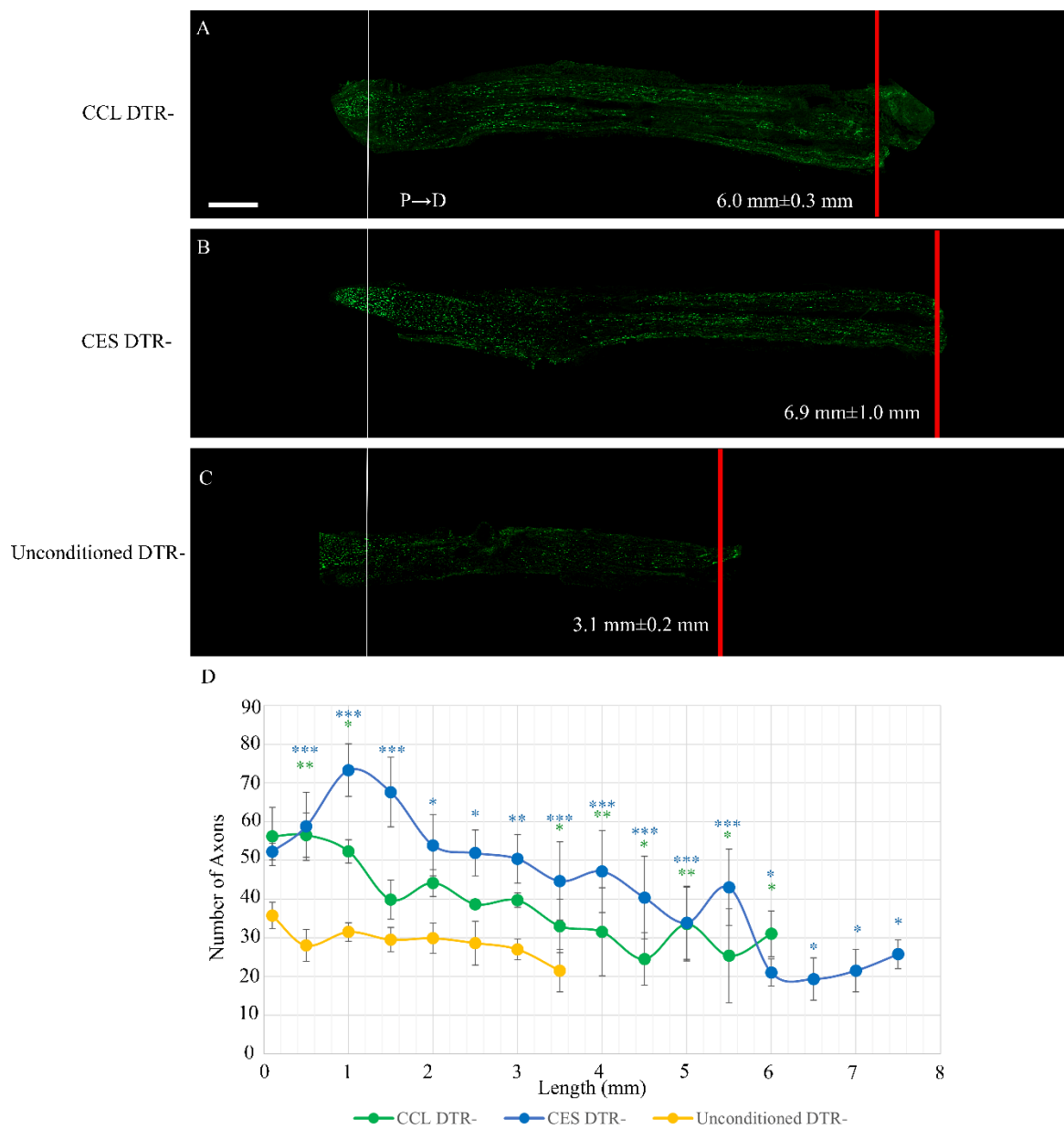


Figure 3.5.10 The pro-regenerative effects of CCL and CES persist in littermate controls of iDTR;CX3CR1 mice.

A-C) NF200 immunofluorescence of the sciatic nerve of iDTR;CX3CR1 control animals that do not express the inducible diphtheria toxin receptor (DTR-) on their CX3CR1 cells 7 days following surgical repair. Cohorts included animals that received either: CCL (A) CES (B) or no-conditioning (C) one-week prior to surgery (n=4/cohort). White lines indicate the site of surgical repair. Red lines indicate the length at which less than 10 axons were counted. D) The number of axons and extent of their regeneration were counted from the surgery repair site distally every 0.5 mm. CES and CCL conditioning accelerated the rate of regeneration in these mice lacking the diphtheria toxin receptor (DTR-) ($*p<0.05$; $**p<0.01$; $***p<0.001$). The scale bar in A indicates a length of 500 μm .

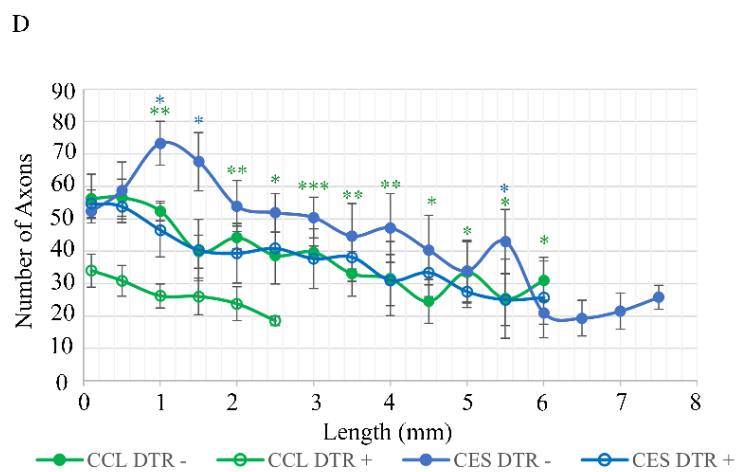
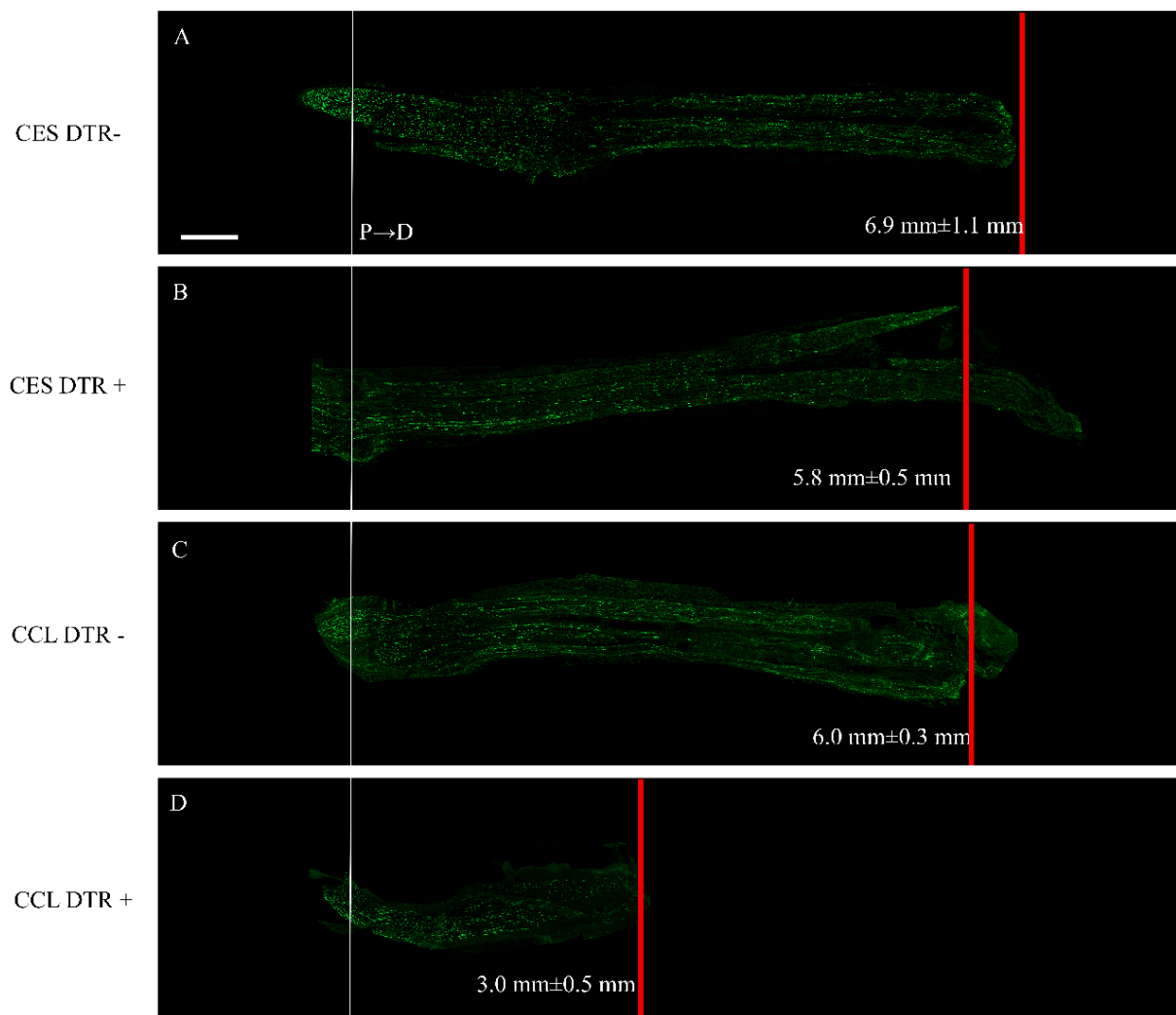


Figure 3.5.11 Unlike CCL, the pro-regenerative effect of CES remains following macrophage ablation in iDTR;CX3CR1 mice.

A-D) NF200 immunofluorescence at the sciatic nerve of iDTR;CX3CR1 control mice that did not express the inducible diphtheria toxin receptor (DTR-) on their CX3CR1-expressing cells (A,C) compared to mice that expressed the inducible diphtheria toxin receptor (DTR+) on their CX3CR1-expressing cells (B,D). The nerves were harvested one week following nerve repair surgery of animals that were conditioned by CES (A, B) or CCL (C,D) one week prior to surgery (n=4/cohort). White lines indicate the site of surgical repair. Red lines indicate the length at which less than 10 axons were counted. E) The number of axons and extent of their regeneration were counted from the surgery repair site distally every 0.5 mm. CES conditioning accelerated the rate of regeneration in these mice in both DTR- and DTR+ iDTR;CX3CR1 mice whereas CCL did not exert its pro-regenerative effect in the absence of CX3CR1 macrophages (* $p < 0.05$; ** $p < 0.01$; *** $p < 0.001$). The scale bar in A indicates a length of 500 μm .

**CHAPTER 4: Investigation of the role of AlphaB-Crystallin in the pro-regenerative effects
of CES and CCL**

4.1 Introduction

AlphaB-crystallin (α BC) is a small heat-shock protein initially discovered in the lens of the eye (Mörner, 1894). While other major proteins of the lens including beta-crystallin and gamma-crystallin are restricted to the lens, α BC has a widespread expression in other tissues including skeletal muscle, heart, the central nervous system (CNS), and the peripheral nervous system (PNS) (Mörner, 1894; Nagaraj et al., 2017). α BC has been shown to contribute to tauopathies such as Alzheimer's disease, progressive supranuclear palsy, frontotemporal dementia with parkinsonism-17, and corticobasal degeneration, as upregulations are found in astrocytes, oligodendrocytes, microglia, and neurons of the brain post-mortem (Mao et al., 2001; Dabir et al., 2004; Richter-Lansberg and Goldbaum, 2003). Although α BC is deemed as neuroprotective earlier on in some neuro-degenerative disease states, particularly Parkinsons disease, its upregulation contributes to toxicity primarily through interactions with glial cell inclusions (Liu et al., 2015). It is possible that the overall benefit/deficit created by α BC depends on phosphorylation state: phosphorylation of serine residues -45 and -59 have been demonstrated to contribute to protection, whereas phosphorylation of Ser-19 supports degeneration (Li and Reiser, 2011; Kuipers et al., 2017). Further complicating this, phosphorylation of Ser-59 has been shown to cause reactive astrogliosis and demyelination in cuprizone-induced MS (Kuipers et al., 2017).

In the PNS, α BC is expressed in both Schwann cells and neuronal axons and cell bodies and its expression is downregulated for up to 28 days following a crush injury. (Lim et al., 2017). Recent studies demonstrate a key role for α BC in remyelination as it is highly expressed in Schwann cells during developmental myelination and remyelination post-injury (after the 28 day downregulation (D'Antonio et al., 2006; Ousman et al., 2017). Further, α BC may have an

anti-inflammatory role in the PNS as α BC^{-/-} mice have increased pro-inflammatory macrophages following nerve injury, and macrophages treated with α BC peptide treatment following lipopolysaccharide (LPS) stimulation had decreased cytokine expression such as interleukin-6 (IL-6), interleukin-1beta (IL-1 β), interleukin-12p40 (IL-12p40), and tumour necrosis factor alpha (TNF α) *in vitro* (Lim et al., 2021). The role of α BC in regeneration determined through axonal measures is unclear as although there was no change in neurite outgrowth of α BC^{-/-} dorsal root ganglion (DRG) neurons compared to their controls, there was an upregulation of phosphorylated protein kinase B (pAKT) which has been shown to promote nerve growth (Lim et al., 2017). The Ousman laboratory determined that the deficits seen in the knock-out mice were due to deficits during myelination and noted deficits in behavioral indices that also impact regeneration, not solely myelination. Our study investigated the role of α BC in nerve regeneration *in vivo* through immunohistochemistry in addition to its potential role in the conditioning effects associated with the conditioning crush lesion (CCL) and conditioning electrical stimulation (CES).

4.2 Methods

Animals: α BC^{-/-} animals were obtained from the Ousman Laboratory at the University of Calgary and bred with Health Sciences Laboratory Animal Services (HSLAS) at the University of Alberta under AUP 00003034 (Lim et al., 2017).

Surgical Procedures: 1) To determine the effect of CES and CCL on WT and α BC^{-/-} animals to determine the effect of α BC on DRG RAG expression (n=4/cohort) as described in Chapter 2. 2) To determine the effect of α BC on the ability of CES and CCL to accelerate nerve regeneration, CES and CCL were performed on WT and α BC^{-/-} animals 7 days prior to cut/coaptation (n=6), as described in Chapter 2. The extent of nerve regeneration was measured after 7 days. 3) In a third cohort, we performed graft experiments to determine if the expression of α BC in the growing axons or within the regeneration milieu (including Schwann cells) is required for nerve regeneration. One week prior to graft surgeries, adult 129S6/SvEvTac (WT) mice and α B-C^{-/-} mice (n=8) underwent a crush lesion as described above to the sciatic nerve. On day 7, the crushed sciatic nerves were isolated from the euthanized mice and placed on ice in saline to be used for grafts (donor nerves). Graft recipients included WT and α BC^{-/-} animals (n=8). The sciatic nerve from animals anesthetized with oral isoflurane was isolated via an incision at the mid-thigh and blunt dissection through the hamstring muscles. A surgical transection to the sciatic was made proximal to the trifurcation point, and a 5 mm section from the donor grafts was inserted with 10-0 sutures and fibrinogen gel to the proximal and distal transected sciatic nerve of the host mouse. The surgical site was closed as described above and animals were given subcutaneous buprenorphine (0.05 mg/Kg/animal). Ten days following graft insertion, the sciatic

nerve was harvested as described above for nerve regeneration studies including 5 mm proximal to the graft and 5 mm distal. The four cohorts of donor grafts to host nerve consisted of: i) WT nerve growing through the WT graft to the WT distal stump (WT \rightarrow WT \rightarrow WT); ii) α BC^{-/-} nerve growing through the WT donor graft to the α BC^{-/-} distal stump (α BC^{-/-} \rightarrow WT \rightarrow α BC^{-/-}); iii) the WT nerve growing through the α BC^{-/-} donor graft to the WT distal stump (WT \rightarrow α BC^{-/-} \rightarrow WT), and iv) α BC^{-/-} nerve growing through the α BC^{-/-} donor graft to the α BC^{-/-} distal stump (α BC^{-/-} \rightarrow α BC^{-/-} \rightarrow α BC^{-/-}).

Tissue Collection: Tissue collection was completed as described in Chapter 2 at 1 and 3 days for DRG analysis (1), 14 days for nerve regeneration analysis (2), and 17 days for nerve graft regeneration analysis (3), respectively. Nerve regeneration microscopy and data analysis were completed by Paige Hardy during an undergraduate research project under my supervision.

Microscopy: Microscopy was completed as described in Chapter 2.

Western Blots: Western blots were completed by Susanne Lingrell. Protein was isolated from DRGs and sciatic nerve seven days following crush or from unconditioned naïve tissue by homogenizing with RIPA buffer (Pierce 89901) supplemented with HALT protease inhibitor (Thermo 1861281), sonication, and centrifuging at 14000 rpm for five minutes. Concentrations of protein were determined using a BCA protein assay kit (Thermo 23227). This included loading 25 μ L of each sample in RIPA buffer and HALT protease inhibitor into each well of gel cassettes and incubated at 37 °C for 30 minutes. The following day, the samples were loaded and underwent electrophoresis by first preparing the samples based on the BCA protein

quantification, supplementing with RIPA buffer and protease inhibitor, and boiling for five minutes. Protein samples (25 μ L/lane) underwent electrophoresis at 60V for 20-30 minutes, and then increased to 100V until the bands reached the bottom of gel. The samples were then transferred onto PVDF membrane and imaged with GAPDH as a loading control. The following day, the membranes were visualized with antibodies by first washing in methanol for 5 minutes followed by TBS for 10 minutes three times. All membranes underwent blocking for one hour in 5% BSA/TBS-T. Membranes were washed two times with TBS-T for 10 minutes each before the primary antibodies were added. Samples were covered and left to incubate overnight at 4°C. The following day, samples were washed twice with 1X TBS and twice with 1X TBS-T for 10 minutes each before the secondary antibody (Anti-rabbit HRP; 1:5000; Invitrogen, 31430) was applied and left for one hour at room temperature. Membranes underwent washing twice with 1X TBS, twice with 1X TBS-T for 10 minutes once more before the membranes were applied to the Chemidoc machine for signal detection and band imaging. Specific procedures are listed below in Figure 4.5.1.

Immunohistochemistry: IHC was completed as stated in Chapter 2, with specific antibody procedures listed below in Figure 4.5.2.

Statistical Analysis: Experimental results are written as the mean \pm standard error mean (s.e.m). Significance of RAG analysis and lengths of regeneration were determined using a one-way analysis of variance (ANOVA) to determine any differences in the mean between groups followed by a post-hoc Dunnett's test to compare experimental groups against unconditioned animals. A level of $p < 0.05$ was the cut-off for statistical significance. To determine statistical

significance between axon counts, a two-way ANOVA was completed to determine differences between the mean of each group in a paired data set followed by Dunnett's post-hoc for comparison against unconditioned animals. To compare between knock-out mice and wildtype mice unpaired t-tests were performed on each group. Statistics were completed using Prism 9.3.1 (GraphPad Software, San Diego, CA).

4.3 Results

4.3.1 Biomics identifies a difference between DRG alphaB-crystallin expression following CES and CCL.

To identify key players that might be involved in the conditioning effect of CES compared to CCL, DRG were harvested from Sprague-Dawley rats 1-day post-conditioning. These tissue samples alongside those from unconditioned animals (n=2 animals/cohort) underwent mass spectrometry and comparative microarray analysis. The heat shock protein, α BC was selected for further analysis as it was decreased 22-fold from naïve tissues following CES and decreased by 4.4-fold following CCL (Figure 4.5.3). We speculated that this 5-fold discrepancy between CES and CCL may lead to a further understanding of the mechanism of these conditioning effects on nerve regeneration.

4.3.2 The heat-shock protein α BC is upregulated 3 days following CES, but not CCL conditioning.

We performed western blot analysis to confirm the expression levels of α BC in CES and CCL conditioning paradigms (Figure 4.5.3). Unfortunately, we determined that unlike our biomics analysis, there were no significant differences in CES or CCL α BC expression 1-day post-conditioning, compared to naïve samples (Figure 4.5.3). Interestingly, we demonstrated that there was an upregulation of α BC in the DRG following CES whereas there was no change in CCL α BC expression.

To investigate the role of α BC in peripheral nerve regeneration further, we obtained α BC $-/-$ mice from the Ousman Laboratory at the University of Calgary (Lim et al., 2017). We first

confirmed that these knock-out mice were the correct phenotype through western blot analysis of α BC DRG and heart (positive control) of WT and α BC^{-/-} mice. Our analysis confirmed α BC^{-/-} mice had a decrease in the 22 kDa α BC protein compared to WT (Figure 4.5.3). We went on to assess Schwann cell protein MP0 to determine if an ablation of α BC affected myelination as it had been identified to be involved in the deficit of their ability to switch from de-differentiating Schwann cells to myelinating Schwann cells, thereby producing impaired remyelination and recovery after nerve injury (Lim et al., 2017). We observed a decrease in Schwann cell protein MP0 in α BC^{-/-} mice which supports the findings by Lim et al., that loss of α BC protein affects Schwann cell function (Figure 4.5.3).

4.3.3 CES and CCL promote DRG RAG upregulation in WT and α BC^{-/-} mice

To determine the role of α BC in the pro-regenerative response to CES and CCL at the DRG, regeneration-associated gene (RAG) levels were measured in α BC^{-/-} and WT mice. The sciatic nerve of α BC^{-/-} mice were conditioned by CES or CCL to compared to unconditioned mice (n=4/cohort). Animals were euthanized on days 1 or 3 post-conditioning, and their L4, L5 DRGs were harvested and processed for tissue sectioning (9 μ m). Immunohistochemistry demonstrated increased cytosolic expression of growth-associated protein 43 (GAP-43) in animals following CES (70.6 a.u. \pm 2.3 a.u.; $p < 0.05$) and CCL (70.9 a.u. \pm 6.8 a.u.; $p < 0.05$) compared to the unconditioned, baseline expression (45.8 a.u. \pm 18.9 a.u.) (Figure 4.5.4). These data confirm that CES and CCL promote RAG upregulation at the DRG regardless of α BC protein expression.

4.3.4 Similar to WT mice, CCL, but not CES α BC^{-/-} mice promotes ATF3 expression within DRG neurons.

One day post-conditioning, CCL showed a significant increase in ATF3 immunofluorescence at the nucleus ($42.3\% \pm 12.8\%$, $p < 0.01$), unlike CES ($5.5\% \pm 1.6\%$, $p > 0.05$) compared to unconditioned controls ($0.0\% \pm 0.0\%$) (Figure 4.5.4). There were no significant differences between $\alpha BC^{-/-}$ mice and WT mice ($p > 0.05$; Figure 4.5.4).

4.3.5 $\alpha BC^{-/-}$ mice display inherently increased pCREB expression compared to WT mice.

At 3 days post-conditioning, no difference was found in phosphorylated cyclic adenosine monophosphate (cAMP) response element binding protein (pCREB) expression at the DRG nuclei following CCL ($42.9\% \pm 3.2\%$) or CES ($45.4\% \pm 1.0\%$) compared to unconditioned animals ($39.8\% \pm 0.4\%$). However, all $\alpha BC^{-/-}$ groups had significantly increased pCREB protein expression compared to their WT counterpart (CES $p < 0.001$; CCL $p < 0.05$; unconditioned $p < 0.01$) (Figure 4.5.4). Furthermore, Western Blot showed an upregulation of pCREB expression in DRGs of knock-out mice compared to WT animals (Figure 4.5.4). After this, we also completed western blot analysis to see if there was an upregulation of pathways interacting with pCREB. We found an upregulation of both phosphorylated extracellular signal-regulated kinases 1/2 (pERK-1/2) and ERK-1/2 protein in $\alpha BC^{-/-}$ mice compared to WT mice DRGs (Figure 4.5.4). Overall, this data indicates $\alpha BC^{-/-}$ mice have a baseline upregulation of pCREB and ERK-1/2 expression.

4.3.6 The loss of αBC protein did not influence the pro-regenerative conditioning effects of CES or CCL.

We investigated the role of αBC in the pro-regenerative effects of CES and CCL by comparing nerve regeneration in WT and $\alpha BC^{-/-}$ mice one week following nerve repair surgery

(Figure 4.5.5). The extent of regeneration in $\alpha BC^{-/-}$ mice was determined seven days following a sciatic nerve repair surgery in which the animals were previously conditioned by CES, CCL or left unconditioned (n=6/cohort). Immunohistochemistry against neurofilament 200 (NF200) allowed the quantification of the number of axons regenerating past the site of coaptation (Figure 4.5.5) Similar to WT animals, both CES and CCL conditioning in $\alpha BC^{-/-}$ mice accelerated nerve regeneration. These nerves had highly significantly increased numbers of axons extending past the site of coaptation with the mean maximum numbers reaching 64.4 ± 6.8 axons and 46.6 ± 3.1 axons, for CES and CCL animals respectively, compared to unconditioned animals with 34.1 ± 3.6 axons. Further, both conditioned groups attained significantly greater distances of regeneration, despite a lack of αBC protein. The distance of regeneration following CES was $5.4 \text{ mm} \pm 0.6 \text{ mm}$ ($p < 0.01$) and CCL was $4.8 \text{ mm} \pm 0.5 \text{ mm}$ ($p < 0.01$), whereas unconditioned animals only reached $2.3 \text{ mm} \pm 0.4 \text{ mm}$, indicating the presence of a pro-regenerative conditioning effect following CES and CCL. Furthermore, there were no significant differences between $\alpha BC^{-/-}$ mice and their WT counterparts including mean WT lengths following CCL ($5.6 \text{ mm} \pm 0.6 \text{ mm}$), CES ($5.4 \text{ mm} \pm 0.2 \text{ mm}$), and unconditioned ($3.1 \text{ mm} \pm 0.7 \text{ mm}$).

4.3.7 Loss of αBC in the regenerating environment does not affect nerve growth.

As αBC affects Schwann cell ability to switch back to a myelinating phenotype (Figure 4.5.3; Lim et al., 2017), we sought to determine if the loss of this heat-shock protein would affect the proliferative environment which includes Schwann cells essential for nerve regeneration distal to the injury site. We investigated how the regenerating axons from $\alpha BC^{-/-}$ mice and WT mice response to nerve grafts distal to the injury site comprised of $\alpha BC^{-/-}$ or WT Schwann cells. A separate cohort of donor mice underwent sciatic nerve graft surgeries. Each donor animal

contributing their sciatic nerve, $\alpha BC^{-/-}$ (n=8) and WT (n=8) underwent a sciatic nerve crush to evoke Wallerian degeneration and subsequent induction of a regenerative environment including enhanced proliferative Schwann cells. Seven days following the donor crush surgery, $\alpha BC^{-/-}$ (n=8) and WT (n=8) host mice were placed under anesthesia, their sciatic nerves were transected, and a 5 mm donor nerve graft was coapted distal to the crush. Ten days following graft insertion these sciatic nerves, consisting of proximal host nerve coapted to donor graft coapted to the distal host nerve, were harvested, cryosectioned, and processed for NF200 immunohistochemistry and analysis to assess the extent of regeneration (Figure 4.5.6). Thus, the regenerating host nerve will extend through the graft to the host's distal nerve stump, depicted hereafter as (Host→Donor→Host). Therefore, the groups consisted of WT nerve growing through the WT graft to the WT distal stump (WT → WT → WT); $\alpha BC^{-/-}$ nerve growing through the WT donor graft to the $\alpha BC^{-/-}$ distal stump ($\alpha BC^{-/-}$ → WT → $\alpha BC^{-/-}$); the WT nerve growing through the $\alpha BC^{-/-}$ donor graft to the WT distal stump (WT → $\alpha BC^{-/-}$ → WT), and the $\alpha BC^{-/-}$ nerve growing through the $\alpha BC^{-/-}$ donor graft to the $\alpha BC^{-/-}$ distal stump ($\alpha BC^{-/-}$ → $\alpha BC^{-/-}$ → $\alpha BC^{-/-}$). The maximal mean lengths of regeneration attained were: 4.2 mm \pm 0.2 mm (WT → WT → WT); 3.1 mm \pm 0.4 mm ($\alpha BC^{-/-}$ → WT → $\alpha BC^{-/-}$); 3.6 mm \pm 0.6 mm (WT → $\alpha BC^{-/-}$ → WT); and 3.0 mm \pm 0.9 mm ($\alpha BC^{-/-}$ → $\alpha BC^{-/-}$ → $\alpha BC^{-/-}$). When all animals/cohort were averaged however, there were no significant differences between any of the experimental groups including no difference in growth through a regenerative environment lacking αBC compared to WT regenerative environments. Furthermore, there were no differences between inherent growth of $\alpha BC^{-/-}$ mice compared to WT mice.

4.4 Discussion

Our western blot data observed a decrease in MP0 and S100 protein expression suggesting a decrease in Schwann cells in $\alpha BC^{-/-}$ tissue. This supports similar findings from the Ousman laboratory who found a significant decrease in S100b protein expression in naïve nerve and a decrease in myelinated Schwann cells but not total Schwann cell counts following nerve injury. Their data demonstrated an increase in proliferating Schwann cells in $\alpha BC^{-/-}$ mice (Lim et al., 2017). As this group showed a decrease in the number of myelinating Schwann cells and their *in vitro* work showed there was similar neurite extension associated with $\alpha BC^{-/-}$ and WT mice following sciatic nerve injury, it suggested that αBC does not affect axonal regeneration. This led us to investigate if αBC affects the environment through which nerves regenerate *in vivo*. Our data showed that there was no difference in the extent of nerve regeneration between naïve $\alpha BC^{-/-}$ and WT nerves. We went on to determine if αBC is involved in the conditioning effect. We confirmed that CES and CCL increased the number of regenerating axons and accelerated their length of nerve regeneration in both $\alpha BC^{-/-}$ and WT mice suggesting that αBC does not have a role in axon regeneration or conditioning.

Despite genetic modification, $\alpha BC^{-/-}$, animals portrayed a similar DRG phenotype to WT animals post-conditioning. ATF3 was upregulated in animals that underwent CCL, consistent with WT animals, supporting our Chapter 2 and 3 findings that demonstrated that CCL, unlike CES, is injurious. Further, animals displayed an upregulation of GAP-43 following both CES and CCL, indicating the persistence of a pro-regenerative effect following conditioning, compared to unconditioned, naïve animals. Interestingly, pCREB was not significantly different in $\alpha BC^{-/-}$ CES, CCL, or unconditioned animals likely due to the increased innate pCREB expression in the $\alpha BC^{-/-}$ mice compared to WT DRG counterparts.

Recent research by Wang et al., revealed a potential reciprocal relationship with CREB and α BC that could explain the discrepancy between α BC^{-/-} mice and pCREB expression (Wang et al., 2020). Interestingly, CREB^{-/-} animals demonstrated an upregulation of α BC protein expression under conditions of stress; CREB was found to suppress the α BC gene through negative regulation of the α BC promoter at multiple sites (Wang et al., 2020). With an inherently elevated expression of pCREB, it might follow that nerve regeneration could be increased in unconditioned α BC^{-/-} animals similar to that produced by a conditioning paradigm, and indeed in literature it has been demonstrated that constitutive activation of CREB increases regeneration (Gao et al., 2004). However, we did not observe a change in length of nerve regeneration of α BC^{-/-} or WT mice *in vivo*. These data support previous studies showing that DRG neurite outgrowth from α BC^{-/-} DRG neurons is similar to WT mice (Lim et al., 2017). Further, the pro-regenerative effects of CES or CCL was not altered in the absence of α BC *in vivo*.

In addition to increased pCREB DRG expression in α BC^{-/-} mice, we found an increase in baseline expression of ERK-1/2 and pERK-1/2 protein at the DRGs of unconditioned α BC^{-/-} mice compared to WT. Increased pERK1/2 expression has been shown to increase nerve regeneration; however, in the α BC^{-/-}, this elevated ERK and pERK did not translate into enhanced regeneration. As well, this finding contrasted with what the Ousman laboratory found, as they did not show changes in pERK1/2 protein expression in naïve and crushed sciatic nerve tissue from α BC^{-/-} mice (Lim et al., 2019). Similarly, it is possible that these inherent upregulations of pCREB and ERK-1/2 are compensating for a loss of α BC, or some necessary interaction of α BC which is why we do not see any effects on nerve regeneration in these knock-out mice compared to WT.

Interestingly, $\alpha\text{BC}^{-/-}$ mice have been demonstrated to display enhanced inflammatory responses as there are elevated IBA-1⁺ cells and increased cytokine release including IL-6, IL-1 β , and TNF- α (Lim et al., 2021). As inflammation is associated with increased regeneration, as shown with our CCL conditioning effect on nerve regeneration discussed in Chapter 3), it is evident that this enhanced inflammation did not translate to mimicking the conditioning effect in unconditioned animals, nor did it affect the impact of CCL or CES to accelerate nerve regeneration. From this data, it is possible that the enhanced inflammation is not enough to elicit a conditioning effect and that potentially this pro-inflammatory response is also not detrimental to the health of these mice in nerve regeneration, though enhanced inflammation was hypothesized to be detrimental in nerve regeneration by prolonging macrophage presence (Lim et al., 2021). More research is needed to determine whether the enhanced inflammatory response associated with $\alpha\text{BC}^{-/-}$ mice is detrimental to functional recovery following nerve injury or enhances the pain response of such injuries, however, based on our findings it is likely that functional recovery would be similar to WT mice, and therefore the elevated inflammatory response is within an acceptable realm.

Next, we wanted to specifically assess whether the regenerative environment lacking αBC affected nerve regeneration. Lim et al., established there is a prolonged presence of proliferative Schwann cells a month following nerve injury and a decrease in myelinating Schwann cell population (Lim et al., 2017). In addition, we observed a decrease in SC protein expression in $\alpha\text{BC}^{-/-}$ following nerve injury (Figure 4.5.3). We speculated, therefore, that the regenerative milieu was altered in $\alpha\text{BC}^{-/-}$ mice which could impact nerve regeneration across the injury site. The insertion of $\alpha\text{BC}^{-/-}$ donor grafts into WT tissue, we allow us to determine if WT axon regeneration was affected as these axons grew into a graft from $\alpha\text{BC}^{-/-}$ mice. Likewise, the

insertion of WT donor grafts into α BC^{-/-} mice, could determine if the WT regenerative milieu rescued any deficits associated with the loss of α BC in the axons. However, we did not observe any differences in WT or α BC^{-/-} axons regenerating through the WT or α BC^{-/-} grafts (Figure 4.5.6) leading us to conclude that nerve regeneration is unaffected by a loss of α BC. It is possible there is compensation by other heat-shock proteins or signaling pathways (such as the upregulation of CREB) that overcomes the loss of α BC. The small number of animals (n=4/cohort) is a limitation of this study and we plan to repeat this experiment to increase our n numbers.

Overall, the data from our studies on α BC indicate that this heat-shock protein does not have a role in innate nerve regeneration or the conditioning effect (CES or CCL) that accelerate nerve regeneration. Further, the innate increase in pCREB, ERK-1/2 and pERK- $\frac{1}{2}$ expression, we demonstrated in the α BC^{-/-} DRG following nerve injury may compensate for the deficits associated with α BC loss. Alternatively, these changes in protein expression may have an independent and unknown role separate from nerve regeneration. In conclusion, the impaired functional recovery, and reduced conduction velocity in α BC^{-/-} mice shown by the Ousman lab may be due solely to remyelination deficits, and not deficits in nerve regeneration (Lim et al., 2017).

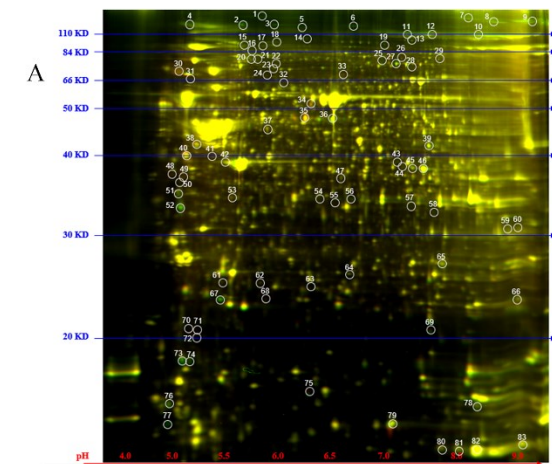
4.5 Figures

Primary Antibody	Tissue Collected	Gel Concentration	Primary Antibody Dilution	Tissue Concentration Loaded
α BC Millipore ABN185	DRG α BC ^{-/-} ; WT	12.5%	1:1000	16 μ g
α BC	Nerve α BC ^{-/-} ; WT	12.5%	1:1000	16 μ g
α BC	Heart α BC ^{-/-} ; WT	12.5%	1:1000	5 μ g
α BC	Brain WT	12.5%	1:1000	10 μ g
α BC	RAT DRG	12.5%	1:5000	25 μ g
pCREB	DRG α BC ^{-/-} ; WT	12.5%	1:1000	25 μ g
ERK1/2 Santa Cruz sc-94	DRG α BC ^{-/-} ; WT	12.5%	1:250	18.5 μ g
pERK-1/2 Cell Signaling 4377	DRG α BC ^{-/-} ; WT	12.5%	1:1000	18.5 μ g
MP0 Millipore ABN363	DRG α BC ^{-/-} ; WT	15%	1:1000	5-6 μ g
S100 Sigma- Aldrich S2644	DRG α BC ^{-/-} ; WT	15%	1:2000	5-6 μ g
GAPDH Ambion 4300	DRG α BC ^{-/-} ; WT	15%	1:10000	10 μ g

Figure 4.5.1 Primary and Secondary Antibody Protocols for Western Blot

Primary Antibody	Antigen Retrieval 40 minutes in 60 °C citrate buffer (10mM sodium citrate, 0.05% Tween-20, pH 6.0)	Primary Antibody Dilution	Secondary Antibody	Secondary Antibody Dilution
ATF3 (rabbit) Abcam 207434	Yes	1:500	AlexaFluor 488 goat anti-rabbit Invitrogen, Carlsbad, CA A-11008	1:1000
pCREB (rabbit) Cell Signalling 9198	Yes	1:500	AlexaFluor 488 goat anti-rabbit	1:1000
NF200 (rabbit) Sigma-Alrich N4142	No	1:500	AlexaFluor 488 goat anti-rabbit	1:500
GAP-43 (rabbit) Novus Biochemicals Centennial, CO NB300-143	No	1:500	Alexa Fluor 488 goat anti-rabbit	1:1000

Figure 4.5.2: Primary and Secondary Antibodies Used for immunohistochemistry



B

Protein Expression Ratio		
#2 CCL / #1 Naive	#3 CES / #1 Naive	#3 CES / #2 CCL
-4.4	-22.2	-5.0

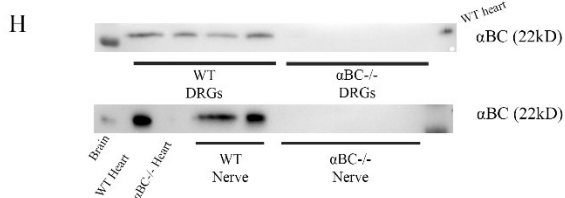
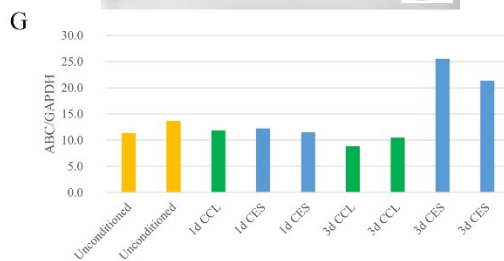
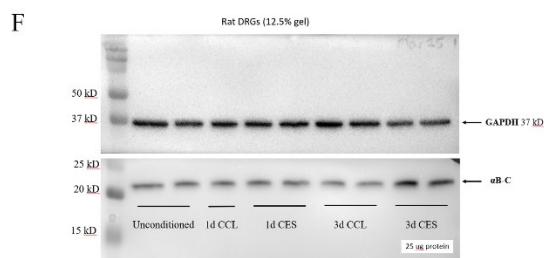
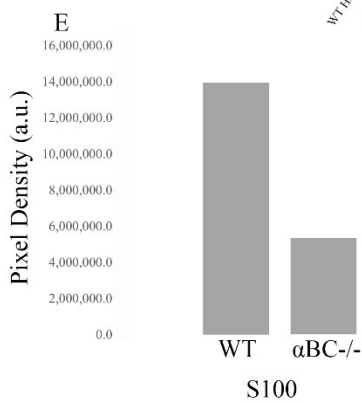
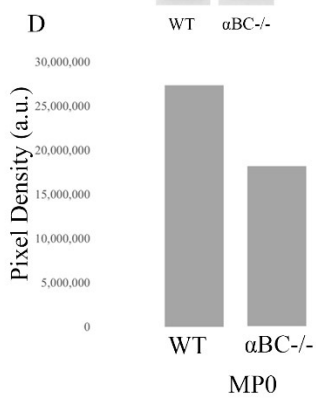
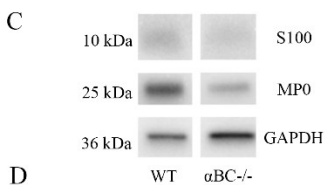


Figure 4.5.3 The heat-shock protein, α BC, is unchanged 1 day following CCL and CES compared to unconditioned Sprague-Dawley rats, but upregulated 3 days post-CES.

A) Microarray analysis of Sprague-Dawley DRGs 1 day following CCL, CES, or no-conditioning separated by mass spectrometry. B) Protein expression ratio of α BC from mass spectrometry showing a 22.2 fold decrease in CES compared to naïve DRG, 4.4 fold decrease in CCL compared to naïve, and a 5.0 fold decrease in CES compared to CCL. C) MP0 western blot analysis of naïve WT and α BC^{-/-} mouse DRGs. D) Western blot densitometry quantification of MP0 protein in arbitrary units of WT and α BC^{-/-} naïve mouse DRG (a.u.) (n=1). E) Western blot densitometry quantification of S100 protein in arbitrary units of WT and α BC^{-/-} naïve mouse DRG (a.u.) (n=1). F) α BC western blot of unconditioned, CCL and CES L4, L5 DRGs. G) Western blot quantification indicating no change in α BC levels at 1 day post-conditioning with an upregulation at 3 days only following CES and not CCL. H) Western blots for α BC protein at 22 kDa of the DRG and sciatic nerve in WT mice compared to α BC^{-/-} mice.

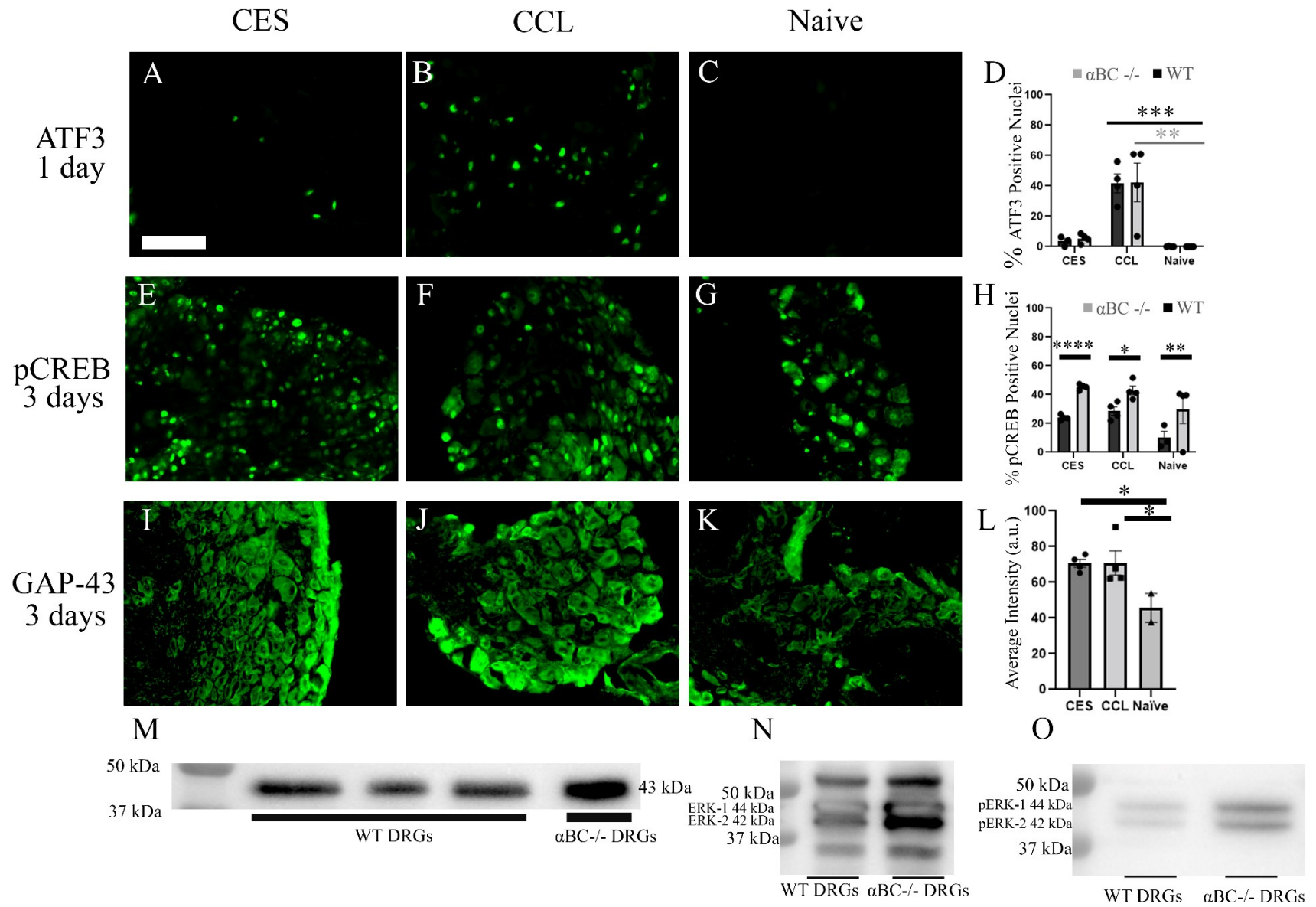


Figure 4.5.4: CES and CCL upregulated RAGs in WT and α BC^{-/-} mice, whereas there is an increase in pCREB expression in the unconditioned α BC^{-/-} DRG.

A-D) The immunohistochemical expression of ATF3 1-day post-conditioning following A) CES, B) CCL, or C) no-conditioning (n=4/cohort). D) The percentage of ATF3 positive nuclei. E-H) The immunohistochemical expression of pCREB 3-days following E) CES, F) CCL, or G) no-conditioning (n=4/cohort). H) The percentage of pCREB positive nuclei. I-L) The average intensity of GAP-43 immunofluorescence 3 days following I) CES J) CCL or K) no-conditioning (n=4/cohort). M) Western blot analysis showing increased pCREB protein at 43 kDa in knockout mice compared to WT. N-O) Western blot of N) ERK-1/2 and O) pERK-1/2 signals that are increased in α BC^{-/-} DRG compared to WT control. The scale bar in A is 100 μ m (*p<0.05, **p<0.01, ***p<0.001).

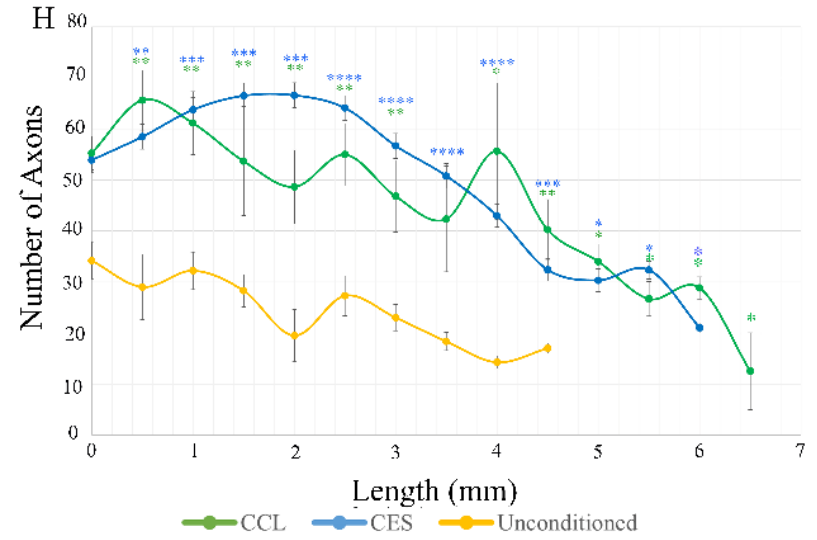
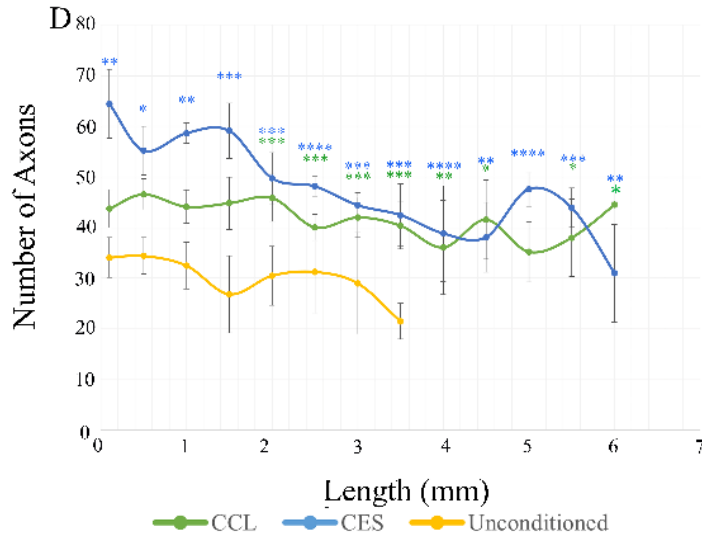
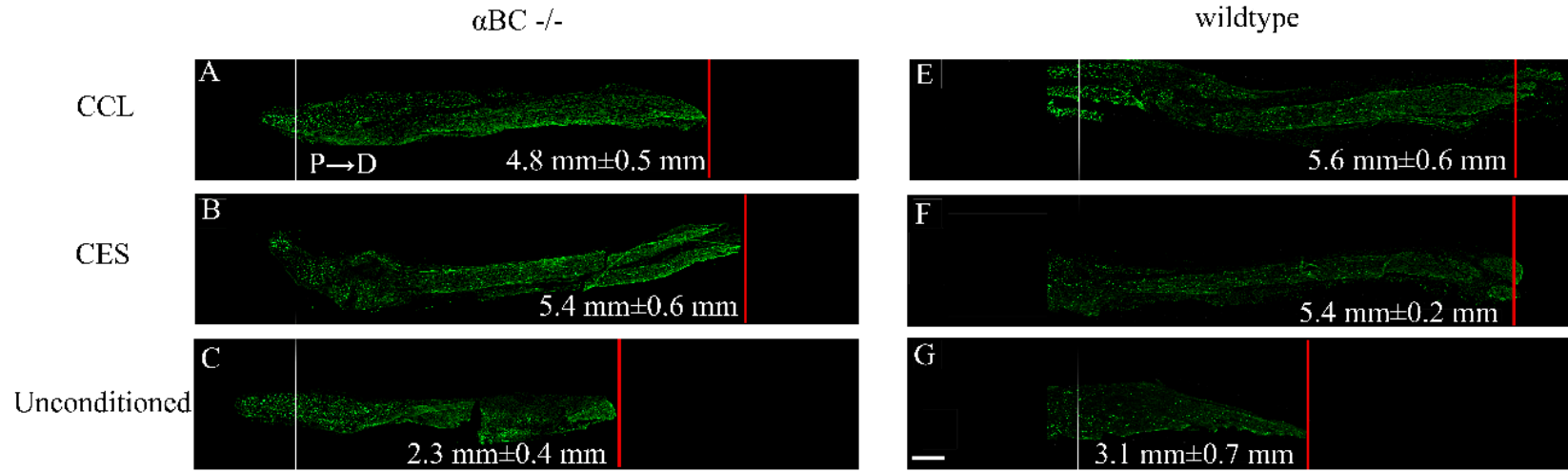


Figure 4.5.5: α BC protein does not influence the pro-regenerative effects of CES and CCL.

A-C) NF200 immunofluorescent images of longitudinal sciatic nerve sections at 7 days following surgical transection and repair of α BC^{-/-} mice that had received either A) CCL, B) CES, or C) no-conditioning (n=6/cohort). The coaptation site was approximated by the white line (A-C). D) The number of axons and extent of nerve regeneration from the surgery repair site in α BC^{-/-} mice was counted every 0.5 mm until less than 10 axons were observed. E-G) Representative NF200 immunofluorescent images of longitudinal sciatic nerve sections at 7 days following surgical transection and repair of WT animals that had received either E) CCL, F) CES, or G) remained unconditioned (n=6/cohort). The coaptation site was approximated by the white line in E-G. H) The number of axons and extent of nerve regeneration from the surgery repair site in wildtype animals were counted every 0.5mm until less than 10 axons were observed. The scale bar indicates a length of 500 μ m (* p <0.05, ** p <0.01, *** p <0.001).

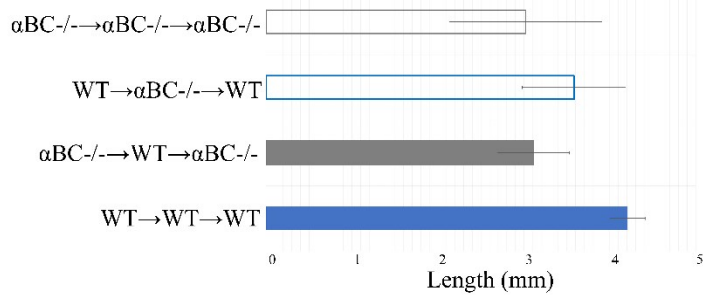
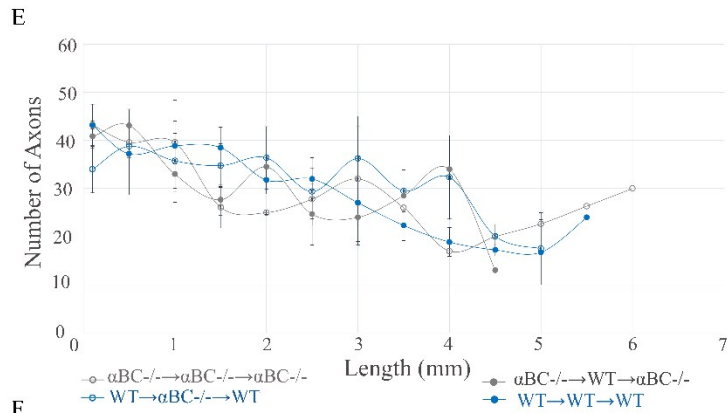
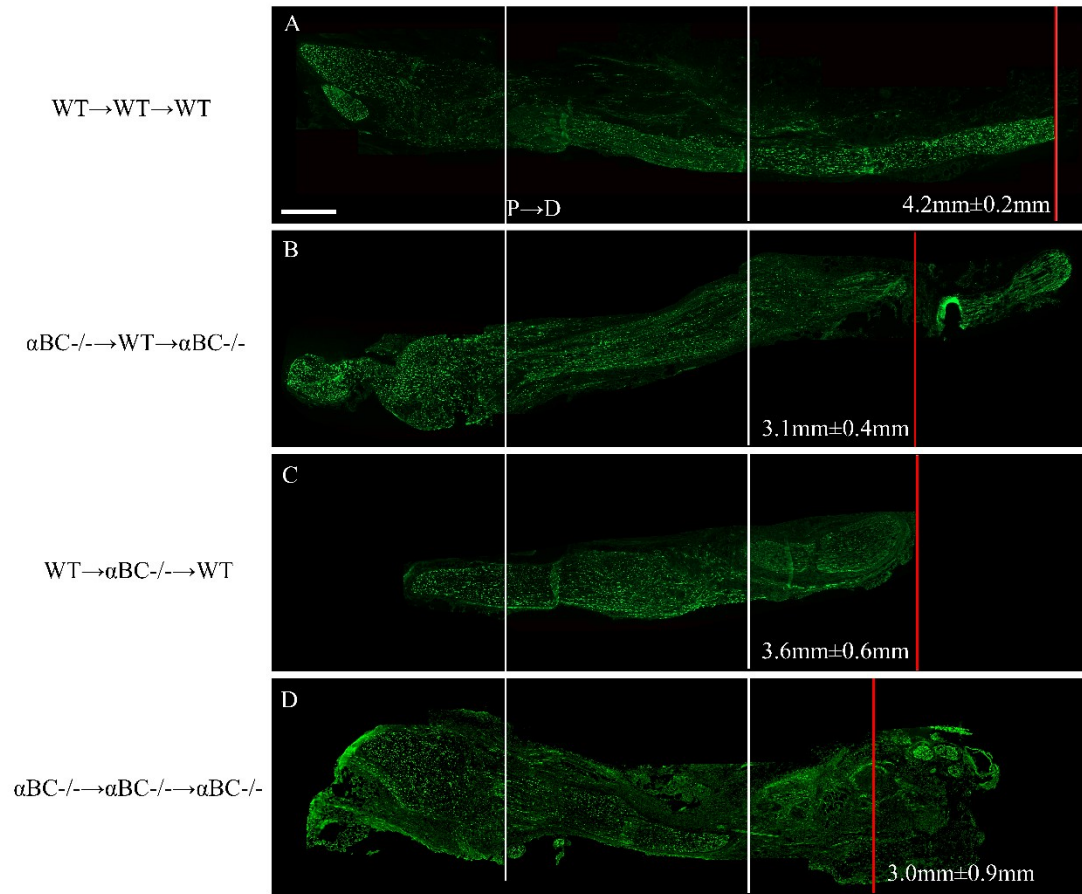


Figure 4.5.6 A lack of α BC in the nerve growth environment does not affect sciatic nerve growth through a graft.

A-D) Representative longitudinal sections of NF200 immunolabelled sciatic nerves 10 days following 5 mm sciatic nerve graft surgery. Grafts (WT or α BC^{-/-}) were inserted into sciatic nerves of host WT or α BC^{-/-} mice. White lines depict proximal and distal sites of coaptation of the donor graft into the host mouse. Nomenclature of donor graft to host combinations depicted as 'host nerve → donor → host nerve' (n=4/cohort). A) WT → WT → WT, B) α BC^{-/-} → WT → α BC^{-/-}, C) WT → α BC^{-/-} → WT, D) α BC^{-/-} → α BC^{-/-} → α BC^{-/-}. E) The number of axons and the extent of regeneration from the first surgery repair site every 0.5 mm until less than 10 axons were observed (red line). F) The mean lengths achieved by each condition of growth. The scale bar in A indicates a length of 500 μ m.

Discussion

Our present data indicate that CES is translatable from Sprague-Dawley rats to mice, with a persistent upregulation of RAGs and enhanced nerve regeneration. Furthermore, our data strongly supports the hypothesis that CES is non-inflammatory and non-injurious as both TRMs and monocyte-derived monocytes were not involved in the conditioning response, and not necessary for pro-regenerative effects following their ablation. Lastly, our data indicates that α BC does not play a role in the conditioning effect but could have potential interactions in various pathways associated with regeneration due to the inherently high pCREB expression associated with decreased α BC.

Our data supports our hypothesis that CES is non-injurious and does not evoke an inflammatory response. In both Sprague-Dawley rats and WT mice, CES generates a pro-regenerative environment through RAG upregulation at the DRG and increasing both the number of regenerating axons and accelerating nerve regeneration. CES does not generate an overt inflammation response as indicated by the lack of swelling through gross observation of the nerve, lack of Wallerian degeneration past the conditioning site, and the lack of injury marker ATF3 at the DRG.

To further support CES as a pro-regenerative conditioning strategy safe for clinical translation, it would be pertinent to demonstrate more data through various other methodologies that indicate improved nerve regeneration. Our immunohistochemical analysis of regenerating axons consisted solely of NF200, which labels larger diameter axons. To be inclusive of all axon fiber types this analysis could be supplemented with other axonal markers including SCG10, a tubulin destabilization marker that accumulates in the regenerative tips of growing axons, PGP 9.5 for small diameter axons, betaIII-tubulin, a pan-specific marker, or CGRP which accumulates

in the growth cones of small diameter neurons (Shin et al., 2014; Dalsgaard et al., 1989; Hossain-Ibrahim et al., 2007; Burry et al., 1992; Ferreira and Caceres, 1992; Zochodne 2009). Assessment of more regeneration markers and indices will allow for not only direct axonal regeneration data, but also whether or not this translates into better motor and sensory recovery in mice.

Strategies other than immunohistochemistry are needed to assess functional recovery from nerve injury. Electrophysiological strategies such as compound muscle axon potentials (CMAPs) assess motor axon function/recovery, and sensory analyses such as von Frey filaments and Hargreaves can test for mechanosensory and heat sensitivity, respectively (Mallik and Weir, 2005; Deuis et al., 2017; Hargreaves et al., 1988). Horizontal ladder testing and sciatic functional index analyses can measure motor and functional recovery (Metz and Whishaw, 2009; Antonow-Schlorke et al., 2013; Shen and Zhu, 1995). We used these motor and sensory assays to show CES promotes nerve regeneration in rats; however, we did not confirm the role of CES in functional recovery in our mice studies (Senger et al., 2019, 2020, 2021). It is reasonable to assume that since CES accelerated nerve regeneration in our mice studies in a comparable manner to our rat studies; however, these experiments should still be performed to ensure there are no interspecies differences that occur following CES.

Our work did not include *in vitro* analyses of nerve regeneration and in the future, we will compare the effect of CES on Sprague-Dawley and WT mice (Filous and Silver, 2016; Zochodne, 2009). Singh et al., (2009) clearly showed electrical stimulation promoted neurite extension in DRG neuronal cultures compared to control (not electrically stimulated) neurons (Singh et al. 2009). We predict that CES prior to culturing mouse WT DRG neurons will have the growth promoting effects shown in rat (Udina et al., 2008; Wei et al., 2014). *In vitro* assays

allow for pathway assessment, and the use of transgenic mice or various antagonistic or pharmacological compounds may determine the signaling pathways responsible for the CES-induced growth promoting effect. Further, our laboratory would like to apply CES prior to mouse neuronal culture as performed by Udina et al., (2008) in rat. Specifically, we intend to quantify neurite extension cultured for 24 hours from DRG neurons harvested 3 days after CES and CCL conditioning. Singh et al., determined that the growth promoting effect of electrical stimulation in DRG neurons was blocked by pharmacological inhibition of the PI3K pathway (Singh et al 2009). It would be interesting to utilize a transgenic mouse that could block the PI3K pathway in DRG neurons prior to CES to determine if this pathway is the mechanism through which CES exerts its conditioning effects *in vivo*.

To support the safe translation of CES, we confirmed this modality does not induce axonal injury or inflammation. PES is deemed clinically safe and uses the same paradigms as CES; however, it is performed after a nerve repair surgery when the nerve has already been transected. Therefore, it is difficult to determine if PES evokes inflammation or nerve injury. As CES is performed prior to nerve repair surgery, we are able to assess if it causes nerve injury or a local inflammatory response. (Chan et al., 2016; Gordon et al., 2010; Wong et al., 2015; Barber et al., 2018; Power et al., 2020; Zuo et al., 2020). Our data confirmed that CES does not cause Wallerian degeneration or gross inflammation (i.e. increase in Iba-1 macrophage expression) at the nerve and it did not upregulate injury marker ATF3 in the DRG neuronal cell bodies. We went on to directly measure specific immune cells responsible for the inflammatory response following nerve regeneration and CCL conditioning. Our data corroborated what is established in the literature: CCL relies on the infiltration and activation of monocyte-derived macrophages to produce a pro-regenerative response (Lu and Richardson, 1991; Kwon et al.,

2015; Niemi et al., 2013; Senger et al., 2019). Alternatively, CES showed minimal monocyte-derived macrophage infiltration comparable to naïve animals suggesting it is not inducing inflammation at the nerve or the DRG.

We initially hypothesized that TRMs may be involved in the conditioning response of CES, as these immune cells have been shown to support homeostatic, reparative, and anti-inflammatory responses more so than monocyte-derived macrophages (Mueller et al., 2003; Ydens et al., 2012; Zhao et al., 2018; Hashimoto et al., 2013). We also hypothesized that TRMs may be upregulated/activated in animals receiving CCL as they have been shown to proliferate and activate following nerve injury (Ydens et al., 2012; Ydens et al., 2020; Davies et al., 2013; Mueller et al., 2001; Krishnan et al., 2018). Our data did not support this conclusion, as the number of TRMs and their activity, determined by dectin-1 expression were comparable in CES and CCL. Though our data thus far indicates TRMs do not play a key role in the mechanisms of CCL and CES, the possibility that they do indeed have some kind of effect cannot be discounted. Repeating our TRM fate-mapping experiment at various time points following conditioning could elucidate a role in the conditioning effect if TRM proliferation happened much earlier than anticipated. A three-day time point was chosen to be able to assess both RAGs and macrophages, as data indicates infiltration of monocyte-derived macrophages starts around day 2 whereas TRM proliferation typically occurs around day 1 and remains elevated at day 3; however, it would be important to fully assess the possibility of a different time-point before completely discounting TRM proliferation in response to CCL or CES (Ydens et al., 2012; Ydens et al., 2020). Likewise, more markers of TRM activation could be assessed with the possibility that TRMs do not upregulate dectin-1 following conditioning. CD68 may be an additional marker of TRM activation and should be measured.

Not only applicable to conditioning, but the possibility of an activation marker unique to TRMs could support the use of analyses such as immunohistochemistry without the use of genetic models, which can be expensive and difficult to implement experimentally. It would be interesting to determine if any receptors or proteins expressed by activated TRMs are different in DRG and nerve, as unique roles of TRMs in various tissues are being increasingly recognized in the literature (Lavin et al., 2014; Ydens et al., 2020). Furthermore, an assessment of cytokines released in CES and CCL would add strength to our data to determine, by ELISAs, if there is an increase in inflammatory cytokines associated with CES. If *in vivo* analysis demonstrated an upregulation of specific cytokines such as IL-6, in CES, but not CCL (or vice-versa), *in vitro* neurite extension with exogenous cytokines added could be assessed. Pharmacological inhibition or antagonizing of these cytokines could determine if a conditioning effect persists, confirming their role in CES-induced neurite extension. Further, co-cultures of TRMs and monocyte-derived macrophages with DRG neurons *in vitro* could provide additional data on the conditioning effect of CES. It would also be possible to assess if there are anti-inflammatory cytokine upregulations during the conditioning effect of CES. As dectin-1 is associated with pro-inflammatory activation, both immunohistochemistry of an anti-inflammatory activation marker or an analysis of anti-inflammatory cytokines following CES could demonstrate if the mechanism associated with CES relies on anti-inflammatory actions by TRMs, or infiltrating monocyte-derived macrophages (Schorey and Lawrence, 2008; Gensel et al., 2015).

Our data suggests that TRMs do not proliferate in response nerve conditioning via crush or electrical stimulation. Though research has shown increased TRM proliferation, activation, and phagocytotic roles in nerve injury, we did not observe these responses following CCL, which was contrary to our expectations (Ydens et al., 2012; Ydens et al., 2020; Davies et al., 2013;

Mueller et al., 2001; Krishnan et al., 2018). Potentially TRMs are only activated in more injurious cases such as complete nerve transection, and any consequences of their activation would need to be determined, as differing prognoses do exist following various types of nerve injury. This could impact how nerve injury patients are treated, for example, if activation of TRMs is deleterious to recovery/conditioning, potentially anti-inflammatory treatments would be beneficial prior to nerve surgery in patients. Overall, our data supports that CCL relies on infiltrating macrophages to produce a pro-regenerative effect following nerve injury and both CCL and CES do not rely on an overt inflammatory response by TRMs. More research is needed to fully determine whether there is any response by TRMs following CES and CCL conditioning, and whether or not this can impact nerve injury treatments beyond supporting CES as clinically feasible.

Finally, our work demonstrated that α BC expression does not affect nerve regeneration. This data supported the Ousman laboratory that showed α BC null mice did not have any differences in neurite extension (Lim et al., 2017). Our data demonstrated an upregulation of pCREB and pERK expression in uninjured α BC^{-/-} mice DRG which is novel and could have ramifications in other research studies. It is surprising that an upregulation of pCREB and pERK did not enhance nerve regeneration as several lines of evidence indicate increases in pCREB and the cAMP have pro-regenerative effects on nerve growth, and upregulation of the cAMP pathway is partly responsible for the mechanism of CCL (Wei et al., 2016; Chan et al., 2014; Gao et al., 2004; Cai et al., 1999; Blesch et al., 2012). Further exploration of pathways and molecules to elucidate this interaction between pCREB, pERK, and α BC will be important, not only to understand the relationship, but also potentially why there is no pro-regenerative response. By rescuing null mice with exogenous α BC and measuring pCREB and pERK levels,

we would be able to determine if their relationship is direct, or if there are other factors involved in these knock-out mice that might be affected by a lack of α BC and are creating the subsequent downstream effect of pCREB upregulation. As α BC has been shown to have beneficial effects on myelination and reducing inflammation, it would be interesting to see if upregulating α BC in WT animals could enhance nerve regeneration (Lim et al., 2017; 2021). As it is possible that the null mice experience deficits which mask any beneficial effects of increased pCREB, by further increasing α BC, potentially naïve nerves will display a pro-regenerative response, similar to conditioning. Furthermore, with α BCs connection to inflammation and the enhanced IBA-1 expression seen with null mice, it would be interesting to explore whether this upregulation is a result of enhanced monocyte-derived monocyte infiltration or TRM proliferation, and elucidate a possible connection between α BC and downregulating inflammation (Lim et al., 2021). Though α BC does not seem to play a role in the conditioning effect thus far, this research could provide beneficial information about nerve regeneration and generate data further indicating therapeutic potential for α BC, not only in supporting remyelination, but also in enhancing nerve regeneration.

Overall, this data indicates that monocyte-derived macrophages, TRMs, and α BC are not responsible for the pro-regenerative effects of CES; therefore, more specific research to determine the underlying mechanism responsible for CES-induced pro-regenerative effects has yet to be determined. As of our research thus far, part of the mechanism of CES is due to its upregulation of DRG RAGs expression, including GAP-43, pCREB, GFAP, and BDNF (Senger et al., 2019; 2020). Much is known about the pathways leading to their upregulation from both nerve injury paradigms and CCL conditioning including upregulation various pathways such as the JAK/STAT3 pathway, cAMP pathway, and PI3K pathway in injured neurons (Senger et al.,

2018; Wu et al., 2007; Cafferty et al., 2001; Cai et al., 1999). To further explore the mechanism of CES and how it may differ from CCL but ultimately produce the same RAG upregulation, targeting these pathways will be necessary. *In vitro* work suggests the PI3K pathway may be responsible for the RAG upregulation following electrical stimulation (Singh et al., 2009). Additionally, the pharmacological inhibition of the JAK/STAT3 pathway using AG490 could be used to assess whether or not CES continues to display a pro-regenerative response. As we are aware of what happens to CCL, it can be used as a control for targeting these pathways. Though the mechanisms of CES and CCL may converge to upregulate the same RAGs, their means to this site must be divergent as CCL relies on the inflammatory response whereas CES does not. Potentially there is stimulation of specific receptors at the cell membrane by the electrical current. Since the injury response causes rapid depolarization at the cell membrane, opening of voltage-gated sodium and calcium channels, and intracellular calcium release, it is possible that even the spike pattern at the axonal membrane could convey a different signal to the cell bodies (George et al., 1995; Iwata et al., 2004; Ohtake et al., 2018). Furthermore, there is the possibility that different channels or channel subtypes are opened at the membrane leading to a different retrograde signal. In summary, determining what pathways are upregulated in CES and tracing these pathways back to specific receptors could provide a detailed analysis of the mechanism associated with CES.

Our data support the clinical translation of CES for nerve injury patients. With the absence of an inflammatory response by monocyte-derived and tissue-resident macrophages and no ATF3 upregulation, coupled with the knowledge that electrical stimulation is routinely applied post-nerve repair surgery, suggests CES is likely safe for patients. Furthermore, while Sprague-Dawley rats and WT mice are much different from humans, the fact that CES has

shown some degree of interspecies validity provides support for the hypothesis that CES will also work in human patients. A strategy to accelerate the rate of nerve regeneration in humans would greatly benefit those suffering from nerve injury, not only by speeding recovery, but also the likelihood of recovery as it is important for regenerating nerves to reach target tissues to avoid poor outcomes that increase with prolonged denervation such as muscle atrophy (Grinsell and Keating, 2014). As peripheral nerve injury is widespread, and many patients suffer despite surgical intervention, CES has the potential to improve quality of life, functional recovery, and prognosis if clinical trials were successful in scheduled nerve repair patients.

Bibliography:

Abrams M, Widenfalk J (2005) Emerging strategies to promote improved functional outcome after peripheral nerve injury. *Restor Neurol Neurosci* **23**(5-6):367-382. PMID: 16477099

Ajami B, Bennett JL, Krieger C, Tetzlaff W, Rossi FM (2007) Local self-renewal can sustain CNS microglia maintenance and function throughout adult life. *Nat Neurosci* **10**(12):1538-1543. doi: 10.1038/nn2014 PMID: 18026097

Al-Majed AA, Neumann CM, Brushart TM, Gordon T (2000) Brief electrical stimulation promotes the speed and accuracy of motor axonal regeneration. *J Neurosci* **20**(7):2602-2608. doi: 10.1523/JNEUROSCI.20-07-02602.2000 PMID: 10729340

Al-Majed AA, Brushart TM, Gordon T (2000) Electrical stimulation accelerates and increases expression of BDNF and trkB mRNA in regenerating rat femoral motoneurons. *Eur J Neurosci* **12**(12):4381-4390. PMID: 11122348

Aldskogius H, Arvidsson J (1978) Nerve cell degeneration and death in the trigeminal ganglion of the adult rat following peripheral nerve transection. *J Neurocytol* **7**(2):229-250. doi: 10.1007/BF01217921 PMID: 650265

Allodi I, Udina E, Navarro X (2012) Specificity of peripheral nerve regeneration: interactions at the axon level. *Prog Neurobiol* **98**(1):16-37 doi: 10.1016/j.pneurobio.2012.05.005 PMID: 22609046

Ambrosini RT, Walters ET (1996) Priming events and retrograde injury signals. A new perspective on the cellular and molecular biology of nerve regeneration. *Mol Neurobiol* **13**(1):61-79. doi: 10.1007/BF02740752 PMID: 8892336

Ambrosini RT, Dulin MF, Zhang XP, Schmied R, Walters ET (1995) Axoplasm enriched in a protein mobilized by nerve injury induces memory-like alterations in *Aplysia* neurons. *J Neurosci* **15**(5 Pt 1):3440-3446. doi: 10.1523/JNEUROSCI.15-05-03440.1995 PMID: 7538559

Antonow-Schlorke I, Ehrhardt J, Knieling M (2013) Modification of the ladder rung walking task-new options for analysis of skilled movements. *Stroke Res Treat* **2013**:418627. doi: 10.1155/2013/418627 PMID: 23577278

Atwal JK, Massie B, Miller FD, Kaplan DR (2000) The TrkB-Shc site signals neuronal survival and local axon growth via MEK and P13-kinase. *Neuron* **27**(2):265-277. doi: 10.1016/s0896-6273(00)00035-0 PMID: 10985347

Arevalo M, Rodríguez-Tébar A (2006) Activation of casein kinase II and inhibition of phosphatase and tensin homologue deleted on chromosome 10 phosphatase by nerve growth factor/p75NTR inhibit glycogen synthase kinase-3beta and stimulate axonal growth. *Mol Biol Cell* **17**(8):3369-3377. doi: 10.1091/mbc.e05-12-1144 PMID: 16723502.

- Arthur-Farraj PJ, Latouche M, Wilton DK, Quintes S, Chabrol E, Banerjee A, Woodhoo A, Jenkins B, Rahman M, Turmaine M, Wicher GK, Mitter R, Greensmith L, Behrens A, Raivich G, Mirsky R, Jessen KR (2012) *Neuron* **75**(4):633-647. doi: 10.1016/j.neuron.2012.06.021 PMID: 22920255
- Barber B, Seikaly H, Chan KM, Beaudry R, Rychlik S, Olson J, Curran M, Dziegielewski P, Biron V, Harris J, McNeely M, O'Connell D (2018) Intraoperative Brief Electrical Stimulation of the Spinal Accessory Nerve (BEST SPIN) for prevention of shoulder dysfunction after oncologic neck dissection: a double-blinded, randomized controlled trial. *J Otolaryngol Head Neck Surg* **47**:7. doi: 10.1186/s40463-017-0244-9 PMID: 29361981.
- Bautista M, Krishnan A (2022) Self-renewal of peripheral nerve resident macrophage: does it represent a unique activation status?. *Neural Regen Res* **17**(5):999-1000. doi: 10.4103/1673-5374.324845 PMID: 34558518
- Blesch A, Lu P, Tsukada S, Alto LT, Roet K, Coppola G, Geschwind D, Tuszynski MH (2012) Conditioning lesions before or after spinal cord injury recruit broad genetic mechanisms that sustain axonal regeneration: superiority to camp-mediated effects. *Exp Neurol* **235**(1):162-173. doi: 10.1016/j.expneurol.2011.12.037 PMID: 22227059
- Boring L, Gosling J, Chensue SW, Kunkel SL, Farese Jr RV, Broxmeyer HE, Charo IF (1997). Impaired monocyte migration and reduced type 1 (Th1) cytokine responses in C-C chemokine receptor 2 knockout mice. *J Clin Invest* **100**(10):2552-2562. doi: 10.1172/JCI119798 PMID: 9366570
- Brown MC, Perry VH, Hunt SP, Lapper SR (1994) Further studies on motor and sensory nerve regeneration in mice with delayed Wallerian degeneration. *Eur J Neurosci* **6**(3):420-428. doi: 10.1111/j.1460-9568.1994.tb00285.x PMID: 8019679
- Brück W, Friede RL (1990) Anti-macrophage CR3 antibody blocks myelin phagocytosis by macrophages in vitro. *Acta Neuropathol* **80**(4):415-418. doi: 10.1007/BF00307696 PMID: 2239153
- Brück W, Friede RL (1991) The role of complement in myelin phagocytosis during PNS Wallerian degeneration. *J Neurol Sci* **103**(2):182-187. doi: 10.1016/0022-510x(91)90162-z PMID: 1880536
- Brunet A, Bonni A, Zigmond MJ, Lin MZ, Juo P, Hu LS, Anderson MJ, Arden KC, Blenis J, Greenberg ME (1999) Akt promotes cell survival by phosphorylating and inhibiting a Forkhead transcription factor. *Cell* **96**(6):857-868. doi: 10.1016/s0092-8674(00)80595-4 PMID: 10102273
- Brushart TM (1988) Preferential reinnervation of motor nerves by regenerating motor axons. *J Neurosci* **8**(3): 1026-1031. doi: 10.1523/JNEUROSCI.08-03-01026.1988 PMID: 3346713
- Brushart TM, Hoffman PN, Royall RM, Murinson BB, Witzel C, Gordon T (2002) Electrical stimulation promotes motoneuron regeneration without increasing its speed or conditioning the

neuron. *J Neurosci* **22**:6631-6638. doi: 10.1523/JNEUROSCI.22-15-06631.2002 PMID: 12151542

Brushart TM, Jari R, Verge V, Rohde C, Gordon T (2005) Electrical stimulation restores the specificity of sensory axon regeneration. *Exp Neurol* **194**(1):221-229. doi: 10.1016/j.expneurol.2005.02.007 PMID: 15899259

Buch T, Heppner FL, Tertilt C, Heinen TJ, Kremer M, Wunderlich FT, Jung S, Waisman A (2005) A Cre-inducible diphtheria toxin receptor mediates cell lineage ablation after toxin administration. *Nat Methods* **2**(6):419-426. doi: 10.1038/nmeth762 PMID: 15908920.

Burry RW, Lah JJ, Hayes DM (1992) GAP-43 distribution is correlated with development of growth cones and presynaptic terminals. *J Neurocytol* **21**(6):413-425. doi: 10.1007/BF01191506 PMID: 1403006

Cai D, Shen Y, De Bellard M, Tang S, Filbin MT (1999) Prior exposure to neurotrophins blocks inhibition of axonal regeneration by MAG and myelin via a cAMP-dependent mechanism. *Neuron* **22**(1):89-101. doi: 10.1016/s0896-6273(00)80681-9 PMID: 10027292

Cai R, Pan C, Ghasemigharagoz A, Todorov MI, Förstera B, Zhao S, Bhatia HS, Parra-Damas A, Mrowka L, Theodorou D, Rempfler M, Xavier AL, Kress BT, Benakis C, Steinke H, Liebscher S, Bechmann I, Liesz A, Menze B, Kerschensteiner M, Nedergaard M, Ertürk A (2019) Panoptic imaging of transparent mice reveals whole-body neuronal projections and skull-meninges connections. *Nat Neurosci* **22**(2):317-327. doi: 10.1038/s41593-018-0301-3 PMID: 30598527

Cafferty WB, Gardiner NJ, Gavazzi I, Powell J, McMahon SB, Heath JK, Munson J, Cohen J, Thompson SW (2001) Leukemia inhibitory factor determines the growth status of injured adult sensory neurons. *J Neurosci* **21**(18):7161-7170. doi: 10.1523/JNEUROSCI.21-18-07161.2001 PMID: 11549727

Cajal SR (1928) Degeneration and Regeneration of the Nervous System. (*May, R.M. (trans.)*) New York, Oxford: Oxford University Press.

Cao Z, Gao Y, Bryson JB, Hou J, Chaudry N, Siddiq M, Martinez J, Spencer T, Carmel J, Hart RB, Filbin MT (2006) The cytokine interleukin-6 is sufficient but not necessary to mimic the peripheral conditioning lesion effect on axonal growth. *J Neurosci* **26**(20):5565-5573. doi: 10.1523/JNEUROSCI.0815-06.2006 PMID: 16707807

Cattin A, Lloyd AC (2016) The multicellular complexity of peripheral nerve regeneration. *Curr Opin Neurobiol* **39**:38-46. doi: 10.1016/j.conb.2016.04.005 PMID: 27128880

Cattin A, Burden JJ, Van Emmenis L, Mackenzie FE, Hoving JJ, Calavia NG, Guo Y, McLaughlin M, Rosenberg LH, Quereda V, Jamecna D, Napoli I, Parrinello S, Enver T, Ruhrberg C, Lloyd AC (2015) Macrophage-Induced Blood Vessels Guide Schwann Cell-Mediated Regeneration of Peripheral Nerves. *Cell* **162**(5):1127-1139. doi:10.1016/j.cell.2015.07.021

Chan KM, Curran MW, Gordon T (2016) The use of brief post-surgical low frequency electrical stimulation to enhance nerve regeneration in clinical practice. *J Physiol* **594**:3553-3559 doi: 10.1113/JP270892 PMID: 26864594

Chan KM, Gordon T, Zochodne DW, Power HA (2014) Improving peripheral nerve regeneration: from molecular mechanisms to potential therapeutic targets. *Exp Neurol* **261**:826-835. doi: 10.1016/j.expneurol.2014.09.006. PMID: 25220611

Chen ZW, Wang MS (1995) Effects of nerve growth factor on crushed sciatic nerve regeneration in rats. *Microsurgery* **16**(8):547-551. doi: 10.1002/micr.1920160808 PMID: 8538432

Chen Z, Yu W, Strickland S (2007) Peripheral regeneration. *Annu Rev Neurosci* **30**:209-233. doi: 10.1146/annurev.neuro.30.051606.094337 PMID: 17341159.

Cheng C, Webber CA, Wang J, Xu Y, Martinez JA, Liu WQ, McDonald D, Guo GF, Nguyen MD, Zochodne DW (2008) Activated RHOA and peripheral axon regeneration. *Exp Neurol* **212**(2):358-369. doi: 10.1016/j.expneurol.2008.04.023 PMID: 18554585

Christie KJ, Webber CA, Martinez JA, Singh B, Zochodne DW (2010) PTEN inhibition to facilitate intrinsic regenerative outgrowth of adult peripheral axons. *J Neurosci* **30**(27):9306-9315. doi: 10.1523/JNEUROSCI.6271-09.2010 PMID: 20610765

Christie KJ, Zochodne D (2013) Peripheral axon regrowth: new molecular approaches. *Neuroscience* **240**:310-324. doi: 10.1016/j.neuroscience.2013.02.059. PMID: 23500101

Cohen MS, Ghosh AK, Kim HJ, Jeon NL, Jaffrey SR (2013) Chemical genetic-mediated spatial regulation of protein expression in neurons reveals an axonal function for WldS. *Chem Biol* **19**(2):179-187. doi: 10.1016/j.chembiol.2012.01.012 PMID: 22365601

Conforti L, Tarlton A, Mack TG, Mi W, Buckmaster EA, Wagner D, Perry VH, Coleman MP (2000) A Ufd2/D4Cole1e chimeric protein and overexpression of Rbp7 in the slow Wallerian degeneration (WldS) mouse. *Proc Natl Acad Sci U S A* **97**(21):11377-11382. doi: 10.1073/pnas.97.21.11377 PMID: 11027338.

Conforti L, Gilley J, Coleman MP (2014) Wallerian degeneration: an emerging axon death pathway linking injury and disease. *Nat Rev Neurosci* **15**(6):394-409. doi: 10.1038/nrn3680 PMID: 24840802

Cross DA, Alessi DR, Cohen P, Andjelkovich M, Hemmings BA (1995) Inhibition of glycogen synthase kinase-3 by insulin mediated by protein kinase B. *Nature* **378**(6559):785-789. doi: 10.1038/378785a0 PMID: 8524413.

Cugurra A, Mamuladze T, Rustenhoven J, Dykstra T, Beroshvili G, Greenberg ZJ, Baker W, Papadopoulos Z, Drieu A, Blackburn S, Kanamori M, Brioschi S, Herz J, Schuettepelz LG, Colonna M, Smirnov I, Kipnis J (2021) Skull and vertebral bone marrow are myeloid cell

resevoirs for the meninges and CNS parenchyma. *Science* **373**(6553):eabf7844. doi: 10.1126/science.abf7844 PMID: 34083447

Cursiefen C, Chen L, Borges LP, Jackson D, Cao J, Radziejewski C, D'Amore PA, Dana MR, Wiegand SJ, Streilein JW (2004) VEGF-A stimulates lymphangiogenesis and hemangiogenesis in inflammatory neovascularization via macrophage recruitment. *J Clin Invest* **113**(7):1040-1050. doi: 10.1172/JCI20465 PMID: 15057311.

Dabir DV, Trojanowski JQ, Richter-Landsberg C, Lee VM, Forman MS (2004) Expression of the small heat-shock protein alphaB-crystallin in tauopathies with glial pathology. *Am J Pathol* **164**(1):155-166. doi: 10.1016/s0002-9440(10)63106-9 PMID: 14695329

Dahlin LB (1992) Stimulation of regeneration of the sciatic nerve by experimentally induced inflammation in rats. *Scand J Plast Reconstr Surg Hand Surg* **26**(2):121-125. doi: 10.3109/02844319209016001 PMID: 1411338

Dalsgaard CJ, Rydh M, Haegerstrand A (1989) Cutaneous innervation in man visualized with protein gene product 9.5 (PGP 9.5) antibodies. *Histochemistry* **92**(5):385-390. doi: 10.1007/BF00492495 PMID: 2531128

D'Antonio M, Michalovich D, Paterson M, Droggiti A, Woodhoo A, Mirsky R, Jessen KR (2006) Gene profiling and bioinformatic analysis of Schwann cell embryonic development and myelination. *Glia* **53**(5):501-515. doi: 10.1002/glia.20309 PMID: 16369933

Davies LC, Jenkins SJ, Allen JE, Taylor PR (2013) Tissue-resident macrophages. *Nat Immunol* **14**(10):986-995. doi: 10.1038/ni.2705 PMID: 24048120

De S, Trigueros MA, Kalyvas A, David S (2003) Phospholipase A2 plays an important role in myelin breakdown and phagocytosis during Wallerian degeneration. *Mol Cell Neurosci* **24**(3):753-765. doi: 10.1016/s1044-7431(03)00241-0 PMID: 14664823

DeFrancesco-Lisowitz A, Lindborg JA, Niemi JP, Zigmond RE (2015) The neuroimmunology of degeneration and regeneration in the peripheral nervous system. *Neuroscience* **302**:174-203. doi: 10.1016/j.neuroscience.2014.09.027 PMID: 25242643

Deuis JR, Dvorakova LS, Vetter I (2017) Methods Used to Evaluate Pain Behaviors in Rodents. *Front Mol Neurosci* **10**:284. doi: 10.3389/fnmol.2017.00284 PMID: 28932184

Ding C, Hammarlund (2020) Mechanisms of injury-induced axon degeneration. *Curr Opin Neurobiol* **57**:171-178. doi: 10.1016/j.conb.2019.03.006 PMID: 31071521

Dudek H, Datta SR, Franke TF, Birnbaum MJ, Yao R, Cooper GM, Segal RA, Kaplan DR, Greenberg ME (1997) Regulation of neuronal survival by the serine-threonine protein kinase Akt. *Science* **275**(5300):661-665. doi: 10.1126/science.275.5300.661 PMID: 9005851

- Duraikannu A, Krishnan A, Chandrasekhar A, Zochodne DW (2019) Beyond Trophic Factors: Exploiting the Intrinsic Regenerative Properties of Adult Neurons. *Front Cell Neurosci* **13**:128. doi: 10.3389/fncel.2019.00128 PMID: 31024258
- Ellenbroek B, Youn J (2016) Rodent models in neuroscience research: is it a rat race?. *Dis Model Mech* **9**(10):1079-1087. doi: 10.1242/dmm.026120 PMID: 27736744
- Essuman K, Summers DW, Sasaki Y, Mao X, DiAntonio A, Milbrandt J (2017) The SARM1 Toll/Interleukin-1 Receptor Domain Possesses Intrinsic NAD⁺ Cleavage Activity that Promotes Pathological Axonal Degeneration. *Neuron* **93**(6):1334-1343. doi: 10.1016/j.neuron.2017.02.022 PMID: 28334607
- Fantin A, Vieira JM, Gestri G, Denti L, Schwarz Q, Prykhozhiy S, Peri F, Wilson SW, Ruhrberg C (2010) Tissue macrophages act as cellular chaperones for vascular anastomosis downstream of VEGF-mediated endothelial tip cell induction. *Blood* **116**(5):829-840. doi: 10.1182/blood-2009-12-257832 PMID: 20404134
- Faroni A, Mobasseri SA, Kingham PJ, Reid AJ (2015) Peripheral nerve regeneration: experimental strategies and future perspectives. *Adv Drug Deliv Rev* **83**:160-167. doi: 10.1016/j.addr.2014.11.010 PMID: 25446133
- Ferreira A, Caceres A (1992) Expression of the class III beta-tubulin isotype in developing neurons in culture. *J Neurosci Res* **32**(4):516-529. doi: 10.1002/jnr.490320407 PMID: 1527798
- Filous AR, Silver J (2015) Neurite Outgrowth Assay. *Bio Protoc* **6**(1):e1694. doi: 10.21769/BioProtoc.1694 PMID: 29082282
- Fleur ML, Underwood JL, Rappolee DA, Werb Z (1996) Basement membrane and repair of injury to peripheral nerve: defining a potential role for macrophages, matrix metalloproteinases, and tissue inhibitor of metalloproteinases-1. *J Exp Med* **184**(6):2311-2326. doi: 10.1084/jem.184.6.2311 PMID: 8976186
- Fogg DK, Sibon C, Miled C, Jung S, Aucouturier P, Littman DR, Cumano A, Geissmann F (2006) A clonogenic bone marrow progenitor specific for macrophages and dendritic cells. *Science* **311**(5757):83-87. doi: 10.1126/science.1117729 PMID: 16322423
- Francis C, Natarajan S, Lee MT, Khaladkar M, Buckley PT, Sul J, Eberwine J, Kim J (2014) *BMC Genomics* **15**(1):883. doi: 10.1186/1471-2164-15-883 PMID: 25301173
- Fricker FR, Lago N, Balarajah S, Tsantoulas C, Tanna S, Zhu N, Fageiry SK, Jenkins M, Garratt AN, Birchmeier C, Bennett DL (2011) Axonally derived neuregulin-1 is required for remyelination and regeneration after nerve injury in adulthood. *J Neurosci* **31**(9):3225-3233. doi: 10.1523/JNEUROSCI.2568-10.2011 PMID: 21368034
- Friedman B, Kleinfeld D, Ip NY, Verge VM, Moulton R, Boland P, Zlotchenko E, Lindsay RM, Liu L (1995) BDNF and NT-4/5 exert neurotrophic influences on injured adult spinal motor

neurons. *J Neurosci* **15**(2):1044-1056. doi: 10.1523/JNEUROSCI.15-02-01044.1995 PMID: 7869082

Fu SY, Gordon T (1997) The cellular and molecular basis of peripheral nerve regeneration. *Mol Neurobiol* **14**(1-2):67-116. doi: 10.1007/BF02740621 PMID: 9170101

Gao Y, Deng K, Hou J, Bryson JB, Barco A, Nikulina E, Spencer T, Mellado W, Kandel ER, Filbin MT (2004) Activated CREB is sufficient to overcome inhibitors in myelin and promote spinal axon regeneration in vivo. *Neuron* **44**(4):609-621. doi: 10.1016/j.neuron.2004.10.030 PMID: 15541310

Gardiner NJ, Moffatt S, Fernyhough P, Humphries MJ, Streuli CH, Tomlinson DR (2007) Preconditioning injury-induced neurite outgrowth of adult rat sensory neurons on fibronectin is mediated by mobilisation of axonal alpha5 integrin. *Mol Cell Neurosci* **35**(2):249-260. doi: 10.1016/j.mcn.2007.02.020 PMID: 17433878

Gaudet AD, Popovich PG, Ramer MS (2011) Wallerian degeneration: gaining perspective on inflammatory events after peripheral nerve injury. *J Neuroinflammation* **8**:110. doi: 10.1186/1742-2094-8-110. PMID: 21878126

George EB, Glass JD, Griffin JW (1995) Axotomy-induced axonal degeneration is mediated by calcium influx through ion-specific channels. *J Neurosci* **15**(10): 6445-6452. doi: 10.1523/JNEUROSCI.15-10-06445.1995 PMID: 7472407

Gensel JC, Wang Y, Guan Z, Beckwith KA, Braun KJ, Wei P, McTigue DM, Popovich PG (2015) Toll-Like Receptors and Dectin-1, a C-Type Lectin Receptor, Trigger Divergent Functions in CNS Macrophages. *J Neurosci* **35**(27):9966-9976. doi: 10.1523/JNEUROSCI.0337-15.2015 PMID: 26156997

Geremia NM, Gordon T, Brushart TM, Al-Majed AA, Verge VM (2007) Electrical stimulation promotes sensory neuron regeneration and growth-associated gene expression. *Exp Neurol* **205**(2):347-359. doi: 10.1016/j.expneurol.2007.01.040 PMID: 17428474

Geremia NM, Pettersson LM, Hasmatali JC, Hryciw T, Danielsen N, Schreyer DJ, Verge VM (2010) Endogenous BDNF regulates induction of intrinsic neuronal growth programs in injured sensory neurons. *Exp Neurol* **223**(1):128-142. doi: 10.1016/j.expneurol.2009.07.022 PMID: 19646438

Ginhoux F, Greter M, Leboeuf M, Nandi S, See P, Gokhan S, Mehler MF, Conway SJ, Ng LG, Stanley ER, Samokhvalov IM, Merad M (2010) Fate mapping analysis reveals that adult microglia derive from primitive macrophages. *Science* **330**(6005):841-845. doi: 10.1126/science.1194637 PMID: 20966214

Gordon T, Amirjani N, Edwards DC, Chan KM (2010) Brief post-surgical electrical stimulation accelerates axon regeneration and muscle reinnervation without affecting the functional

measures in carpal tunnel syndrome patients. *Exp Neurol* **223**(1):192-202. doi: 10.1016/j.expneurol.2009.09.020 PMID: 19800329

Gordon T (2020) Peripheral Nerve Regeneration and Muscle Reinnervation. *Int J Mol Sci* **21**(22):8652 doi: 10.3390/ijms21228652 PMID: 33212795

Gregson NA, Hall SM (1973) A quantitative analysis of the effects of the intraneural injection of lysophosphatidyl choline. *J Cell Sci* **13**(1):257-277. doi: 10.1242/jcs.13.1.257 PMID: 4729938.

Grinsell D, Keating CP (2014) Peripheral nerve reconstruction after injury: a review of clinical and experimental therapies. *Biomed Res Int*: 698256. doi: 10.1155/2014/698256 PMID: 25276813

Hall SM (1972) The effect of injections of lysophosphatidyl choline into white matter of the adult mouse spinal cord. *J Cell Sci* **10**(2):535-546. doi: 10.1242/jcs.10.2.535 PMID: 5018033.

Hall A, Lalli G (2010) Rho and Ras GTPases in axon growth, guidance, and branching. *Cold Spring Harb Perspect Biol* **2**(2):a001818 doi: 10.1101/cshperspect.a001818 PMID: 20182621

Hanani M (2005) Satellite glial cells in sensory ganglia: from form to function. *Brain Res Brain Res Rev* **48**(3):457-476. doi: 10.1016/j.brainresrev.2004.09.001 PMID: 15914252

Hannila SS, Filbin MT (2008) The role of cyclic AMP signaling in promoting axonal regeneration after spinal cord injury. *Exp Neurol* **209**(2):321-332. doi: 10.1016/j.expneurol.2007.06.020 PMID: 17720160

Hanz S, Perlson E, Willis D, Zheng J, Massarwa R, Huerta JJ, Koltzenburg M, Kohler M, van-Minnen J, Twiss JL, Fainzilber M (2003) Axoplasmic importins enable retrograde injury signaling in lesioned nerve. *Neuron* **40**(6):1095-1104. doi: 10.1016/s0896-6273(03)00770-0 PMID: 14687545

Hargreaves K, Dubner R, Brown F, Flores C, Joris J (1988) A new and sensitive method for measuring thermal nociception in cutaneous hyperalgesia. *Pain* **32**(1):77-88. doi: 10.1016/0304-3959(88)90026-7 PMID: 3340425

Hashimoto D, Chow A, Noizat C, Teo P, Beasley MB, Leboeuf M, Becker CD, See P, Price J, Lucas D, Greter M, Mortha A, Boyer SW, Forsberg EC, Tanaka M, van Rooijen N, García-Sastre A, Stanley ER, Ginhoux F, Frenette PS, Merad M (2013) Tissue-resident macrophages self-maintain locally throughout adult life with minimal contribution from circulating monocytes. *Immunity* **38**:792-804. doi: 10.1016/j.immuni.2013.04.004 PMID: 23601688

Hausott B, Klimaschewski L (2019) Promotion of Peripheral Nerve Regeneration by Stimulation of the Extracellular Signal-Regulated Kinase (ERK) Pathway. *Anat Rec (Hoboken)* **302**(8):1261-1267. doi: 10.1002/ar.24126 PMID: 30951263.

Harrisingh MC, Perez-Nadales E, Parkinson DB, Malcolm DS, Mudge AW, Lloyd AC (2004) The Ras/Raf/ERK signalling pathway drives Schwann cell dedifferentiation. *EMBO J* **23**(15):3061-3071. doi: 10.1038/sj.emboj.7600309 PMID: 15241478

Hemmings BA, Restuccia DF (2012) PI3K-PKB/Akt Pathway. *Cold Spring Harb Perspect Biol* **4**(9):a011189. doi: 10.1101/cshperspect.a011189 PMID: 22952397

Herisson F, Frodermann V, Courties G, Rohde D, Sun Y, Vandoorne K, Wojtkiewicz GR, Masson GS, Vinegoni C, Kim J, Kim D, Weissleder R, Swirski FK, Moskowitz MA, Nahrendorf M (2018) Direct vascular channels connect skull bone marrow and the brain surface enabling myeloid cell migration. *Nat Neurosci* **21**(9):1209-1217. doi: 10.1038/s41593-018-0213-2 PMID: 30150661.

Hetman M, Kanning K, Cavanaugh JE, Xia Z (1999) Neuroprotection by brain-derived neurotrophic factor is mediated by extracellular signal-regulated kinase and phosphatidylinositol 3-kinase. *J Biol Chem* **274**(32):22569-22580. doi: 10.1074/jbc.274.32.22569 PMID: 10428835.

Heumann R, Lindholm D, Bandtlow C, Meyer M, Radeke MJ, Misko TP, Shooter E, Toenen H (1987) Differential regulation of mRNA encoding nerve growth factor and its receptor in rat sciatic nerve during development, degeneration, and regeneration: role of macrophages. *Proc Natl Acad Sci U S A* **84**(23):8735-8739. doi: 10.1073/pnas.84.23.8735 PMID: 2825206

Hikawa N, Takenaka T (1996) Myelin-stimulated macrophages release neurotrophic factors for adult dorsal root ganglion neurons in culture. *Cell Mol Neurobiol* **16**(4):517-528. doi: 10.1007/BF02150231 PMID: 8879753

Hilton BJ, Husch A, Schaffran B, Lin T, Burnside ER, Dupraz S, Schelski M, Kim J, Müller JA, Schoch S, Imig C, Brose N, Bradke F (2022) An active vesicle priming machinery suppresses axon regeneration upon adult CNS injury. *Neuron* **110**(1):51-69. doi: 10.1016/j.neuron.2021.10.007 PMID: 34706221

Horie H, Bando Y, Chi H, Takenaka T (1991) NGF enhances neurite regeneration from nerve-transected terminals of young adult and aged mouse dorsal root ganglia in vitro. *Neurosci Lett* **121**(1-2):125-128. doi: 10.1016/0304-3940(91)90665-g PMID: 2020368

Hossain-Ibrahim MK, Rezajooi K, Stallcup WB, Lieberman AR, Anderson PN (2007) Analysis of axonal regeneration in the central and peripheral nervous systems of the NG2-deficient mouse. *BMC Neurosci* **8**:80. doi: 10.1186/1471-2202-8-80 PMID: 17900358

Huang J, Ye Z, Hu X, Lu L, Luo Z (2010) Electrical stimulation induces calcium-dependent release of NGF from cultured Schwann cells. *Glia* **58**(5):622-631. doi: 10.1002/glia.20951 PMID: 19998481

Imai Y, Ibata I, Ito D, Ohsawa K, Kohsaka S (1996) A novel gene *iba1* in the major histocompatibility complex class III region encoding an EF hand protein expressed in a monocytic lineage. *Biochem Biophys Res Commun* **224**(3):855-862.

doi: 10.1006/bbrc.1996.1112 PMID: 8713135

Iwata A, Stys PK, Wolf JA, Chen X, Taylor AG, Meaney DF, Smith DH (2004) Traumatic axonal injury induces proteolytic cleavage of the voltage-gated sodium channels modulated by tetrodotoxin and protease inhibitors. *J Neurosci* **24**(19):4605-4613. doi: 10.1523/JNEUROSCI.0515-03.2004. PMID: 15140932

Jacobson RD, Virág I, Skene JH (1986) A protein associated with axon growth, GAP-43, is widely distributed and developmentally regulated in rat CNS. *J Neurosci* **6**(6):1843-1855. doi: 10.1523/JNEUROSCI.06-06-01843.1986 PMID: 3712014

Jang SY, Shin YK, Park SY, Park JY, Lee HJ, Yoo YH, Kim JK, Park HT (2016) Autophagic myelin destruction by Schwann cells during Wallerian degeneration and segmental demyelination. *Glia* **64**(5):&30-742. doi: 10.1002/glia.22957 PMID: 26712109

Jaworski J, Spangler S, Seeburg DP, Hoogenraad CC, Sheng M (2005) Control of dendritic arborization by the phosphoinositide-3'-kinase-Akt-mammalian target of rapamycin pathway. *J Neurosci* **25**(49): 11300-11312. doi: 10.1523/JNEUROSCI.2270-05.2005 PMID: 16339025

Jessen KR, Mirsky R, Lloyd AC (2015) Schwann cells: development and role in nerve repair. *Cold Spring Harb Perspect Biol* **7**(7):a020487. doi: 10.1101/cshperspect.a020487 PMID: 25957303

Jha MK, Passero JV, Rawat A, Ament XH, Yang F, Vidensky S, Collins SL, Horton MR, Hoke A, Rutter GA, Latemoliere A, Rothstein JD, Morrison BM (2021) Macrophage monocarboxylate transporter 1 promotes peripheral nerve regeneration after injury in mice. *J Clin Invest* **131**(21):e141964. doi: 10.1172/JCI141964 PMID: 34491913

Jopling , Boue S, Belmonte JC (2011) Dedifferentiation, transdifferentiation and reprogramming: three routes to regeneration. *Nat Rev Mol Cell Biol* **12**(2):79-89. doi: 10.1038/nrm3043 PMID: 21252997

Kaplan DR, Miller FD (2000) Neurotrophin signal transduction in the nervous system. *Curr Opin Neurobiol* **10**(3): 381-391. doi: 10.1016/s0959-4388(00)00092-1 PMID: 10851172

Kaplan HM, Mishra P, Kohn J (2015) The overwhelming use of rat models in nerve regeneration research may compromise designs of nerve guidance conduits for humans. *J Mater Sci Mater Med* **26**(8):226. doi: 10.1007/s10856-015-5558-4 PMID: 26296419

Klesse LJ, Meyers KA, Marshall CJ, Parada LF (1999) Nerve growth factor induces survival and differentiation through two distinct signaling cascades in PC12 cells. *Oncogene* **18**(12):2055-2068. doi: 10.1038/sj.onc.1202524 PMID: 10321730

Köhler C (2007) Allograft inflammatory factor-1/Ionized calcium-binding adapter molecule 1 is specifically expressed by most subpopulations of macrophages and spermatids in testis. *Cell Tissue Res* **330**(2):291-302. doi: 10.1007/s00441-007-0474-7 PMID: 17874251

- Krishnan A, Bhavanam S, Zochodne D (2018) An Intimate Role for Adult Dorsal Root Ganglia Resident Cycling Cells in the Generation of Local Macrophages and Satellite Glial Cells. *J Neuropathol Exp Neurol* **77**(10):929-941. doi: 10.1093/jnen/nly072 PMID: 30169768
- Kuipers HF, Yoon J, van Horssen J, Han MH, Bollyky PL, Palmer TD, Steinman L (2017) Phosphorylation of α B-crystallin supports reactive astrogliosis in demyelination. *Proc Natl Acad Sci USA* **114**(9):E1747-E1754. doi: 10.1073/pnas.1621314114 PMID: 28196893
- Kuziel WA, Morgan SJ, Dawson TC, Griffin S, Smithies O, Ley K, Maeda N (1997) Severe reduction in leukocyte adhesion and monocyte extravasation in mice deficient in CC chemokine receptor 2. *Proc Natl Acad Sci U S A* **94**(22):12053-12058. doi: 10.1073/pnas.94.22.12053 PMID: 9342361
- Kwon MJ, Shin HY, Cui Y, Kim H, Thi AH, Choi JY, Kim EY, Hwang DH, Kim BG (2015) CCL2 Mediates Neuron-Macrophage Interactions to Drive Proregenerative Macrophage Activation Following Preconditioning Injury. *J Neurosci* **35**(48):15934-15947. doi: 10.1523/JNEUROSCI.1924-15.2015 PMID: 26631474
- Lavin Y, Winter D, Blecher-Gonen R, David E, Keren-Shaul H, Merad M, Jung S, Amit I (2014) Tissue-resident macrophage enhancer landscapes are shaped by the local microenvironment. *Cell* **159**(6):1312-1326. doi: 10.1016/j.cell.2014.11.018 PMID: 25480296
- Leslie NR, Batty IH, Maccario H, Davidson L, Downes CP (2008). *Oncogene* **27**(41):5464-5476. doi: 10.1038/onc.2008.243 PMID: 18794881.
- Levi-Montalcini R (1987) The nerve growth factor: thirty-five years later. *Biosci Rep* **7**(9):681-699. doi: 10.1007/BF01116861 PMID: 3322422.
- Levine S, Saltzman A, Kumar AR (2004) A method for peripheral chromatolysis in neurons of trigeminal and dorsal root ganglia, produced in rats by lithium. *J Neurosci Methods* **132**(1):1-7doi: 10.1016/j.jneumeth.2003.07.001PMID: 14687669
- Li R, Reiser G (2011) Phosphorylation of Ser45 and Ser59 of α B-crystallin and p38/extracellular regulated kinase activity determine α B-crystallin-mediated protection of rat brain astrocytes from C2-ceramide- and staurosporine-induced cell death. *J Neurochem* **118**(3):354-364. doi: 10.1111/j.1471-4159.2011.07317.x PMID: 21615407
- Li Y, Kang S, Halawani D, Wang Y, Alves CJ, Ramakrishnan A, Estill M, Shen L, Li F, He X, Friedel RH, Zou H (2022) Macrophages facilitate peripheral nerve regeneration by organizing regeneration tracks through Plexin-B2. *Genes Dev* **36**(3-4):133-148. doi:10.1101/gad.349063.121 PMID: 35086862
- Lim EF, Nakanishi ST, Hoghooghi V, Eaton SE, Palmer AL, Frederick A, Stratton JA, Stykel MG, Whelan PJ, Zochodne DW, Biernaskie J, Ousman SS (2017) AlphaB-crystallin regulates

remyelination after peripheral nerve injury. *Proc Natl Acad Sci U S A* **114**(9):E1707-E1716 doi: 10.1073/pnas.1612136114 PMID: 28137843

Lim EF, Hoghooghi V, Hagen KM, Kapoor K, Frederick A, Finlay TM, Ousman SS (2021) Presence and activation of pro-inflammatory macrophages are associated with CRYAB expression in vitro and after peripheral nerve injury. *J Neuroinflammation* **18**(1):82 doi: 10.1186/s12974-021-02108-z PMID: 33761953

Lindå H, Sköld MK, Ochsmann T (2011) Activating transcription factor 3, a useful marker for regenerative response after nerve root injury. *Front Neurol* **2**:30 doi: 10.3389/fneur.2011.00030 PMID: 21629765

Lindborg JA, Mack M, Zigmond RE (2017) Neutrophils Are Critical for Myelin Removal in a Peripheral Nerve Injury Model of Wallerian Degeneration. *J Neurosci* **37**(43):10258-10277. doi: 10.1523/JNEUROSCI.2085-17.2017 PMID: 28912156

Liu RY, Snider WD (2001) Different signaling pathways mediate regenerative versus developmental sensory axon growth. *J Neurosci* **21**(17):RC164. doi: 10.1523/JNEUROSCI.21-17-j0003.2001 PMID: 11511695

Liu P, Peng J, Han G, Ding X, Wei S, Gao G, Huang K, Chang F, Wang Y (2019) Role of macrophages in peripheral nerve injury and repair. *Neural Regen Res* **14**(8):1335-1342. doi: 10.4103/1673-5374.253510 PMID: 30964051

Liu Y, Zhou Q, Tang M, Fu N, Shao W, Zhang S, Yin Y, Zeng R, Wang X, Hu G, Zhou J (2015) Upregulation of alphaB-crystallin expression in the substantia nigra of patients with Parkinson's disease. *Neurobiol Aging* **36**(4):1686-1691. doi: 10.1016/j.neurobiolaging.2015.01.015 PMID: 25683516

Lowery LA, Van Vactor D (2009) The trip of the tip: understanding the growth cone machinery. *Nat Rev Mol Cell Biol* **10**(5):332-343. doi: 10.1038/nrm2679 PMID: 19373241

Lu C, Santosa KB, Jablonka-Shariff A, Vannucci B, Fuchs A, Turnbull I, Pan D, Wood MD, Snyder-Warwick AK (2020) Macrophage-Derived Vascular Endothelial Growth Factor-A Is Integral to Neuromuscular Junction Reinnervation after Nerve Injury. *J Neurosci* **40**(50):9602-9616. doi: 10.1523/JNEUROSCI.1736-20.2020 PMID: 33158964

Lu X, Richardson PM (1993) Responses of macrophages in rat dorsal root ganglia following peripheral nerve injury. *J Neurocytol* **22**(5):334-341. doi: 10.1007/BF01195557 PMID: 8315414

Mack TG, Reiner M, Beirowski B, Mi W, Emanuelli M, Wagner D, Thomson D, Gillingwater T, Court F, Conforti L, Fernando FS, Tarlton A, Andressen C, Addicks K, Magni G, Ribchester RR, Perry VH, Coleman MP (2001) Wallerian degeneration of injured axons and synapses is delayed by a Ube4b/Nmnat chimeric gene. *Nat Neurosci* **4**(12):1199-1206. doi: 10.1038/nm770 PMID: 11770485

Mahar M, Cavalli V (2018) Intrinsic mechanisms of neuronal axon regeneration. *Nat Rev Neurosci* **19**(6):323-337. doi: 10.1038/s41583-018-0001-8 PMID: 29666508

Mallik A, Weir AI (2005) Nerve conduction studies: essentials and pitfalls in practice. *J Neurol Neurosurg Psychiatry* **76**:ii23-31. doi: 10.1136/jnnp.2005.069138 PMID: 15961865

Mandolesi G, Madeddu F, Bozzi Y, Maffei L, Ratto GM (2004) Acute physiological response of mammalian central neurons to axotomy: ionic regulation and electrical activity. *FASEB J* **18**(15):1934-1936. doi: 10.1096/fj.04-1805fje PMID: 15451889

Mao JJ, Katayama S, Watanabe C, Harada Y, Noda K, Yamamura Y, Nakamura S (2001) The relationship between alphaB-crystallin and neurofibrillary tangles in Alzheimer's disease. *Neuropathol Appl Neurobiol* **27**(3):180-188. doi: 10.1046/j.1365-2990.2001.00310.x PMID: 11489137

Mazzoni IE, Saïd FA, Aloyz R, Miller FD, Kaplan D (1999) Ras regulates sympathetic neuron survival by suppressing the p53-mediated cell death pathway. *J Neurosci* **19**(22):9716-9727. doi: 10.1523/JNEUROSCI.19-22-09716.1999 PMID: 10559381

McLean NA, Popescu BF, Gordon T, Zochodne DW, Verge VM (2014) Delayed nerve stimulation promotes axon-protective neurofilament phosphorylation, accelerates immune cell clearance and enhances remyelination in vivo in focally demyelinated nerves. *PLoS One* **9**(10):e110174. doi: 10.1371/journal.pone.0110174 PMID: 25310564

McQuarrie IG, Jacob JM (1991) Conditioning nerve crush accelerates cytoskeletal protein transport in sprouts that form after a subsequent crush. *J Comp Neurol* **305**(1):139-147. doi: 10.1002/cne.903050113 PMID: 1709646

Meiri KF, Pfenninger KH, Willard MB (1986) Growth-associated protein, GAP-43, a polypeptide that is induced when neurons extend axons, is a component of growth cones and corresponds to pp46, a major polypeptide of a subcellular fraction enriched in growth cones. *Proc Natl Acad Sci U S A* **83**(10):3537-3541. doi: 10.1073/pnas.83.10.3537 PMID: 3517863

Metz GA, Wishaw IQ (2009) The ladder rung walking task: a scoring system and its practical application. *J Vis Exp* **12**(28):1204. doi: 10.3791/1204 PMID: 19525918

Mirsky R, Woodhoo A, Parkinson DB, Arthur-Farraj P, Bhaskaran A, Jessen KR (2008) Novel signals controlling embryonic Schwann cell development, myelination and dedifferentiation. *J Peripher Nerv Syst* **13**(2): 122-135. doi: 10.1111/j.1529-8027.2008.00168.x PMID: 18601657

Mörner, C (1894) Th., *Z. physiol. Chemie*, 18, 61 (1894).

Mueller M, Wacker K, Ringelstein EB, Hickey WF, Imai Y, Kiefer R (2001) Rapid response of identified resident endoneurial macrophages to nerve injury. *Am J Pathol* **159**(6):2187-2197. doi: 10.1016/S0002-9440(10)63070-2 PMID: 11733369

Mueller M, Leonhard C, Wacker K, Ringelstein EB, Okabe M, Hickey WF, Kiefer R (2003) Macrophage response to peripheral nerve injury: the quantitative contribution of resident and hematogenous macrophages. *Lab Invest* **83**(2):175-185. doi: 10.1097/01.lab.0000056993.28149.bf PMID: 12594233

Murakami M, Nakatani Y, Atsumi G, Inoue K, Kudo I (1997) Regulatory functions of phospholipase A2. *Crit Rev Immunol* **17**(3-4):225-283. doi: 10.1615/critrevimmunol.v17.i3-4.10 PMID: 9202883

Napoli I, Noon LA, Ribeiro S, Kerai AP, Parrinello S, Rosenberg LH, Collins MJ, Harrisingh MC, White IJ, Woodhoo A, Lloyd AC (2012) A central role for the ERK-signaling pathway in controlling Schwann cell plasticity and peripheral nerve regeneration in vivo. *Neuron* **73**(4):729-742. doi: 10.1016/j.neuron.2011.11.031 PMID: 22365547

Nagaraj RH, Nahomi RB, Mueller NH, Raghavan CT, Ammar DA, Petrash JM (2017) Therapeutic Potential of α -Crystallin. *Biochim Biophys Acta* **1860**(1 Pt B):252-257. doi: 10.1016/j.bbagen.2015.03.012 PMID: 25840354

Navarro X, Kennedy WR (1990) The effect of a conditioning lesion on sudomotor axon regeneration. *Brain Res* **509**(2):232-236. doi: 10.1016/0006-8993(90)90547-o PMID: 2322820

Neumann S, Woolf CJ (1999) Regeneration of dorsal column fibers into and beyond the lesion site following adult spinal cord injury. *Neuron* **23**(1):83-91. doi: 10.1016/s0896-6273(00)80755-2 PMID: 10402195

Niemi JP, DeFrancesco-Lisowitz A, Roldán-Hernández L, Lindborg JA, Mandell D, Zigmond RE (2013) A critical role for macrophages near axotomized neuronal cell bodies in stimulating nerve regeneration. *J Neurosci* **33**:16236-16248. doi: <https://doi.org/10.1523/JNEUROSCI.3319-12.2013> PMID: 24107955

Niemi JP, DeFrancesco-Lisowitz A, Cregg JM, Howarth M, Zigmond RE (2016) Overexpression of the monocyte chemokine CCL2 in dorsal root ganglion neurons causes a conditioning-like increase in neurite outgrowth and does so via a STAT3 dependent mechanism. *Exp Neurol* **275** Pt 1:25-37. doi: 10.1016/j.expneurol.2015.09.018 PMID: 26431741

Ohtake Y, Hayat U, Li S (2015) PTEN inhibition and axon regeneration and neural repair. *Neural Regen Res* **10**(9):1363-1368. doi: 10.4103/1673-5374.165496 PMID: 26604880.

Ohtake Y, Matsuhisa K, Kaneko M, Kanemoto S, Asada R, Imaizumi K, Saito A (2018) Axonal Activation of the Unfolded Protein Response Promotes Axonal Regeneration Following Peripheral Nerve Injury. *Neuroscience* **375**:34-48 doi: 10.1016/j.neuroscience.2018.02.003 PMID: 29438804

Ohtori S, Takahashi K, Moriya H, Myers RR (2004) TNF- α and TNF- α receptor type 1 upregulation in glia and neurons after peripheral nerve injury studies in murine DRG and spinal cord. *Spine (Phila Pa 1976)* **29**(10):1082-1088. doi: 10.1097/00007632-200405150-00006 PMID: 15131433

Oliveira AL (2001) Apoptosis of sensory neurons and satellite cells after sciatic nerve transection in C57BL/6J mice. *Braz J Med Biol Res* **34**(3):375-380. doi: 10.1590/s0100-879x2001000300012 PMID: 11262589

Ousman SS, David S (2000) Lysophosphatidylcholine induces rapid recruitment and activation of macrophages in the adult mouse spinal cord. *Glia* **30**(1):92-104. PMID: 10696148

Ousman SS, David S (2001) MIP-1 α , MCP-1, GM-CSF, and TNF- α control the immune cell response that mediates rapid phagocytosis of myelin from the adult mouse spinal cord. *J Neurosci* **21**(13):4649-4656. doi: 10.1523/JNEUROSCI.21-13-04649.2001 PMID: 11425892

Ousman SS, Frederick A, Lim EF (2017) Chaperone Proteins in the Central Nervous System and Peripheral Nervous System after Nerve Injury. *Front Neurosci* **11**:79. doi:10.3389/fnins.2017.00079 PMID: 28270745

Pannese E, Procacci P (2002) Ultrastructural localization of NGF receptors in satellite cells of the rat spinal ganglia. *J Neurocytol* **31**(8-9):755-763. doi: 10.1023/a:1025708132119 PMID: 14501212

Parrinello S, Napoli I, Ribeiro S, Wingfield Digby P, Fedorova M, Parkinson DB, Doddrell RD, Nakayama M, Adams RH, Lloyd AC (2010) EphB signaling directs peripheral nerve regeneration through Sox2-dependent Schwann cell sorting. *Cell* **143**(1): 145–155 doi: 10.1016/j.cell.2010.08.039 PMID: 20869108

Patodia S, Raivich G (2012) Role of transcription factors in peripheral nerve regeneration. *Front Mol Neurosci* **5**:8 doi: 10.3389/fnmol.2012.00008 PMID: 22363260.

Perkins NM, Tracey DJ (2000) Hyperalgesia due to nerve injury: role of neutrophils. *Neuroscience* **101**(3):745-757. doi: 10.1016/s0306-4522(00)00396-1 PMID: 11113323.

Perlson E, Hanz S, Ben-Yaakov K, Segal-Ruder Y, Seger R, Fainzilber M (2005) Vimentin-dependent spatial translocation of an activated MAP kinase in injured nerve. *Neuron* **45**(5):715-726. doi: 10.1016/j.neuron.2005.01.023 PMID: 15748847

Perlson E, Michaelevski I, Kowalsman N, Ben-Yaakov K, Shaked M, Seger R, Eisenstein M, Fainzilber M (2006) Vimentin binding to phosphorylated Erk sterically hinders enzymatic dephosphorylation of the kinase. *J Mol Biol* **364**(5):938-944. doi: 10.1016/j.jmb.2006.09.056 PMID: 17046786

- Pernet V, Hauswirth WW, Polo AD (2005) Extracellular signal-regulated kinase 1/2 mediates survival, but not axon regeneration, of adult injured central nervous system neurons in vivo. *J Neurochem* **93**(1):72-83. doi: 10.1111/j.1471-4159.2005.03002.x PMID: 15773907
- Perrin FE, Lacroix S, Avilés-Trigueros M, David S (2005) Involvement of monocyte chemoattractant protein-1, macrophage inflammatory protein-1alpha and interleukin-1beta in Wallerian degeneration. *Brain* **128**(Pt 4):854-866. doi: 10.1093/brain/awh407 PMID: 15689362
- Perry RB, Fainzilber M (2009) Nuclear transport factors in neuronal function. *Semin Cell Dev Biol* **20**(5):600-606. doi: 10.1016/j.semcdb.2009.04.014 PMID: 19409503
- Plemel JR, Stratton JA, Michaels NJ, Rawji KS, Zhang E, Sinha S, Baaklini CS, Dong Y, Ho M, Thorburn K, Firedman TN, Jawad S, Silva C, Caprariello AV, Hoghooghi V, Yue J, Jaffer A, Lee K, Kerr BJ, Midha R, Stys PK, Biernaskie J, Yong VW (2020) Microglia response following acute demyelination is heterogeneous and limits infiltrating macrophage dispersion. *Sci Adv* **6**(3):eaay6324. doi: 10.1126/sciadv.aay6324 PMID: 31998844
- Pollard JW (2009) Trophic macrophages in development and disease. *Nat Rev Immunol* **9**(4):259-270. doi: 10.1038/nri2528 PMID: 19282852
- Power HA, Morhart MJ, Olson JL, Chan KM (2020) Postsurgical Electrical Stimulation Enhances Recovery Following Surgery for Severe Cubital Tunnel Syndrome: A Double-Blind Randomized Controlled Trial. *Neurosurgery* **86**(6):769-777. doi: 10.1093/neuros/nyz322 PMID: 31432080
- Qui J, Cafferty WB, McMahon SB, Thompson SW (2005) Conditioning injury-induced spinal axon regeneration requires signal transducer and activator of transcription 3 activation. *J Neurosci* **25**(7):1645-1653. doi: 10.1523/JNEUROSCI.3269-04.2005 PMID: 15716400
- Read DE, Gorman AM (2009) Involvement of Akt in neurite outgrowth. *Cell Mol Life Sci* **66**(18):2975-2984. doi: 10.1007/s00018-009-0057-8 PMID: 19504044
- Rich KM, Luszyczynski JR, Osborne PA, Johnson Jr EM (1987) Nerve growth factor protects adult sensory neurons from cell death and atrophy caused by nerve injury. *J Neurocytol* **16**(2):261-268. doi: 10.1007/BF01795309 PMID: 3625240
- Richardson PM, Issa VM (1984) Peripheral injury enhances central regeneration of primary sensory neurones. *Nature* **309**:791-793. doi: 10.1038/309791a0 PMID: 6204205
- Richner M, Ferreira N, Dudele A, Jensen TS, Vaegter CB, Gonçalves NP (2019) Functional and Structural Changes of the Blood-Nerve-Barrier in Diabetic Neuropathy. *Front Neurosci* **12**:1038. doi: 10.3389/fnins.2018.01038 PMID: 30692907
- Richter-Lansberg C, Goldbaum O (2003) Stress proteins in neural cells: functional roles in health and disease. *Cell Mol Life Sci* **60**(2):337-349. doi: 10.1007/s000180300028 PMID: 12678498

- Rigoni M, Negro S (2020) Signals Orchestrating Peripheral Nerve Repair. *Cells* **9**(8):1768. doi: 10.3390/cells9081768 PMID: 32722089
- Rishal I, Fainzilber M (2014) Axon-soma communication in neuronal injury. *Nat Rev Neurosci* **15**(1):32-42. doi: 10.1038/nrn3609 PMID: 24326686
- Rosenberg AF, Isaacman-Beck J, Franzini-Armstrong C, Granato M (2014) Schwann cells and deleted in colorectal carcinoma direct regenerating motor axons towards their original path. *J Neurosci* **34**(44):14668-14681. doi: 10.1523/JNEUROSCI.2007-14.2014 PMID: 25355219
- Rosenthal A, Goeddel DV, Nguyden T, Lewis M, Shih A, Laramée GR, Nikolics K, Winslow JW (1990) Primary structure and biological activity of a novel human neurotrophic factor. *Neuron* **4**(5):767-773. doi: 10.1016/0896-6273(90)90203-r PMID: 2344409
- Rossi D, Zlotnik A (2000) The biology of chemokines and their receptors. *Annu Rev Immunol* **18**:217-242. doi: 10.1146/annurev.immunol.18.1.217 PMID: 10837058.
- Rotshenker S (2003) Microglia and macrophage activation and the regulation of complement-receptor-3 (CR3/MAC-1)-mediated myelin phagocytosis in injury and disease. *J Mol Neurosci* **21**(1):65-72. doi: 10.1385/JMN:21:1:65 PMID: 14500997.
- Rotshenker S (2011) Wallerian degeneration: the innate-immune response to traumatic nerve injury. *J Neuroinflammation* **8**:109. doi: 10.1186/1742-2094-8-109 PMID: 21878125
- Ruijs AC, Jaquet J, Kalmijn S, Giele H, Hovius SE (2005) Median and ulnar nerve injuries: a meta-analysis of predictors of motor and sensory recovery after modern microsurgical nerve repair. *Plast Reconstr Surg* **116**(2):484-494. doi: 10.1097/01.prs.0000172896.86594.07 PMID: 16079678
- Salegio EA, Pollard AN, Smith M, Zhou X (2011) Macrophage presence is essential for the regeneration of ascending afferent fibres following a conditioning sciatic nerve lesion in adult rats. *BMC Neurosci* **12**:11 doi: 10.1186/1471-2202-12-11 PMID: 21251261
- Sassone-Corsi P (2012) The cyclic AMP pathway. *Cold Spring Harb Perspect Biol* **4**(12):a011148. doi: 10.1101/cshperspect.a011148 PMID: 23209152
- Schmidt RE, Modert CW (1984) Orthograde, retrograde, and turnaround axonal transport of dopamine-beta-hydroxylase: response to axonal injury. *J Neurochem* **43**(3):865-870. doi: 10.1111/j.1471-4159.1984.tb12810.x PMID: 6205123
- Scholz J, Broom DC, Youn D, Mills CD, Kohno T, Suter MR, Moore KA, Decosterd I, Coggeshall RE, Woolf CJ (2005) Blocking Caspase Activity Prevents Transsynaptic Neuronal Apoptosis and the Loss of Inhibition in Lamina II of the Dorsal Horn after Peripheral Nerve Injury. *J Neurosci* **25**(32):7317-7323. doi: 10.1523/JNEUROSCI.1526-05.2005 PMID: 16093381

- Schorey JS, Lawrence C (2008) The pattern recognition receptor Dectin-1: from fungi to mycobacteria. *Curr Drug Targets* **9**(2):123-129. doi: 10.2174/138945008783502430 PMID: 18288963
- Seddon HJ (1942) A Classification of Nerve Injuries. *Br Med J* **2**(4260):237-239. doi: 10.1136/bmj.2.4260.237 PMID: 20784403
- Seiffers R, Allchorne AJ, Woolf CJ (2006) The transcription factor ATF-3 promotes neurite outgrowth. *Mol Cell Neurosci* **32**(1-2):143-154. doi: 10.1016/j.mcn.2006.03.005 PMID: 16713293
- Seiffers R, Mills CD, Woolf CJ (2007) ATF3 increases the intrinsic growth state of DRG neurons to enhance peripheral nerve regeneration. *J Neurosci* **27**(30):7911-7920. doi: 10.1523/JNEUROSCI.5313-06.2007 PMID: 17652582
- Senger JB, Verge VM, Chan KM, Webber CA (2018): The nerve conditioning lesion: A strategy to enhance nerve regeneration. *Ann Neurol* **83**(4):691-702. doi: 10.1002/ana.25209 PMID: 29537631
- Senger J, Chan KM, Macandili H, Chan AW, Verge VM, Jones KE, Webber CA (2019) Conditioning electrical stimulation promotes functional nerve regeneration. *Exp Neurol* **315**:60-71. doi: 10.1016/j.expneurol.2019.02.001 PMID: 30731076
- Senger JL, Chan KM, Webber CA (2020) Conditioning electrical stimulation is superior to postoperative electrical stimulation, resulting in enhanced nerve regeneration and functional recovery. *Exp Neurol* **325**:113147 doi: 10.1016/j.expneurol.2019.113147 PMID: 31837321
- Shen N, Zhu J (1995) Application of sciatic functional index in nerve functional assessment. *Microsurgery* **16**(8):552-555. doi: 10.1002/micr.1920160809 PMID: 8538433
- Shen ZL, Lassner F, Bader A, Becker M, Walter GF, Berger A (2000) Cellular activity of resident macrophages during Wallerian degeneration. *Microsurgery* **20**(5):255-261. doi: 10.1002/1098-2752(2000)20:5<255::aid-micr6>3.0.co;2-a PMID: 11015722
- Shin JE, Geisler S, DiAntonio A (2014) Dynamic regulation of SCG10 in regenerating axons after injury. *Exp Neurol* **252**:1-11. doi: 10.1016/j.expneurol.2013.11.007 PMID: 24246279
- Shinder V, Govrin-Lippmann R, Cohen S, Belenky M, Ilin P, Fried K, Wilkinson HA, Devor M (1999) Structural basis of sympathetic-sensory coupling in rat and human dorsal root ganglia following peripheral nerve injury. *J Neurocytol* **28**(9):743-761. doi: 10.1023/a:1007090105840 PMID: 10859576
- Simpson EM, Linder CC, Sargent EE, Davisson MT, Mobraaten LE, Sharp JJ (1997) Genetic variation among 129 substrains and its importance for targeted mutagenesis in mice. *Nat Genet* **16**(1):19-27. doi: 10.1038/ng0597-19 PMID: 9140391

Singh B, Xu Q, Franz CK, Zhang R, Dalton C, Gordon T, Verge VM, Midha R, Zochodne DW (2012) Accelerated axon outgrowth, guidance, and target reinnervation across nerve transection gaps following a brief electrical stimulation paradigm. *J Neurosurg* **116**(3):498-512. doi: 10.3171/2011.10.JNS11612 PMID: 22149377

Singh B, Krishnan A, Micu I, Koshy K, Singh V, Martinez JA, Koshy D, Xu F, Chandrasekhar A, Dalton C, Syed N, Stys PK, Zochodne DW (2015) Peripheral neuron plasticity is enhanced by brief electrical stimulation and overrides attenuated regrowth in experimental diabetes. *Neurobiol Dis* **83**:134-151. doi: 10.1016/j.nbd.2015.08.009 PMID: 26297317

Skene JH, Willard M (1981) Axonally transported proteins associated with axon growth in rabbit central and peripheral nervous system. *J Cell Biol* **89**(1):96-103. doi: 10.1083/jcb.89.1.96 PMID: 6164683.

Song X, Li F, Zhang F, Zhong J, Zhou X (2008) Peripherally-derived BDNF promotes regeneration of ascending sensory neurons after spinal cord injury. *PLoS One* **3**(3):e1707. doi: 10.1371/journal.pone.0001707 PMID: 18320028

Stassart RM, Fledrich R, Velanach V, Brinkmann BG, Schwab MH, Meijer D, Sereda MW, Nave K (2013) A role for Schwann cell-derived neuregulin-1 in remyelination. *Nat Neurosci* **16**(1):48-54. doi: 10.1038/nn.3281 PMID: 23222914

Streppel M, Azzolin N, Dohm S, Guntinas-Lichius O, Haas C, Grothe C, Wevers A, Neiss WF, Angelov DN (2002) Focal application of neutralizing antibodies to soluble neurotrophic factors reduces collateral axonal branching after peripheral nerve lesion. *Eur J Neurosci* **15**(8):1327-1342. doi: 10.1046/j.1460-9568.2002.01971.x PMID: 11994127

Sunderland S (1951) A classification of peripheral nerve injuries producing loss of function. *Brain* **74**(4):491-516. doi: 10.1093/brain/74.4.491 PMID: 14895767

Tanaka K, Zhang QL, Webster HD (1992) Myelinated fiber regeneration after sciatic nerve crush: morphometric observations in young adult and aging mice and the effects of macrophage suppression and conditioning lesions. *Exp Neurol* **118**(1):53-61. doi: 10.1016/0014-4886(92)90022-i PMID: 1397176

Tanaka T, Minami M, Nakagawa T, Satoh M (2004) Enhanced production of monocyte chemoattractant protein-1 in the dorsal root ganglia in a rat model of neuropathic pain: possible involvement in the development of neuropathic pain. *Neurosci Res* **48**(4):463-469. doi: 10.1016/j.neures.2004.01.004 PMID: 15041200

Tedeschi A, Bradke F (2013) The DLK signalling pathway—a double-edged sword in neural development and regeneration. *EMBO Rep* **14**(7):605-614. doi: 10.1038/embor.2013.64. PMID: 23681442

- Tonge D, Edström A, Ekström P (1998) Use of explant cultures of peripheral nerves of adult vertebrates to study axonal regeneration in vitro. *Prog Neurobiol* **54**(4): 459-480. doi: 10.1016/s0301-0082(97)00072-5 PMID: 9522396
- Topp KS, Boyd BS (2006) Structure and Biomechanics of Peripheral Nerves: Nerve Responses to Physical Stresses and Implications for Physical Therapist Practice. *Phys Ther* **86**(1):92-109. doi: 10.1093/ptj/86.1.92 PMID: 16386065
- Tsujino H, Kondo E, Fukuoka T, Dai Y, Tokunaga A, Miki K, Yonenobu K, Ochi T, Noguchi K (2000) Activating transcription factor 3 (ATF3) induction by axotomy in sensory and motoneurons: A novel neuronal marker of nerve injury. *Mol Cell Neurosci* **15**(2):170-182. doi: 10.1006/mcne.1999.0814 PMID: 10673325
- Udina E, Fuery M, Busch S, Silver J, Gordon T, Fouad K (2008) Electrical stimulation of intact peripheral sensory axons in rats promotes outgrowth of their central projections. *Exp Neurol* **210**(1):238-247. doi: 10.1016/j.expneurol.2007.11.007 PMID: 18164293
- Van der Laan, LJ, Ruuls SR, Weber KS, Lodder IJ, Döpp EA, Dijkstra CD (1996) Macrophage phagocytosis of myelin in vitro determined by flow cytometry: phagocytosis is mediated by CR3 and induces production of tumor necrosis factor-alpha and nitric oxide. *J Neuroimmunol* **70**(2):145-152. doi: 10.1016/s0165-5728(96)00110-5 PMID: 8898723.
- Vanhaesebroeck B, Alessi DR (2000) The PI3K–PDK1 connection: more than just a road to PKB. *Biochem J* **345** Pt 3 (Pt3):561-576. PMID: 10698680
- Van Rooijen N, van Nieuwmegen R (1984) Elimination of phagocytic cells in the spleen after intravenous injection of liposome-encapsulated dichloromethylene diphosphonate. An enzyme-histochemical study. *Cell Tissue Res* **238**(2):355-358. doi: 10.1007/BF00217308 PMID: 6239690
- Vargas ME, Barres BA (2007) Why is Wallerian degeneration in the CNS so slow? *Annu Rev Neurosci* **30**:153-179. doi: 10.1146/annurev.neuro.30.051606.094354 PMID: 17506644
- Vargas ME, Watanabe J, Singh SJ, Robinson WH, Barres BA (2010) Endogenous antibodies promote rapid myelin clearance and effective axon regeneration after nerve injury. *Proc Natl Acad Sci U S A* **107**(26):11993-11998. doi: 10.1073/pnas.1001948107 PMID: 20547838
- Vela FJ, Martínez-Chacón G, Ballestín A, Campos JL, Sánchez-Margallo FM, Abellán E (2020) Animal models used to study direct peripheral nerve repair: a systematic review. *Neural Regen Res* **15**(3):491-502. doi: 10.4103/1673-5374.266068 PMID: 31571661
- Verdú E, Ceballos D, Vilches JJ, Navarro X (2000) Influence of aging on peripheral nerve function and regeneration. *J Peripher Nerv Syst* **5**(4):191-208. doi: 10.1046/j.1529-8027.2000.00026.x PMID: 11151980

Verge VM, Riopelle RJ, Richardson PM (1989) Nerve growth factor receptors on normal and injured sensory neurons. *J Neurosci* **9**(3):914-922. doi: 10.1523/JNEUROSCI.09-03-00914.1989 PMID: 2538586.

Verge VM, Gratto KA, Karchewski LA, Richardson PM (1996) Neurotrophins and nerve injury in the adult. *Philos Trans R Soc Lond B Biol Sci* **351**(1338):423-430. doi:10.1098/rstb.1996.0038 PMID: 8730781

Walker LJ, Summers DW, Sasaki Y, Brace EJ, Milbrandt J, DiAntonio A (2017) MAPK signaling promotes axonal degeneration by speeding the turnover of the axonal maintenance factor NMNAT2. *eLIFE* **6**:e22540. doi: 10.7554/eLife.22540 PMID: 28095293

Wang L, Nie Q, Gao M, Yang L, Xiang J, Xiao Y, Liu F, Gong X, Fu J, Wang Y, Nguyen QD, Liu Y, Liu M, Li DW (2020) The transcription factor CREB acts as an important regulator mediating oxidative stress-induced apoptosis by suppressing α B-crystallin expression. *Aging (Albany NY)* **12**(13):13594-13617. doi: 10.18632/aging.103474 PMID: 32554860

Wang PL, Yim AK, Kim K, Avey D, Czepielewski RS, Colonna M, Milbrandt J, Randolph GJ (2020) Peripheral nerve resident macrophages share tissue-specific programming and features of activated microglia. *Nat Commun* **11**(1):2552. doi: 10.1038/s41467-020-16355-w PMID: 32439942

Wang S, Watanabe T, Noritake J, Fukata M, Yoshimura T, Itoh N, Harada T, Nakagawa M, Matsuura Y, Arimura N, Kaibuchi K (2007) IQGAP3, a novel effector of Rac1 and Cdc42, regulates neurite outgrowth. *J Cell Sci* **120**(Pt 4):567-577. doi: 10.1242/jcs.03356 PMID: 17244649

Wang Y, Song M, Song F (2018) Neuronal autophagy and axon degeneration. *Cell Mol Life Sci* **75**(13):2389-2406. doi: 10.1007/s00018-018-2812-1 PMID: 29675785

Webber CA, Xu Y, Vanneste KJ, Martinez JA, Verge VM, Zochodne DW (2008) Guiding adult Mammalian sensory axons during regeneration. *J Neuropathol Exp Neurol* **67**(3):212-222. doi: 10.1097/NEN.0b013e3181654972 PMID: 18344912

Webber CA, Zochodne DW (2010) The nerve regenerative microenvironment: early behavior and partnership of axons and Schwann cells. *Exp Neurol* **223**(1):51-59. doi:10.1016/j.expneurol.2009.05.037 PMID: 19501085

Webber CA, Christie KJ, Cheng C, Martinez JA, Singh B, Singh V, Thomas D, Zochodne DW (2011) Schwann cells direct peripheral nerve regeneration through the Netrin-1 receptors, DCC and Unc5H2. *Glia* **59**(10):1503-1517. doi: 10.1002/glia.21194 PMID: 21656855

Wei D, Hurd C, Galleguillos D, Singh J, Fenrich KK, Webber CA, Sipione S, Fouad K (2016) Inhibiting cortical protein kinase A in spinal cord injured rats enhances efficacy of rehabilitative training. *Exp Neurol* **283**(Pt A):365-374. doi: 10.1016/j.expneurol.2016.07.001 PMID: 27401133

Wetmore C, Olson L (1995) Neuronal and nonneuronal expression of neurotrophins and their receptors in sensory and sympathetic ganglia suggest new intercellular trophic interactions. *J Comp Neurol* **353**(1):143-159. doi: 10.1002/cne.903530113 PMID: 7714245

White FA, Sun J, Waters SM, Ma C, Ren D, Ripsch M, Steflik J, Cortright DN, Lamotte RH, Miller RJ (2005) Excitatory monocyte chemoattractant protein-1 signaling is up-regulated in sensory neurons after chronic compression of the dorsal root ganglion. *Proc Natl Acad Sci U S A* **102**(39):14092-14097. doi: 10.1073/pnas.0503496102 PMID: 16174730

Witzel C, Rohde C, Brushart TM (2005) Pathway sampling by regenerating peripheral axons. *J Comp Neurol* **485**(3):183-190. doi: 10.1002/cne.20436 PMID: 15791642

Wong JN, Olson JL, Morhart MJ, Chan KM (2015) Electrical stimulation enhances sensory recovery: a randomized controlled trial. *Ann Neurol* **77**(6):996-1006. doi: 10.1002/ana.24397 PMID: 25727139

Woodho A, Sommer L (2008) Development of the Schwann cell lineage: from the neural crest to the myelinated nerve. *Glia* **56**(14):1481-1490. doi: 10.1002/glia.20723 PMID: 18803317

Wu KY, Hengst U, Cox LJ, Macosko EZ, Jeromin A, Urquhart ER, Jaffrey SR (2005) Local translation of RhoA regulates growth cone collapse. *Nature* **436**(7053):1020-1024. doi: 10.1038/nature03885 PMID: 16107849

Wu D, Zhang Y, Bo X, Huang W, Xiao F, Zhang X, Miao T, Magoulas C, Subang MC, Richardson PM (2007) Actions of neuropoietic cytokines and cyclic AMP in regenerative conditioning of rat primary sensory neurons. *Exp Neurol* **204**(1):66-76. doi: 10.1016/j.expneurol.2006.09.017 PMID: 17112514

Xiao Y, Faucherre A, Pola-Morell L, Heddleston JM, Liu T, Chew T, Sato F, Sehara-Fujisawa A, Kawakami K, López-Schier H (2015) High-resolution live imaging reveals axon-glia interactions during peripheral nerve injury and repair in zebrafish. *Dis Model Mech* **8**(6):553-564. doi: 10.1242/dmm.018184 PMID: 26035865

Xiong X, Hao Y, Sun K, Li J, Li X, Mishra B, Soppina P, Wu C, Hume RI, Collins CA (2012) The Highwire ubiquitin ligase promotes axonal degeneration by tuning levels of Nmnat protein. *PLoS Biol* **10**:e1001440 doi: 10.1371/journal.pbio.1001440 PMID: 23226106

Yamagishi Y, Tessier-Lavigne M (2016) An atypical SCF-life ubiquitin ligase complex promotes Wallerian degeneration through regulation of axonal Nmnat2. *Cell Rep* **17**:774-782. <https://doi.org/10.1016/j.celrep.2016.09.043> PMID: 27732853

Yang J, Weimer RM, Kallop D, Olsen O, Wu Z, Renier N, Uryu K, Tessier-Lavigne M (2013) Regulation of axon degeneration after injury and in development by the endogenous calpain inhibitor calpastatin. *Neuron* **80**(5):1175-1189. doi: 10.1016/j.neuron.2013.08.034 PMID: 24210906.

Yao H, Price TT, Cantelli G, Ngo B, Warner MJ, Olivere L, Ridge SM, Jablonski EM, Therrien J, Tannheimer S, McCall CM, Chenn A, Sipkins DA (2018) Leukaemia hijacks a neural mechanism to invade the central nervous system. *Nature* **560**(7716):55-60. doi: 10.1038/s41586-018-0342-5 PMID: 30022166.

Ydens E, Cauwels A, Asselbergh B, Goethals S, Peeraer L, Lornet G, Almeida-Souza L, Van Ginderachter JA, Timmerman V, Janssens S (2012) Acute injury in the peripheral nervous system triggers an alternative macrophage response. *J Neuroinflammation* **9**:176. doi: 10.1186/1742-2094-9-176 PMID: 22818207

Ydens E, Amann L, Asselbergh B, Scott CL, Martens L, Sichien D, Mossad O, Blank T, De Prijck S, Low D, Masuda T, Saeys Y, Timmerman V, Stumm R, Ginhoux F, Prinz M, Janssens S, Guillemins M (2020) Profiling peripheral nerve macrophages reveals two macrophage subsets with distinct localization, transcriptome and response to injury. *Nat Neurosci* **23**(5):676-689. doi: 10.1038/s41593-020-0618-6 PMID: 32284604

Yin Q, Kemp GJ, Yu LG, Wagstaff SC, Frostick SP (2001) Neurotrophin-4 delivered by fibrin glue promotes peripheral nerve regeneration. *Muscle Nerve* **24**(3):345-351. doi: 10.1002/1097-4598(200103)24:3<345::aid-mus1004>3.0.co;2-p PMID: 11353418

Yona S, Kim K, Wolf Y, Mildner A, Varol D, Breker M, Strauss-Ayali D, Viukov S, Guillemins M, Misharin A, Hume DA, Perlman H, Malissen B, Zelzer E, Jung S (2013) Fate mapping reveals origins and dynamics of monocytes and tissue macrophages under homeostasis. *Immunity* **38**(1):79-91. doi: 10.1016/j.immuni.2012.12.001 PMID: 23273845

Zhang JY, Luo XG, Xian CJ, Liu ZH, Zhou XF (2000) Endogenous BDNF is required for myelination and regeneration of injured sciatic nerve in rodents. *Eur J Neurosci* **12**(12):4171-4180. PMID: 11122329

Zhang J, De Koninck Y (2006) Spatial and temporal relationship between monocyte chemoattractant protein-1 expression and spinal glial activation following peripheral nerve injury. *J Neurochem* **97**(3):772-783 PMID: 16524371

Zhao Y, Zou W, Du J, Zhao Y (2018) The origins and homeostasis of monocytes and tissue resident macrophages in physiological situation. *J Cell Physiol* **233**:642. doi: 10.1002/jcp.26461 PMID: 29323706

Zhao X, Alam MM, Liao Y, Huang T, Mathur R, Zhu X, Huang Y (2019) Targeting Microglia Using Cx3cr1-Cre Lines: Revisiting the Specificity. *eNeuro* **6**(4):ENEURO.0114-19.2019. doi: 10.1523/ENEURO.0114-19.2019 PMID: 31201215.

Zhou XF, Deng YS, Chie E, Xue Q, Zhong JH, McLachlan EM, Rush RA, Xian CJ (1999) Satellite-cell-derived nerve growth factor and neurotrophin-3 are involved in noradrenergic sprouting in the dorsal root ganglia following peripheral nerve injury in the rat. *Eur J Neurosci* **11**(5):1711-1722. doi: 10.1046/j.1460-9568.1999.00589.x PMID: 10215925

Zochodne DW (2012) The challenges and beauty of peripheral nerve regrowth. *J Peripher Nerv Syst* **17**(1):1-18. doi: 10.1111/j.1529-8027.2012.00378.x PMID: 22462663

Zochodne DW (2008) Neurobiology of peripheral nerve regeneration. *Cambridge University press*, Cambridge

Zuo KJ, Gordon T, Chan KM, Borschel GH (2020) Electrical stimulation to enhance peripheral nerve regeneration: Update in molecular investigations and clinical translation. *Exp Neurol* **332**:113397. doi: 10.1016/j.expneurol.2020.113397 PMID: 32628968

Recovering the regenerative potential in chronically injured nerves by using conditioning electrical stimulation

Jenna-Lynn B. Senger, MD, PhD,¹ Karyne N. Rabey, PhD,^{2,4} Leah Acton, BSc,²
Ying-Ho S. Lin, BSc,² Susanne Lingrell,² K. Ming Chan, MD, FRCPC,³ and
Christine A. Webber, PhD²

¹Division of Plastic Surgery, Department of Surgery, Faculty of Medicine and Dentistry, University of Alberta; ²Division of Anatomy, Department of Surgery, Faculty of Medicine and Dentistry, University of Alberta; ³Division of Physical Medicine and Rehabilitation, Department of Medicine, Faculty of Medicine and Dentistry, University of Alberta; and ⁴Department of Anthropology, Faculty of Science, University of Alberta, Edmonton, Alberta, Canada

OBJECTIVE Chronically injured nerves pose a significant clinical challenge despite surgical management. There is no clinically feasible perioperative technique to upregulate a proregenerative environment in a chronic nerve injury. Conditioning electrical stimulation (CES) significantly improves sensorimotor recovery following acute nerve injury to the tibial and common fibular nerves. The authors' objective was to determine if CES could foster a proregenerative environment following chronically injured nerve reconstruction.

METHODS The tibial nerve of 60 Sprague Dawley rats was cut, and the proximal ends were inserted into the hamstring muscles to prevent spontaneous reinnervation. Eleven weeks postinjury, these chronically injured animals were randomized, and half were treated with CES proximal to the tibial nerve cut site. Three days later, 24 animals were killed to evaluate the effects of CES on the expression of regeneration-associated genes at the cell body ($n = 18$) and Schwann cell proliferation ($n = 6$). In the remaining animals, the tibial nerve defect was reconstructed using a 10-mm isograft. Length of nerve regeneration was assessed 3 weeks postgrafting ($n = 16$), and functional recovery was evaluated weekly between 7 and 19 weeks of regeneration ($n = 20$).

RESULTS Three weeks after nerve isograft surgery, tibial nerves treated with CES prior to grafting had a significantly longer length of nerve regeneration ($p < 0.01$). Von Frey analysis identified improved sensory recovery among animals treated with CES ($p < 0.01$). Motor reinnervation, assessed by kinetics, kinematics, and skilled motor tasks, showed significant recovery ($p < 0.05$ to $p < 0.001$). These findings were supported by immunohistochemical quantification of motor endplate reinnervation ($p < 0.05$). Mechanisms to support the role of CES in reinvigorating the regenerative response were assessed, and it was demonstrated that CES increased the proliferation of Schwann cells in chronically injured nerves ($p < 0.05$). Furthermore, CES upregulated regeneration-associated gene expression to increase growth-associated protein-43 (GAP-43), phosphorylated cAMP response element binding protein (pCREB) at the neuronal cell bodies, and upregulated glial fibrillary acidic protein expression in the surrounding satellite glial cells ($p < 0.05$ to $p < 0.001$).

CONCLUSIONS Regeneration following chronic axotomy is impaired due to downregulation of the proregenerative environment generated following nerve injury. CES delivered to a chronically injured nerve influences the cell body and the nerve to re-upregulate an environment that accelerates axon regeneration, resulting in significant improvements in sensory and motor functional recovery. Percutaneous CES may be a preoperative strategy to significantly improve outcomes for patients undergoing delayed nerve reconstruction.

<https://thejns.org/doi/abs/10.3171/2021.4.JNS21398>

KEYWORDS chronic nerve injury; nerve reconstruction; conditioning electrical stimulation; rat; peripheral nerve

ABBREVIATIONS ATF3 = activation transcription factor 3; CES = conditioning electrical stimulation; DRG = dorsal root ganglion; GAP-43 = growth-associated protein-43; GFAP = glial fibrillary acidic protein; NF200 = neurofilament-200; NMJ = neuromuscular junction; PBS = phosphate-buffered saline; pCREB = phosphorylated cAMP response element binding protein; RAG = regeneration-associated gene.

SUBMITTED February 11, 2021. **ACCEPTED** April 28, 2021.

INCLUDE WHEN CITING Published online October 15, 2021; DOI: 10.3171/2021.4.JNS21398.



Original Research Article



Neurorehabilitation and
Neural Repair
2020, Vol. 34(4) 299–308
© The Author(s) 2020
Article reuse guidelines:
sagepub.com/journalsPermissions.nav
DOI: 10.1177/1545968220955801
journals.sagepub.com/home/nrr

Conditioning Electrical Stimulation Is Superior to Postoperative Electrical Stimulation in Enhanced Regeneration and Functional Recovery Following Nerve Graft Repair

Jenna-Lynn B. Senger, MD, PhD¹, Ashley W. M. Chan¹,
K. Ming Chan, MDC¹, Terence Kwan-Wong, MD², Leah Acton¹,
Jaret Olson, MD¹, and Christine A. Webber, PhD¹

Abstract

Background. Autologous nerve graft is the most common clinical intervention for repairing a nerve gap. However, its regenerative capacity is decreased in part because, unlike a primary repair, the regenerating axons must traverse 2 repair sites. Means to promote nerve regeneration across a graft are needed. Postoperative electrical stimulation (PES) improves nerve growth by reducing staggered regeneration at the coaptation site whereas conditioning electrical stimulation (CES) accelerates axon extension. In this study, we directly compared these electrical stimulation paradigms in a model of nerve autograft repair. **Methods.** To lay the foundation for clinical translation, regeneration and reinnervation outcomes of CES and PES in a 5-mm nerve autograft model were compared. Sprague-Dawley rats were divided into: (a) CES, (b) PES, and (c) no stimulation cohorts. CES was delivered 1 week prior to nerve cut/coaptation, and PES was delivered immediately following coaptation. Length of nerve regeneration ($n = 6$ /cohort), and behavioral testing ($n = 16$ /cohort) were performed at 14 days and 6 to 14 weeks post-coaptation, respectively. **Results.** CES treated axons extended 5.9 ± 0.2 mm, significantly longer than PES (3.8 ± 0.2 mm), or no stimulation (2.5 ± 0.2 mm) ($P < .01$). Compared with PES animals, the CES animals had significantly improved sensory recovery (von Frey filament testing, intraepidermal nerve fiber reinnervation) ($P < .001$) and motor reinnervation (horizontal ladder, gait analysis, nerve conduction studies, neuromuscular junction analysis) ($P < .01$). **Conclusion.** CES resulted in faster regeneration through the nerve graft and improved sensorimotor recovery compared to all other cohorts. It is a promising treatment to improve outcomes in patients undergoing nerve autograft repair.

Keywords

conditioning electrical stimulation, nerve graft, predinical, peripheral nerve, nerve regeneration

Introduction

Outcomes following peripheral nerve injury are strongly influenced by the time required for regenerating motor and sensory axons to reach their target tissue. Functional outcomes can be improved by accelerating the intrinsic rate of nerve regeneration. Although a conditioning crush lesion (CCL) delivered to a nerve 1 week prior to transection and nerve repair has been shown to be capable of markedly accelerating nerve regrowth, it cannot be translated to the clinic due to its injurious nature.¹ Recently, however, we demonstrated that 1 hour of conditioning electrical stimulation (CES) delivered to a nerve 7 days prior to injury and repair induces a conditioning effect comparable to a CCL, but in a noninjurious, thus clinically feasible manner.²⁻⁴

While the use of CES is novel, postoperative electrical stimulation (PES) is well described to improve outcomes in animal and human models of nerve injury, and it is the only adjunct to nerve repair that has been successfully translated to the clinic.^{5,6} However, unlike a conditioning lesion (CCL or CES), PES does not accelerate axon extension, but rather enhances regeneration of axons as they

¹University of Alberta, Alberta, Edmonton, Canada

²The Hospital for Sick Children, Toronto, Ontario, Canada

Corresponding Author:

Christine A. Webber, Division of Plastic Surgery, Department of Surgery, University of Alberta, 501 Medical Sciences Building, Edmonton, Alberta, T6G 2N1, Canada.
Email: webber2@ualberta.ca